



Faculté : Sciences de la Nature et de la Vie Département: Sciences Alimentaires
Laboratoire Biomathématique, Biophysique, Biochimie et Scientrometrie

THÈSE
EN VUE DE L'OBTENTION DU DIPLOME
DE DOCTORAT

Domaine : Sciences de la Nature et de la Vie
Filière : Sciences Biologiques
Spécialité : Bio-ressources, Environnement et Technologie Agro-alimentaire

Présentée par
BELHAMEL Chiraz

Thème

**Recherche des Activités Biologiques de deux Plantes Médicinales
et des Nanoparticules de Synthèse**

Soutenue le : 10 avril 2021

Devant le Jury composé de :

Nom et Prénom	Grade		
Mr Madani K.	Professeur	Univ. de Bejaia	Président
Mme Boulekbache L.	Professeur	Univ. de Bejaia	Rapporteur
Mme Ghemghar H.	MCA	Univ. de Bejaia	Co- Rapporteur
Mme Brahmi F.	MCA	Univ. de Bejaia	Examineur
Mr Kadri N.	MCA	Univ. de Bouira	Examineur

Année Universitaire : 2020-2021

République Algérienne Démocratique et Populaire
People's Democratic Republic of Algeria
Ministry of Higher Education and Scientific Research
A.MIRA-BEJAIA University



Faculty: Natural and Life Sciences

Department: Food Sciences

Laboratory of Biomathematics, Biophysics, Biochemistry and Scientrometry

In partial fulfillment of requirements for the degree of Doctorate

Domaine : Sciences de la Nature et de la Vie

Filière : Sciences Biologiques

Spécialité : Bio-ressources, Environnement et Technologie Agro-alimentaire

Presented by
BELHAMEL Chiraz
Title

**Research of the Biological Activities of two Medicinal Plants and
Nanoparticles of Synthesis**

Defended on : 10 april 2021

Jury Members:

First and Last name

Mr Madani K.	Professor	Univ. of Bejaia	President
Mrs Boulekbache L.	Professor	Univ. of Bejaia	Supervisor
Mrs Ghemghar H.	Assoc. Professor	Univ. of Bejaia	Co- Supervisor
Mrs Brahmi F.	Assoc. Professor	Univ. of Bejaia	Examiner
Mr Kadri N.	Assoc. Professor	Univ. de Bouira	Examiner

University year : 2020-2021

This thesis has been written to meet the requirements for obtaining a PhD diploma from the University of Bejaia. It is structured in two parts:

Part I : Biological activities of two medicinal plants (*Rhamnus alaternus* and *Phillyrea angustifolia*).

Part II: Synthesis of nanostructured alumina using two methods (sol-gel and green synthesis) and their applications in farming.

The research work within the framework of this thesis led to the publication of paper in an international renowned journal : Journal stored products Research. Moreover, I presented 9 communications in national and international conferences.

- 01 publication:

Chiraz Belhamel, Lila Boulekbache-Makhlouf, Stefano Bedini, Camilla Tani, Tiziana Lombardi, Paolo Giannotti, Khodir Madani, Kamel Belhamel, Barbara Conti, Nanostructured alumina as seed protectant against insect pests. *Journal stored products research*, 87, 2020, 101607.

- 09 communications:

1. S. Guemouni, **Chiraz Belhamel**, K. MADANI .Participation au séminaire International, Les produits du terroir un outil du développement de l'agriculture de montagne avec une communication affichée intitulée : Séchage comparé de la tomate « *Lycopersicon esculentum* Mill » entre la micro-onde et l'étuve, organisé à Chemini wilaya de Bejaia-Algérie- 15 et 16 décembre 2018.
2. **Chiraz Belhamel**, Lila Boulekbache-Makhlouf, Hayatte Haddadi-Ghemghar, Nacim Nabet. Participation au séminaire International, Les produits du terroir un outil du développement de l'agriculture de montagne avec une communication affichée intitulée « La culture Hors sol : pour une agriculture saine, rentable et respectueuse de l'environnement organisé à Chemini wilaya de Bejaia- Algérie- 15 et 16 décembre 2018.
3. **Chiraz Belhamel** , Lila Boulekbache-Makhlouf, Hayatte Haddadi-Ghemghar , l'orge hydroponique : un potentiel en antioxydants , Congrès International : les Rencontres de l'Agriculture et de la Biologie, Université de Constantine - Algeria, 5-7 Mai 2018
4. **Chiraz Belhamel**, Dahia Meridja, kamel Belhamel, Evaluation de l'activité Antioxydante et pharmacologique des extraits des feuilles d'*Urtica dioca* et *Urtica pilulifera*, Séminaire International sur les plantes Médicinales Université d'el Oued-Algérie 17-18 janvier 2018

5. **Chiraz Belhamel**, Lila Boulekbeche-Makhlouf, Hayatte Haddadi-Ghemghar, Sara GUEMOUNI. Plantes bio-pesticide, alternative aux produits phytosanitaires chimiques et protection des céréales, Séminaire National : Durabilité au Service de notre Alimentation, Santé et Environnement, Université de Bejaia- Algérie 15-16 janvier 2018.
6. **Chiraz Belhamel**, Lila Boulekbeche-Makhlouf, Hayatte Haddadi-Ghemghar. K. Madani. Céréales germées et fourrages hydroponiques: un potentiel en antioxidant , Séminaire d'Echange National: aux Interfaces du Développement Durables, Université de Bejaia- Algérie 20-21 décembre 2017.
7. S. Guemouni, **Chiraz Belhamel**, K. MADANI. Séminaire d'échange national : Aux interfaces du développement durable avec poster affichée intitulée Optimisation de deux méthodes de séchage d'une plante aromatique « Allium sativum » à l'université Abderrahmane Mira de Bejaia 20 et 21 Décembre 2017.
8. S. Guemouni, **Chiraz Belhamel**, K. MADANI. Participation au séminaire international, « Environnement, Agriculture et Biotechnologie » (SIEB-2017) avec communication affichée intitulée : Séchage comparé de l'ail « Allium sativum » entre la micro-onde et l'étuve à l'université Akli Mohand Oulhadj de Bouira. 27 et 28 novembre 2017.
9. **Chiraz Belhamel**, Dahia Meridja, Etude phytochimique et évaluation de l'activité antioxydante des extraits de plantes médicinales de la pharmacopée traditionnelle d'Algérie, International Congress on Biotechnologies for Sustainable Development, Boumerdes- Algeria 24-25 October 2017.

Acknowledgement

This work has been carried out at the laboratory of Biomathematic, Biophysic, Biochemistry and scientromerty, Faculty of Natural Life and Sciences, University of Bejaia with the collaboration of the Department of Agriculture, Food and Environment (DAFE) University of Pisa, Italy and Organic Chemistry department, University of Aveiro, Portugal. Part of the work has been carried out in the frame of the research project funded by the Algerian Ministry of Higher Education.

I would like to express my sincere gratitude to my director, Prof. Boulekbache-makhlouf lila and co-director Dr. Ghumghar Hayet, who have been going along with me during my PhD thesis. Their immense knowledge, valuable advices as well as great patience have helped me all the time in doing research and writing this thesis.

My sincere thanks go to Dr. Susana Cardoso and Dr. Barbara Conti for their warm welcome, their availability and great generosity during my training period at the University of Aveiro and the University of Pisa.

I also would like to thank Prof. Madani Khodir, Dr. Brahmi fatiha and Dr. Kadri Nabil for accepting to become my jury members. It is obvious that their insightful comments would improve my thesis quite a lot and aid me to widen not only my knowledge but also my research views from numerous perspectives.

I would like to express my warm thanks to Dr. Nabet Nacim and Dr. Bedini Stefano for their help and support in the correction of the published paper.

I am grateful to Prof. Nabeti Hafidh and Dr. Bensidehoum Lila for their supporting in the implementation of anti-microbial activities.

Special thanks for my best friends Bensidehoum Lila, Belkhir Sara, Sara Guemouni, and Zeghib Walid for their support, help and encouragements.

Thanks to all the members of laboratory of Biomathematic, Biophysic, Biochemistry and scientromertie (3BS) and Laboratory Organic materials (LMO) for their help, good humour and kindness.

Finally, I would like to thank my sisters, Nour El Houda and Nouara Yasmine, my parents and my husband for their unconditional love and encouragement.

List of abbreviations

ABTS^{•+}: Acide 2,2'-azino-bis(3-ethylbenzothiazoline-6-sulphonique)

ATCC : American Type Culture Collection

Al₂O₃ :Alumina

Al₂O₃-Nps : Alumina nanoarticles

ARO: Antibiotic Resistant Bacteria

AlCl₃ : Aluminium trichloride

BHA: Butylated Hydroxyanisole

BHT: Butylated Hydroxytoluene

CIP : Collection of the Institut de Pasteur

CMB: Minimum Bactericidal Concentration

DMSO: Dimethylsulfoxide

DPPH: 1,1 diphenyl-2-picrylhydrazyl

DZI: Diameter of Muting Zone

EDX: Energy Dispersive X-Ray

EAC: Equivalent in Catechin Acid.

EAG : Equivalent in Gallic Acid

EASC: Equivalent in Ascorbic Acid

EAQ: Equivalent in Quercetin Acid

ERO: Oxygen Reactive Species

EtOH: Ethanol

Fe²⁺: Ferrous iron

Fe³⁺ : Ferric Iron

FeCl₃: Ferric chloride

FeCl₂ : Iron chloride

FRAP: Ferric reducing antioxidant power.

FeSO₄: Ferrous sulphate

FTIR: Fourier Transform InfraRed spectroscopy analysis

JCPDS: Joint Committee on Powder Diffraction Standards

HCl : Hydrochloric acid

H₃PMO₁₂O₄₀: Phosphomolybdic acid

H₃PW₁₂O₄₀ : Phosphotungstic acid

H₂SO₄ : Sulphuric acid

LC: Liquid Chromatography

IC₅₀: 50% inhibitory concentration

K₃Fe (CN) ₆: Potassium Ferricyanide

KOH: Potassium hydroxide

LSD: Low significant difference

MIC: Minimum Inhibitory Concentration

[M-H]⁻ : Molar mass of ion in negative ionisation mode

[M-H]⁺ : Molar mass of ion in positive ionisation mode

MH: Mueller Hinton.

DM: Dry Matter

NSA: Nanostructured alumina

NaOH: Sodium hydroxide

P : *Phillyrea*

R: *Rhamnus*

RSD: Relative Standard Deviation

RSM: Response Surface Method.

SEM: Scanning Electron Microscopy

TCA: Trichloroacetic Acid

UV: Ultra violet Visible

UFC: Unité Formant Colonie

XRD : X-Ray diffraction

List of Figures

Part I

Figure 1. Mesomeric forms of phenol.	13
Figure 2. Formation of Activated Oxygen Species (AOS).	15
Figure 3. Standardized Pareto charts of <i>R. alaternus</i> for polyphenol (mg EAG/g DM).	35
Figure 4. Standardized Pareto charts of <i>R. alaternus</i> for antioxidant activity DPPH (ug EAG/ml).	36
Figure 5. Three-dimensional diagram of the response surface for the effects of time and solvent.	37
Figure 6. Standardized Pareto charts of <i>P. angustifolia</i> for polyphenols.	39
Figure 7. Interaction between the ratio and extraction time and their effect on the polyphenols of <i>P. angustifolia</i>	39
Figure 8. Standardized Pareto charts of <i>P. angustifolia</i> . for antioxidant activity DPPH.	40
Figure 9. Three dimensional plots of surface response using <i>P. angustifolia</i>	42
Figure 10. Flavonoid contents of the plants studied.	42
Figure 11. Condensed tannin contents of the plants studied.	43
Figure 12. Reducing power test of the plant extracts studied.	44
Figure 13. Ammonium phosphomolybdate test of the plant extracts studied.	45
Figure 14. Test ABTS of the plant extracts studied.	46
Figure 15. Superoxide radical scavenging test of the plant extract studied.	47
Figure 16: Antibacterial activities of <i>R. alaternus</i> and <i>P. angustifolia</i> extracts.	50

Part II

Figure 1. Nanoparticle production: top-down and bottom-up.....	83
Figure 2. Scheme of the crystal structure of Al_2O_3	91
Figure 3. Alumina production worldwide from 2010 to 2019.	93
Figure 4. Alumina production worldwide in 2019	94
Figure 5. Schematic representation of green synthesis of Al_2O_3 NPs.....	107
Figure 6. XRD spectra nanostructured alumina obtained after drying gel at 1000°C	109
Figure 7. FTIR spectra of nanostructured alumina calcined at 1000°C	111
Figure 8. Scanning Electron Microscopy of nanostructured alumina.	112
Figure 9. EDX spectrum of nanostructured alumina.....	113
Figure 10. Mortality (%) (mean \pm SE) of <i>T. confusum</i> (a) and <i>O. surinamensis</i> (b) <i>S. paniceum</i> (c) adults fed on beans treated with nanostructured alumina (NSA) particles	114
Figure 11. SEM observed in leaves <i>Phaseolus vulgaris</i> treated with nanostructured alumina....	119
Figure 12. EDX spectrum of in leaves <i>Phaseolus vulgaris</i> treated with nanostructured alumina.	120
Figure 13. XRD spectra of the Al_2O_3 NPs using extract of <i>Rhamnus alaternus</i>	126
Figure 14. Scanning Electron Microscopy image spherical agglomeration alumina nanostructured using <i>Rhamnus alaternus</i> extract.....	126

List of Tables

Part I

Table I: Ecological characteristics of the place where the plants are harvested.	21
Table II: Experimental design used for the extraction of bioactive compounds from the two plants studied.....	23
Table III: Levels of the three selected parameters.	24
Table V. Experimental design and observed results for all investigated responses from <i>R. alaternus</i>	34
Table VI. Predicted and observed values of each individual response for the optimal <i>R. alaternus</i>	37
Table VII. Experimental design and observed results for all investigated responses from <i>P. angustifolia</i>	38
Table VIII: Predicted and observed values of each individual response for <i>P. angustifolia</i>	41
Table IX: Antibacterial properties minimal inhibition concentration (MIC) of <i>Rhamnus alaternus</i> and <i>Phillyrea angustifolia</i> extracts.....	52
Table X. Inhibitory activities of <i>Rhamnus alaternus</i> and <i>Phillyrea angustifolia</i> towards α -amylase and α -glucosidase	56

Part II

Table 1 : Examples of current applications of nanomaterials (INRS 2012).....	81
Table II: X-ray diffraction (XRD) analysis of the nanostructured alumina.....	110
Table III: Mineral composition of nanostructured alumina.	113
Table IV. Adjusted estimated marginal (EM) means on mortality of <i>Tribolium confusum</i> , <i>Oryzaephilus surinamensis</i> , and <i>Stegobium paniceum</i> exposed to nanostructured alumina (NSA).	115
Table V: Toxicity of nanostructured alumina against adult <i>Oryzaephilus surinamensis</i> , <i>Stegobium paniceum</i> and <i>Tribolium confusum</i>	116
Table VI: Effect of nanostructured alumina (NSA) on seed germination and radicle and shoot elongation of <i>Phaseolus vulgaris</i> seedling.	117

Table VII: Effects of nanostructured alumina (NSA) on plant of <i>Phaseolus vulgaris</i> in pot culture.	118
Table VIII: Effect of nanostructured alumina on spore germination of different fungi.	121
Table XI: Zone of inhibition by nanostructured alumina against different fungi	122
Table X: X-ray diffraction (XRD) analysis of the Al ₂ O ₃ NPs using extract of <i>Rhamnus alaternus</i>	125

TABLE OF CONTENTS

Fist Part: Biological Activities of medicinal plants. Literature review

CHAPITRE I	1
I. Introduction	1
I.1. Presentation of the medicinal plants studied	4
I.1.1. <i>Rhamnus alaternus</i>	4
I.1.1.1 Botanical description	4
I.1.1.2 Nomenclatures	4
I.1.1.3 Botanical classification	5
I.1.1.4. Therapeutic properties and uses	5
I.1.1.5. Chemical compositions of the Rhamnaceae	5
I.1.1.6. Main biological properties of secondary metabolites	6
I.1.2. <i>Phillyrea angustifolia</i> L.	6
I.1.2.1. Botanical description	7
I.1.2.2. Botanical classification	8
I.1.2.3 Therapeutic properties and uses	8
I.1.2.4. Chemical compositions from Phillyrea.....	8
I.1.2.5 Main biological properties of secondary metabolites	9
I.2. Natural antioxidants	9
I.2.1. Definition	9
I.2.2. The different types of antioxidants	10
I.2.3 Polyphenols.....	10
I.2.3.1 Classification of phenolic compounds	11
I.2.3.2. Simple phenol compounds	11
I.2.3.3. Complex phenolic compounds.....	12

I.3. Chemical properties of polyphenols	12
I.3.1 Nucleophilia	13
I.3.2 Reducing properties	13
I.3.3 Polarisability	13
I.3.4 Hydrogen bond	14
I.4-Oxidative Stress	14
I.4.1. Reactive Oxygen Species	14
I.5. Therapeutic properties of polyphenol and biological properties <i>In vitro</i>	16
I.5.1 Anti-inflammatory effects	16
I.5.2. Antidiabetic	17
I.5.3 Antimicrobial activity	18
 CHAPITRE II	
II. Material and methods	21
II.1.1. Harvesting	21
II.1.2. Drying	21
II.1.3. Crushing and Sieving	21
II.2.Optimization of extraction conditions	22
II.2.1 Experimental model	22
II.2.2. Application of the Box-Behnken (BB) plan	22
II.3. Extraction of phenolic compounds	23
II.3.1. Procedure	23
II.4. Determination of phenolic compounds	23
II.4.1.1. Principle	23
II.4.1.2. Method of operation	24
II.4.2. Determination of flavonoids	24
II.4.2.1. Principle	24

II.4.2.2. Operating procedure	24
II.4.3. Determination of condensed tannins	24
II.4.3.1. Principle.....	24
II.4.3.2. Operating procedure	25
II.5. Measurement of antioxidant activities	25
II.5.1. DPPH free radical scavenging test	25
II.5.1.1. Principle.....	25
II.5.1.2. Operating procedure	26
II.5.2. Reducing power.....	26
II.5.2.1 Principle.....	26
II.5.2.2. Procedure	26
II.5.3. Ammonium phosphomolybdate test.....	26
II.5.3.2. Procedure	26
II.5.3.1 Principle.....	26
II.5.3.2. Procedure	26
II.5.4 ABTS [•] radical scavenging.....	27
II.5.4.1 ABTS [•] radical scavenging Principle	27
II.5.4.2 ABTS [•] radical scavenging.....	27
II.5.5. No enzymatic superoxide radical scavenging	27
II.5.5.1. Principle.....	27
II.5.5.2. Procedure	27
II.6. Determination of antibacterial activities.....	28
II.6.1. Preparation of dry extracts.....	28
II.6.2. Culture medium used.....	28
II.6.3. Standardization of strains	28
II.6.4. Agar disc diffusion test.....	28
II.6.5. Micro-dilution method.....	28
II.7. Assessment <i>in vitro</i> of anti-inflammatory activities	29
II.7.1. Test of Inhibition BSA denaturation.	29
II.7.2. Test of antiproteinase action.....	29
II.7.3. Membrane stabilization by hypotonicity induced hemolysis.	30

II.7.4. Hypotonicity induced hemolysis	31
II.7.5. Cyto-toxicity assay	32
II.8. Enzyme Inhibitory Activity	32
II.8.1. α -Amylase inhibitory activity	32
II.8.2. α -Glucosidase activity	33
II.9. Liquid chromatography–mass spectrometry (LC–MS) characterization of Optimum extract of study plants	33

CHAPITRE III

III. Results and discussion	34
III.1. Response surface methodology (RSM) experimental designs	34
III.1.1. Extraction optimization of total polyphenol content for <i>Rhamnus alaternus</i>	34
III.1.2. Optimisation of the DPPH free radical scavenging effect	35
III.1.3. Optimization of multiple surface responses of <i>Rhamnus alaternus</i> extracts	37
III.2. <i>Phillyrea angustifolia</i>	38
III.2.1. Optimisation of the total polyphenol content of <i>P. angustifolia</i>	38
III.2.2. Optimisation of the DPPH free radical scavenging effect	40
III.2.3. Optimization of multi-surface responses of <i>P. angustifolia</i> extracts	41
III.3. Evaluation of antioxydants of extracts obtain under optimum condition	42
III.3.1. Flavonoid content	42
III.3.2. Condensed tannin contents	43
III.4. Antioxidant activities of the plant extracts studied under optimized condition	44
III.4.1. Reducing power	44
III.4.2. Ammonium phosphomolybdate test	45
III.4.3. ABTS [•] radical scavenging	46
III.4.4. No enzymatic superoxide radical scavenging	47
III.5. Determination of antibacterial activities	48
III.5.1. Sensitivity of the strains tested to antibiotics	48
III.5.2. Antibacterial activity of <i>P. angustifolia</i> and <i>R. alaternus</i> extracts	49

III.5.3. Micro-dilution method minimal (MIC)	51
III.6. Anti-inflammatory activities	51
III.6.1. Inhibition of BSA denaturation	53
III.6.2. Proteinase Inhibitory Action	54
III.6.3. Anti-hemolytic activity	55
III.7. Cyto-toxicity assay	55
III.8. Enzymatic activities	56
III.8.1. α -Amylase Inhibition	56
III.8.2. α -Glucosidase Inhibition	57
VI. Conclusion of the first part	59
V. References	62

Second Part: Synthesis of alumina nanostructured and biological activity. Literature review

CHAPITRE I

I.1. Generalities on Nanomaterials	77
I.1.1. Nano-objects	77
I.1.2. Nanostructured materials	78
I.2. Classification of Nanoparticles	79
I.2.1. Organic nanoparticles	79
I.2.2. Inorganic nanoparticles	79
I.2.3. Metal based	79
I.2.4. Metal oxides based.....	80
I.2.5. Carbon based.....	80
I.3. Some application of nanomaterials	80
I.3.1. Nanoparticles for direct application to humans	81

I.4. Synthesis of nanoparticles	82
I.5. Physical methods.....	83
I.5. 1. Evaporation/condensation.....	83
I.5. 2. Laser pyrolysis	83
I.5. 3. Aerosol method	84
I.6. Chemical methods.....	84
I.6.1. Sol-gel method	84
I.6.2. Liposome production	84
I.6.3. Solvo-thermal and hydro-thermal methods	85
I.7. Biological methods (Biosynthesis) of nanoparticules.....	85
I.7.1. Biological Synthesis of Nanoparticles by Microorganisms.....	85
I.7.1.1. Biological Synthesis of Nanoparticles by Bacteria.....	85
I.7.1.2. Biological Synthesis of Nanoparticles by Fungal	86
I.7.1.3. Biological Synthesis of Nanoparticles by Yeast	87
I.7.2. Biological Synthesis of Nanoparticles by plant	88
I.7.3. Biological Synthesis of Nanoparticles by marine algae	88
I.8. Generalities on Alumina (Al₂O₃)	90
I.8.1. Properties of Alumina (Al ₂ O ₃).....	90
I.8.1.1. Structure of Alumina (Al ₂ O ₃)	91
I.8.1.2. Electrical and chemical properties of Alumina (Al ₂ O ₃).....	92
I.8.2. Aluminium oxide nanoparticles	92
I.8.3. Synthesis of Aluminium oxide nanoparticles	95
I.8.3. 1. Alumina Sol-Gel	96
I.9. Some application of alumina nanoparticules.....	97
I.9.1. Antimicrobial activity of alumina oxide nanoparticles.....	97
I.9.2. Use of alumina nanoparticles in potential clinical applications.....	98
I.9.2. 1. In membranes	98
I.9.2. 1. Drug delivery	98
I.9.2. 2. Use of alumina nanoparticles as insecticide powder	98

I.9.2. 3. Use nanoparticles in plant growth and development	99
--	-----------

CHAPITRE II

II. Material and methods	102
II.1. Nanostructured alumina (NSA) preparation	102
II.2. Characterization of NSA	102
II.2.1. Scanning Electron Microscopy (SEM) with Energy Dispersive X-Ray Analysis (EDX) microanalysis	102
II.3. Insect rearing	103
II.4. Insecticidal activity of NSA	103
II.5. Effects of NSA on <i>P. Vulgaris</i>	104
II.5.1. <i>In vitro</i> tests	104
II.5.2. In pot tests	104
II.6. Antifungal assay	105
II.6.1. Test organisms	105
II.6.2. Spore germination assay	105
II.6.3. Agar well diffusion assay	106
II.7. Biosynthesis of alumina nanoarticles using <i>Rhamnus alaternus</i>	106
II.7. 1. Preparation of <i>Rhamnus alaternus</i> leaf extract.....	106
II.7. 2. Synthesis of the alumina nanoarticles (Al ₂ O ₃ -Nps) using <i>Rhamnus alaternus</i> leaf extract	106
II.7.3 Characterization of synthesis of the alumina nanoarticles (Al ₂ O ₃ -Nps) using <i>Rhamnus alaternus</i> leaf extract	107
II.8. Data analysis	107

CHAPITRE III

III. Results and discussions	108
---	------------

III.1. Nanostuctured alumina-gel characterization	108
III.1.1. X-Ray diffraction (XRD)	108
III.1.2. Fourier Transform InfraRed spectroscopy analysis(FT-IR).....	110
III.1.3. Energy Dispersive X-Ray (EDX) system coupled with Scanning Electron Microscopy (SEM)	112
III.1.3.1 . Nanostructured alumina stucture.....	112
III.1.3.2. Insecticidal effect of NSA	113
III.1.3.3. Effects of NSA on growth and germination of <i>P. Vulgaris</i>	117
III.1.3.4. SEM coupled with EDX of leaves <i>Pheseolus vulgaris</i> treated with Nanostructured alumina	119
III.1.4. Antifungal assay	121
III.1.4.1. Effect of different concentrations of nanostructured alumina on the spore germination of some fungal pathogens	121
III.1.4.2. Agar well diffusion assay	122
III.1.5. Biosynthesis alumina nanoparticules(Al_2O_3 NPs) using extract of <i>Rhamnus alaternus</i> .	123
 IV. Conclusion of the second part	128
V. Global Conclusion and outlook	129
 VI. References	130
VII. Annexes	142

Introduction

I. Introduction

The plants continue to be an important source of compounds for human health. This is mainly due to the fact they are a source of a huge variety of potential medicines, while being accessible to many people. Pharmacognosy and phytochemistry are the study of the physical, chemical, biochemical, and biological properties of drugs as well as the search for new drugs from natural sources (Silva et al., 2007; Tiwari et al., 2020, Martínez-Cruz and Paredes-López, 2014, Nagy et al., 2011). In Algeria, the population resorts to traditional medicine, using the plants medicinal products, of which there are an estimation of 3,000 species, 15% of those plants are endemic (Amadeo et al., 2020; Benkiki, 2006).

Our research is focused on the study of two medicinal plants growing wild in Algeria. the choice is carried on *Rhamnus alaternus* and *Phillyrea angustifolia* due to their use in traditional medicine and lack of information of these two species. This study is constantly evolving and being refined with the improvement of the instruments of investigation.

Phillyrea angustifolia belongs to Oleaceae family count about 600 species divided into 24 genres, growing mainly in Mediterranean regions, South Europe, North Africa, West Asia (Fernández et al., 2006). In Algeria, infusions prepared from the leaves and berry of *P. angustifolia* were used for their astringent and antiseptic properties, commonly used also as a poultice on injuries and sores (Hamel et al., 2018b). Concerning the chemical composition of *P. angustifolia*, few studies (Mebirouk-Boudechiche et al., 2015a; Romani et al., 1996a) have been done. This plant is characterized by the presence of large amounts of phenolic compounds (Romani et al., 1996b). Leaves are rich in flavonoids and oleuropein derivatives, carbohydrates, tannins (Gajić et al., 2020). Indeed (Lanza et al., 2001a) reported eight lignans derivatives (lignan epoxide, pinoresinol, pinoresinol-4-O-b-D-glucopyranoside, pinoresinol monomethyl ether-4-O-b-D-glucopyranoside, lariciresinol, lariciresinol-4-O-b-D-glucopyranoside, lariciresinol-4-O-b-D-glucopyranoside, syringaresinol monoglucopyranoside) in the Aerial parts of *P. angustifolia*. Diaz et al. (2000) have reported the presence of iridoids.

Rhamnus alaternus belong to Rhamnaceae family contains about 50 genus and 900 species that are native of the Mediterranean basin (in north Africa and Europe). *Rhamnus* species are known to be used in traditional medicine for the treatment of various diseases, besides, they have significant pharmacologic activities (Ammar et al., 2005a). The various phytochemical

studies carried out on species of the Rhamnaceae family have shown the presence of various quantities of anthraquinones, coumarins, tannins and in particular flavonoids (Ammar et al., 2008). Considering the interest of these plants that have been reported as good sources of bioactive compounds with promising health benefits including antioxidant, anti-inflammatory, antibacterial, antidiabetic and anti-hepato protectors (Ammar et al., 2008; Benchiha et al., 2015; Dommée, 1992; Hamel et al., 2018a; Janakat and Al-Merie, 2002).

In general, the obtaining of these compounds often requires numerous and time-consuming and costly steps such as extraction, isolation and identification (Dahmoune et al., 2013, (Bezerra et al., 2008) and often involves thermal degradation of the various bioactive constituents (Đorđević and Antov, 2017). As there are a few research works were conducted on these species, It is interesting to study their phyto-composition and antioxidant activities. For this purpose, we are interested in the extraction processes of bioactive compounds from plants growing wild in Algeria using response surface methodology (RSM) and the study of the different interactions between the experimental factors and responses obtained in order to optimize the extraction conditions and reducing the number of experiments.

In the first part of this thesis, we were interested in the optimization of the extraction effect on antioxydants capacity, phenolic content and DPPH radical scavenging assay, using the BOX-BENKEN plan with three levels. This design was used to evaluate the most significant parameters on extraction, and to find the optimal extraction conditions. In order to obtain the best conditions for the extraction of total polyphenols and antioxidant activity, three independent variables were chosen as relevant: ratio, green solvents percentage and extraction time. In addition, the metabolite profiling of the optimum extracts was studied for the first time for *P. angustifolia* by LC/MS. Given the lack of information, the present study constitutes attempt to elucidate the phenolic composition as well as test *In vitro* of antioxidant activities, activity anti diabetic, antimicrobial activities, anti-inflammatory and Cyto-toxicity assay using the optimal extract for *Phillyrea. angustifolia* and *Rhamnus alaternus*.

In the second part of this thesis, we were interested in the synthesis of nanoparticles and their applications in the biological field.

Nanotechnologies are based on the ability to manipulate material at the same time on the smallest possible scale, i.e. 10^{-9} m. The use of nanoparticles on a global scale is considerable and continues to grow, particularly in the field of the medical, environmental and industrial.

The use of nanoparticles makes it possible to create new classes of materials in the innovative properties. A great deal of work has been published on this subject over the last decade and nanoparticles are still attracting a great deal of interest in the economic, industrial medical and an alternative to improve the effectiveness of treatments in agriculture.

Crop protection represents a major challenge for the quality of the agricultural production and requires the use of pesticides, which is essential to reduce the number of crop pests, plant diseases, and the number of proliferation of weeds. Every year, crop pests and plant diseases destroy up to 40% of the world's harvests and these losses could be greater without the use of pesticides (Huang et al., 2018). However, the unreasonable use of pesticides has increased the capacity of insects to develop resistance mechanisms against insecticides.

The main objectives of the second part of this thesis was the synthesis of alumina nanostructured which could constitute an alternative effective in improving the efficiency of treatments in agriculture as an insecticide and anti-fungal against crop pest, also to estimate the toxicity of this material. We have studied the possibility of syntheses alumina nanoparticles using extracts from the leaves of *Rhamnus alaternus*, and characterisation of these nanoparticles by X-ray diffraction (XRD) and Scanning Electron Microscopy (SEM).

Fist Part

Chapter I

Literature review

Approximately 35,000 plant species are used worldwide for medicinal purposes, forming the largest range of biodiversity used by humans (Grenez, 2019). In Algeria, the Flora is characterized by their diversity : Mediterranean flora, Saharan flora and a Paleo Tropical flora belonging to several botanical families (Amirouche and Misset, 2009). From 3,000 species growing wild in Algeria, 15% of those plants are endemic (Amadeo et al., 2020; Benkiki, 2006).

The extractions of high added value active ingredients from plant material, especially the case of secondary metabolites, which are currently attracting a lot of interest due to their antioxidant power, is a very important step in the isolation as well as in the identification of bioactive compounds such as antioxidants, vitamins and minerals, are produced by different plant species. Their antioxidant properties and possible uses in different industries have been studied over the last few years. Different extraction methods for natural substances are known, such as maceration, solvent extraction, ultrasound-assisted extraction, microwave-assisted extraction and supercritical fluid extraction (SFE) (Bezerra et al., 2020).

I.1. Presentation of the medicinal plants studied

I.1.1. *Rhamnus alaternus*

I.1.1.1 Botanical description

Rhamnacees are a cosmopolitan family, shrubs and herbaceous plants with shiny, ovoid or lanceolate, alternate, smooth, petiolate leaves (3 to 6 cm long by 2 to 3 cm wide), with cartilaginous and toothed edges. The leaves remain on the tree for about two years. They are tough, thick midrib, trinulate at the base; linear stipules, deciduous, axillary clusters longer than the petiole. The stem is erect and stalked, and the twigs are alternate, not spiny. It is a multifloral species, with dioecious greenish flowers, arranged in dense, tetra-pentamerous, zero petals, and very small clusters. The seedless fruit is a drupe with 2 or 3 external furrows, red then black, with 4 stones. It is found almost everywhere, in brush and hedges containing about 50 genera and 900 species. In Algeria, 9 plant species belonging to 3 genera have been recorded in various regions and classified according to their morphological characteristics (Fromont, 1997; Hauenschild et al., 2016).

I.1.1.2 Nomenclatures

The name *Rhamnus* is a Greek word *Rhamnos*, the ancient Latin name of the plant is alaternus. Several names are attributed.

Arabe : M'lila, Oud el khir ou bien Safir

Kabyle : Mélilés.

French: Nerprun.

English :Boucktrun.

Latin : *Rhamnus alaternus*.

I.1.1.3 Botanical classification

The botanical classification of *Rhamnus alaternus* is given as follows:

Reign: Plantae-vegetal

Class: Magnoliopsida-dicotyledones

Subclass: Rhosidae

Super order: Rhamnanae

Order: Rhamnales

Family: Rhamnaceae

Genre: *Rhamnus*

Species: *Rhamnus alaternus*

I.1.1.4. Therapeutic properties and uses

Rhamnus alaternus is used in traditional medicine as a laxative, purgative, diuretic, antihypertensive, depurative, hypotensive and for the treatment of diabetes, The decoction of the aerial parts of *R. alaternus* as the bark is used in the treatment of dermatological and hepatic ailments(Ammar et al., 2005b; Ammar et al., 2008).

The stems and leaves of *R. alaternus* are used in Algeria against jaundice and liver disorders.

In Morocco, *R. alaternus* is used in decoction to treat various liver infections.

The fruits of *R. alaternus* contain an active ingredient

I.1.1.5. Chemical compositions of the Rhamnaceae

The various phytochemical studies carried out on species of the Rhamnaceae family have shown the presence of varied quantities of anthraquinones, coumarins, tannins and in particular flavonoids (Ammar et al., 2008).

Three tri-glycosidic flavonoids were isolated from the leaves of *R. alaternus*, Kaempferol 3-O- β -isorhamninoside, rhamnocitrin 3-O- β -isorhamninoside and rhamnetin-3-O- β -

isorhamninoside, on the other hand, three aglyconic flavonoids were identified: apigenin, kaempferol and quercetin.(Ammar et al., 2009).

Ben Ammar et al. (2019) report in their studies the isolation of three new anthraquinone glycosides isolated from extracts of leaves and roots of *R. alaternus*, namely alaternosides A-C (1,4,6,8 tetrahydroxy-3-methyl anthraquinone 1-O- β -D-glucopyranosyl-4,6-di-O- α -L-rhamnopyranoside; 1,2,6,8 3-tetrahydroxy-3-methyl anthraquinone 8-O- β -D-glucopyranoside and 1,6 dihydroxy-3-methyl-6 [2'-Me (heptoxy)] anthraquinone were isolated and elucidated together with the two anthraquinone glycosides, Physcion-8-O-rutinoside and emodin 6-O- α -L-rhamnoside as well as with the known kaempferol 7-methyl ether, β -sitosterol and β -sitosterol-3-O-glycoside.

I.1.1.6. Main biological properties of secondary metabolites

Phenolic compounds class presents a large set of substances with quite variable structural elements. These important structural differences are responsible for the diverse biological properties, the following activities are cited;

- ✚ The anti-inflammatory activities of the isolated flavonoids, quercetin 3-O-methyl ether, kaempferol, and quercetin, from *Rhamnus nakaharai*, and anthraquinone, frangulin B, from *Rhamnus formosana*, inhibit the enzymes involved in the inflammatory process (the chemical mediators released by mast cells, neutrophils, macrophages and microglial cells), quercetin 3-O-methyl ether inhibits the release of β -glucuronidase and lysozyme from neutrophils, also inhibits the formation of superoxide anions in fMLP/CB or neutrophils and thus has a strong inhibitory effect on the formation of tumor necrosis factor A (TNF- α) in lipopolysaccharides (LPS).(Wei et al., 2001) .
- ✚ Kaempferol 3-O- β -isorhamninoside (K_3O -ir) and rhamnocitrin 3-O- β -isorhamninoside (R_3O -ir), isolated from *R. alaternus* have genotoxic and antigenotoxic properties exhibited one against H_2O_2 -induced DNA damage in human TK6 lymphoblastoid cells and its derivative, the deficient cell line p53 NH₃(Ammar et al., 2007). These two flavonoids, also studied for their antioxidant capacities, using different antioxidant tests, such as: Cuprac, Frap and Reduction revealed an important activity due to their capacity to transfer electrons (Ammar et al., 2007).
- ✚ Phenolic compounds are formidable antioxidant agents, this activity translates *In-vivo* by inhibiting the formation of peroxide derivatives responsible for oxidative stress explains their beneficial effects as hepato-protectors (Abdelkrim et al., 2015; Ammar et al., 2007; Benchiha et al., 2015) .

- ✚ Total oligomeric flavonoids of *R. alaternus* induce apoptotic death of human cell line K56 (myelogenous leukemia). Thus the reduction of oxidative stress and protection of lipid peroxidation (Ammar et al., 2011).
- ✚ Anthraquinone is considered a source of natural antioxidants and has the potential for anti-acetylcholinesterase activity (Benamar et al., 2019b).
- ✚ The remarkable cytotoxicity of kaempferol and rhamnocitrin glycoside derivatives (Boussahel et al., 2015; Chen et al., 2016).
- ✚ Recent studies have shown that the anticancer effects of *Rhamnus frangula* extract has apoptotic effect on breast cancer cells, this activity is due to the richness of the plant in anthraquinones mainly aloe-emodine (1,8-dihydroxy-3-hydroxyl-methylanthraquinone; AE) and emodine (1,3,8-trihydroxy-6-methylanthraquinone; EM). (Vahid Shahani1, 2019).
- ✚ Anthraquinones also have bacterial activity against some bacteria in the Gram+ and Gram- group (Kosalec et al., 2013b).
- ✚ The extract of *Rhamnus alaternus* has enzymatic inhibitory properties such as α -glucosidase, tyrosinase, acetylcholinesterase (AChE), and butyrylcholinesterase (BChE). On the basis of correlation coefficients calculated separately for all pairs of experimental parameters, tyrosols are highly correlated with BChE activity (Rocchetti et al., 2019).

I.1.2. *Phillyrea angustifolia* L.

The genus *Phillyrea* from Oleaceae family includes two species: *Phillyrea angustifolia* and *Phillyrea latifolia* L. (Gucci et al., 1997; Lucchesini and Mensuali-Sodi, 2004) Before twenty years, this genus was cited very rarely in ethnobotanical literature (Pieroni et al., 2000b) It is used in the historical medicine of the Mediterranean region for its oropharyngeal anti-inflammatory effect its fruits were probably in the past harvested and eaten as wild olives (Pieroni et al., 2000b).

P. angustifolia L. is a wind-pollinated shrub and one of the handful of species reported to be androecium. It is a native Mediterranean species, which has recently been considered to be suitable for landscaping purposes (DellaGreca et al., 2011).

I.1.2.1. Botanical description

P. angustifolia is an evergreen shrub that can reach 4m high. It is a dense, branched bush form containing many buds. Leaves are linear-lanceolate or lanceolate-sharp, opposite,

leathery, with 4-6 pairs of veins. Males have a greater number of twigs and have better vegetative growth and longer life span than hermaphrodites.

Flowers are yellowish-white or greenish-white in color, close together in small clusters that are placed in the leaf axils, blooming in April and May. The fruit of *P. angustifolia* is fleshy, glaucous, blackish, with a small point at the top, with pea-sized stones, ripening in August and September (ASSILIADIS, 1999).

I.1.2.2. Botanical classification

The botanical classification of *Phillyrea angustifolia* is given as follows:

Kingdom: Plantae

Under the reign of: Tracheobionta

Superdivision: Semaphores

Division: Magnoliophyta

Class: Magnoliopsida

Subclass: Asteridae

Order: Scrophularian

Family: Oleaceae

Genre: Phillyrea

Species : *Phillyrea angustifolia* (Dommée, 1992).

I.1.2.3 Therapeutic properties and uses

P. angustifolia is used in traditional medicine against intermittent fevers. The flowers are used to make poultices recommended against headaches. The leaves were used as emmenagogue and in gargle. Moreover, the leaves and fruit of this plant were recommended as a febrifuge against intermittent fevers. Thus they were used for their astringent and antiseptic properties (Hamel et al., 2018a).

I.1.2.4. Chemical compositions from *Phillyrea*

The leaves of *P. angustifolia* are rich in flavonoids and oleuropein derivatives. The soluble carbohydrate composition of phillyrea leaves does not differ significantly from that of *Olea europaea* L. leaves, except for a higher mannitol/glucose ratio (Romani et al., 1996a). Among the isolated flavonoid structures, apigenin-7-O-glucoside, apigenin-7-O-rutinoside, luteolin-4%-O-glucoside, luteolin-7-O-glucoside and ligustroflavone showed remarkable activity (Pieroni et al., 2000a).

A study carried out by DellaGreca et al. (2011) on lignans isolated from the whole plant of *P. angustifolia* L. were able to identify a new lignan epoxide and seven known lignans: pinoresinol, pinoresinol-O-b-D-glucopyranoside, pinoresinol monomethyl ether-O-b-D-glucopyranoside, lariciresinol, lariciresinol-4-Ob-D-glucopyranoside, lariciresinol-40-O-b-D-glucopyranoside, and syringaresinol monoglucopyranoside.

The leaves of *Phillyrea latifolia* present mainly the oleuropein compound and minor compounds: ligustroside, secologanoside, secoxyloganin, 8-epikingisic acid (Damtoft et al., 1993).

The leaves of *P. angustifolia* analyzed by phytochemical tests revealing the presence of hydrolyzable tannins as well as saponis (Mebirouk-Boudechiche et al., 2015a).

I.1.2.5 Main biological properties of secondary metabolites

The leaves of *Phillyrea latifolia* L. (Oleaceae) were tested for their anti-inflammatory activities *In vitro*. Three phenylpropanoid glycosides (salidroside, syringin and coniferin) and one lignan (phillyrine) were isolated from the leaves. These compounds are capable of exerting inhibitory actions on the enzymes of the arachidonate cascade (Lanza et al., 2001b).

- ✚ Tannin-rich extracts of *P. latifolia* have anthelmintic activity that inhibits the exudation of gastrointestinal nematode larvae (Azaizeh et al., 2013).
- ✚ *Phillyrea* leaves used for weight loss by modifying certain biochemical parameters. The bioactive molecules luteolin 7-O-glucoside and chlorogenic acid, Luteolin and the 7-O-glucoside compound isolated may have a role in fat metabolism.(Yazici-Tutunis et al., 2016).
- ✚ *Phillyrea* extracts have antioxidant, superoxide dismutase (SOD) and peroxidase (POX) activity(Caravaca et al., 2005).
- ✚ Recent studies have shown the hepatoprotective effect of phillyrea extract would be effective in the treatment of jaundice, however both bilirubin level and alkaline phosphatase (ALP) activity were reduced when treated with aqueous extract of *Phillyrea latifolia* without reducing the activity of alanine aminotransferase (ALT) and aspartate aminotransferase (AST) (Janakat and Al-Merie, 2002).

I.2. Natural antioxidants

I.2.1. Definition

An antioxidant is a molecule that can inhibit or even delay the phenomenon of oxidation, hence the term "oxidizable substrate" includes any type of molecule *In vivo*, the presence of

an antioxidant at a very low concentration in the medium compared to those of an oxidizable substrate that does not significantly delay or prevent the oxidation of the substrate (Halliwell, 1995).

Among the most important mechanisms in which antioxidants intervene is the interruption of oxidation reactions and by definition oxidation is part of a redox reaction that transfers electrons from a substance to an oxidizing agent. This reaction can produce free radicals that leads to destructive chain reactions. Antioxidants are able to stop these chain reactions by oxidizing with the free radicals and thereby inhibiting their action. These properties can be found in the thiol and phenol families(Cornelli, 2009).

Although oxidation reactions are necessary for life, they can also be destructive: plants and animals use and produce many antioxidants to protect themselves, such as glutathione, vitamin C and vitamin E, or enzymes such as catalase, superoxide dismutase and certain peroxidases. A deficiency or lack of production of antioxidant enzymes leads to oxidative stress that can damage or destroy cells (huang et al., 2005).

I.2.2. The different types of antioxidants

Cellular antioxidants build a sophisticated defense system against radical aggression. They are characterized by a mechanism of action which can be direct as in the case of enzymatic and non-enzymatic antioxidants or indirect as part of the structure of enzymes and/or cofactors of antioxidant enzymes. (halliwell, 1990).

In this work, we are interested in exogenous non-enzymatic antioxidants and more specifically in polyphenols.

I.2.3 polyphenols

Numerous epidemiological studies and *In vivo* experiments carried out on animals reveal that the polyphenols present in certain fruits and vegetables have antioxidant properties and exert anti-inflammatory, anticarcinogenic, antibacterial, anti-mutagenic, antiviral, anti-tumoral effects and can also protect against degenerative diseases, their biological activities are attributed to chemical structures.(Ali Asgar, 2012). The polyphenol studied in our work comes from medicinal plants.

Polyphenols are also called phenolic compounds, they are secondary metabolites of plants, containing one or more hydroxyl groups, modified or not, attached to an aromatic structure, the association of aromatic rings and hydroxyl functions (OH) gives them a particular reactivity, due to the presence of conjugated double bonds (Balasundram et al., 2006). This

structure favours departures and captures of hydrogen atoms giving these molecules antioxidant properties (Vermerris and Nicholson, 2007). Phenolic compounds are derived from the pentose phosphate, or shikimate, or phenylpropanoid pathway.

I.2.3.1 Classification of phenolic compounds

Phenolic compounds can be grouped into numerous classes which differ firstly by the complexity of the basic skeleton (ranging from a simple C₆ to highly polymerised forms), secondly by the degree of modification of this skeleton (degree of oxidation, hydroxylation, methylation, etc.), and finally by the possible links of these basic molecules with other molecules (carbohydrates, lipids, proteins, other secondary metabolites which may or may not be phenolic compounds, etc.) (Vermerris and Nicholson, 2008).

I.2.3.2. Simple phenol compounds

The simplest phenolic forms have chemical structures ranging from simple C₆ phenol to C₁₅ flavonoids. (Macheix et al., 2005).

a) Acids phenolic

They consist of two groups, hydroxybenzoic acids and hydroxycinnamic acids. (Macheix et al., 2005).

Hydroxybenzoic acids

Hydroxybenzoic acids (p-hydroxybenzoic, protocatechic, vanillic, gallic, syringic, salicylic, gentisic...) are derived from benzoic acid and have a basic formula of C₆-C₁ type. They frequently exist in the form of esters or glucosides and can also be integrated into complex structures such as certain tannins (Macheix et al., 2005).

Hydroxycinnamic acids

Hydroxycinnamic acids are a very important class with the structure base (C₆-C₃) derived from that of cinnamic acid. The basic molecules of the hydroxycinnamic acids are p-coumaric acid (and its isomers, o- and m-coumaric acids), caffeic acid, ferulic acid and its 5-hydroxy derivative and finally sinapic acid. The whole is often reported under the common vocabulary of phenylpropanoids. (Macheix et al., 2005).

b) Flavonoides

Flavonoids are phenolic pigments that are responsible for most of the colouring of flowers and fruits. They are defined by the nature of their carbon skeleton which comprises 15 carbon atoms distributed according to the C₆-C₃-C₆ sequence common to all flavonoids and in which two benzene rings A and B are connected by an element with 3 carbon atoms. The

attachment of the ring B and the substitution on either of the 3 carbon atoms of the intermediate chain(Ribéreau-Gayon, 1968).

Balasundram et al. (2006) report that the major classes of flavonoids are flavonols, flavones, flavanones, flavanols (or catechins), isoflavones and anthocyanidins. This classification takes into account the number and position of oxidation in the central nucleus.

I.2.3.3. Complex phenolic compounds

I.2.3.3. 1. Tannins

Tannins are phenolic compounds capable of precipitating alkaloids, gelatin and other proteins, and are present in plant tissues in the form of polymers. They are responsible for the astringency of many fruits and vegetables and products derived from them (wine, tea, beer...). According to their chemical reactivity and composition, tannins are subdivided into two groups: hydrolysable tannins and condensed tannins (Haslam, 1989; Macheix et al., 2005).

a) Tannins hydrolysables

They are derived from the binding of a carbohydrate moiety and a phenolic moiety (gallic acid or ellagic acid) and formation of an ester-like bond. These compounds can be found in all plant organs: roots, stems, leaves, fruit before maturity, they can be degraded by chemical or enzymatic hydrolysis(Guignard, 2000).

b) Condensed tannins (proanthocyanidins)

Condensed tannins are oligomers or polymers of flavan-3-ols derived from (+)-catechin or its numerous isomers. Unlike hydrolysable tannins, they are resistant to hydrolysis and can only be degraded by strong chemical attacks. Thus, by hot acid treatment, they are transformed into red pigments (Haslam, 1989).

I.2.3.3. 2. Lignines

These high-molecular weight compounds contribute to the formation, together with cellulose and hemicellulosic derivatives, the lining of plant cells. They're polymers resulting from the condensation (copolymerisation) of three alcohols phenylpropenes

I.3. Chemical properties of polyphenols

The chemical properties of polyphenols are essentially related to those of the Phenolic nuclei, especially substituents with a mesomeric electron-withdrawing effect (-M) and substituents with a mesomeric donor effect (+M). The conjugation of one of the two pairs free from the oxygen atom with the ring reflects the (+M) effect of the OH group. This phenomenon

increases electronic delocalization and produces a partial negative charge on the atoms C2, C4, C6(Nkhili, 2009).

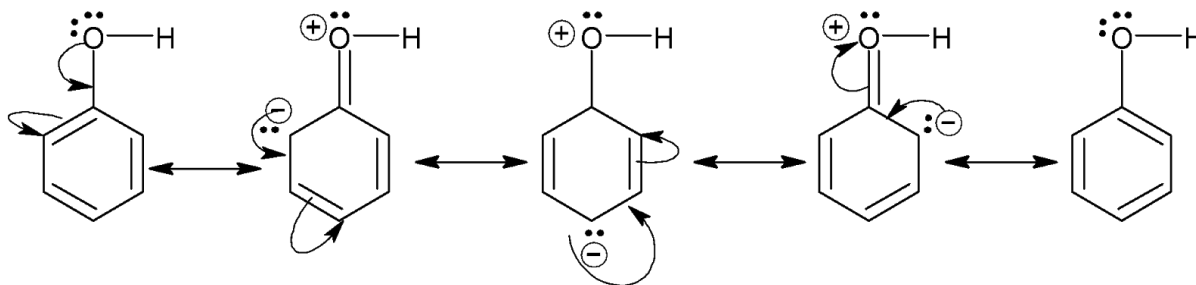


Figure 1. Mesomeric forms of phenol

From these basic characteristics the following different physico-chemical properties are derived:

I.3.1 Nucleophilia

This property is at the origin of the reactions of aromatic electrophilic substituents (alkylation, acylation, etc.) regioselective of the ortho and para positions. The 1,3-dihydroxy (resorcinol) and 1,3,5-trihydroxy (phloroglucinol) type substituents allow an accumulation of electron density on the C2, C4 and C6 summits (all ortho or para of the OH groups), thus accentuating the nucleophilic character.

The flavanols ring has two C6 and C8 centres which are highly nucleophilic because they are ortho and para to three OH or OR groups with (+M) effect. The A ring is also activated by the saturated C4(Nkhili, 2009).

I.3.2 Reducing properties

The ionization potential (IP) of a molecule is the minimum energy that must be supplied to the molecule in order to remove an electron from it. The more an aromatic compound is substituted with electron-donating groups, the lower its PI is and the greater it's reducing character. It can then undergo mono-electron oxidation which leads to the corresponding radical(Nkhili, 2009).

I.3.3 Polarisability

The polarisability of phenols allows them to develop strong molecular dispersion interactions (the attractive component of Vander Waals interactions) with other polarisable compounds. This phenomenon results from the coupling between the electronic fluctuations of two neighbouring molecules. Thus, in aqueous solution, the interaction of the apolar benzene ring

of the phenol with another polarizable entity such as a second aromatic ring is favored by the hydrophobic effect(Nkhili, 2009).

I.3.4 Hydrogen bond

Phenols are hydrogen bond (H bond) donors due to the acidic nature of the proton of the OH group. They are also H-bond acceptors. In fact, only the free pair of the O atom that is not conjugated with the ring is capable of accepting an H-bond from a donor. Thus, a phenol is capable of giving an H bond and receiving only one. Note that these H bonds are mutually reinforcing (cooperativity). For example, by giving an H bond, the phenol lengthens its OH bond. This state of predissociation accentuates the electron density on the O centre and thus its H-bond acceptor character(Nkhili, 2009)

I.4-Oxidative Stress

I.4.1. Reactive Oxygen Species

Under physiological conditions, oxygen, an essential element for life, produces reactive oxygen species (ROS) in the mitochondria, which are particularly toxic to cell integrity. These ROS, which include free radicals, have oxidizing properties that cause them to react, in the environment where they are produced, with a whole range of biological substrates (lipids, proteins, DNA, glucose, etc.). Long considered to be toxic agents responsible for cell dysfunction and death, it is currently accepted that ROS are true secondary messengers involved in the expression and regulation of cell proliferation and death functions. In addition, they are inflammatory mediators involved in various neurodegenerative or vascular pathologies such as atherosclerosis or hypertension(Bravo and Anaconda, 2001) (Labieniec and Gabryelak, 2006)

Cells generate various types of ROS with different reactivity(Labieniec and Gabryelak, 2006; Puppo, 1992)

- The superoxide ion $O_2^{\cdot -}$ and hydrogen peroxide H_2O_2 represent a class that is not very active. $O_2^{\cdot -}$ can capture an H^+ to give HO_2^{\cdot} (pKa) which would be the reactive form of $O_2^{\cdot -}$ capable of initiating lipid peroxidation. $O_2^{\cdot -}$ can dismutate into H_2O_2 and O_2 (spontaneous or superoxide dismutase catalyzed reaction), react with NO^{\cdot} to form the peroxynitrite anion $ONOO^{\cdot -}$, a strong oxidant, or reduce transition metal ions. $O_2^{\cdot -}$ is produced in particular by monoelectronic reduction of O_2 in the mitochondria, by NADPH oxidase, an enzyme of the macrophages which participates in the destruction of viruses and bacteria, or by xanthine oxidase, an enzyme of the purine metabolism(Sakihama et al., 2002).

- The hydroxyl radical HO^\bullet is one of the most oxidizing chemical species and can attack most biological molecules very quickly. HO^\bullet is produced by monoelectronic reduction of H_2O_2 by low-valent metal ions such as Fe_2^+ or Cu^+ , free or complexed (heme) (Fenton reaction).
- The singlet oxygen $^1\text{O}_2$ can be generated by excitation of $^3\text{O}_2$ in the presence of photosensitizers but also by chemical processes (e.g. reaction of H_2O_2 with ClO^-). $^1\text{O}_2$ is highly reactive and can, for example, add rapidly to carbon-carbon double bonds. The different processes of free radical formation are shown in Figure 2.

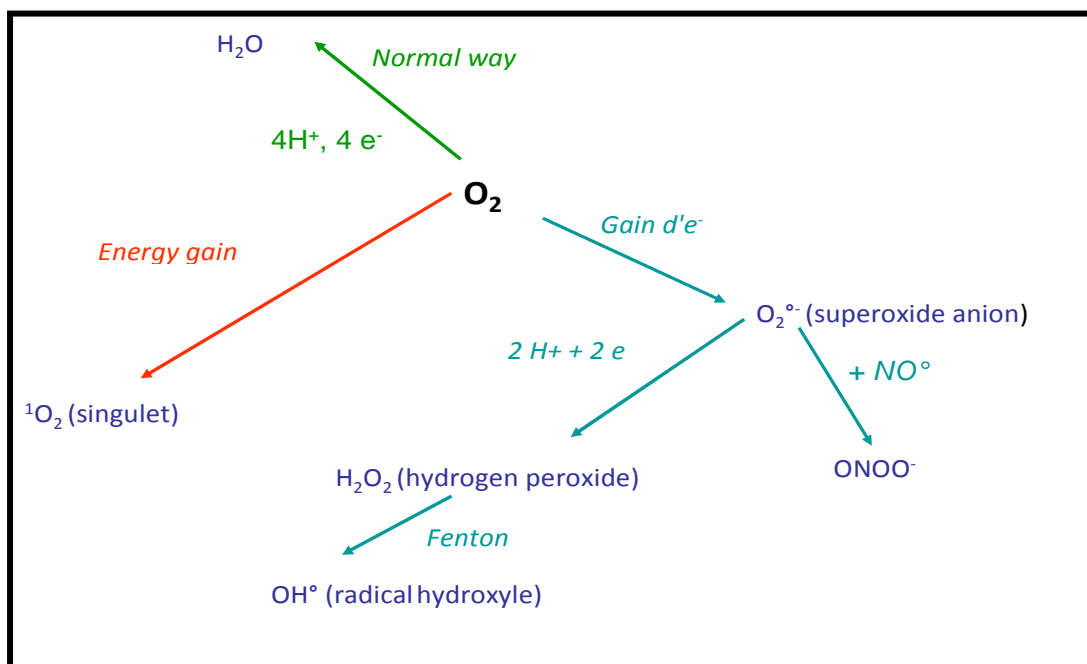


Figure 2. Formation of Activated Oxygen Species (AOS)

EORs are also generated as a result of environmental oxidants. Indeed, pollution (e.g. nitrogen oxides), absorption of alcohol or certain medications (e.g. catecholamines), prolonged exposure to the sun and smoking are all situations that cause an overproduction of EOR in our bodies, which can overwhelm our natural antioxidant defenses (superoxide dismutase, catalase, glutathione peroxidase and other antioxidant enzymes), thus causing cellular damage. This is oxidative stress. In addition, the current diet is not rich enough in vegetable products (fruit, vegetables and derived products) which provide us with a wide variety of antioxidants (polyphenols, carotenoids, vitamins C and E...) that can act as a complement to our natural defences. Oxidative stress can be of accidental origin such as inflammation, exposure to radiation and pro-oxidant xenobiotics, or genetic (deficiency in the expression of antioxidant defence enzymes). In general, oxidative stress is defined as the result of an

imbalance between the balance of pro-oxidants and defence systems (antioxidants), with the result that often irreversible damage to the cell occurs. Chronic exposure to oxidative stress can promote the development of cancer and cardiovascular disease(Halliwell, 1994)

I.5. Therapeutic properties of polyphenol and biological activities studied *In vitro*

The biological properties of polyphenols are essentially established *In vitro* and derive from their reducing activity (anti- or even pro-oxidant effects) and their affinity for a wide variety of proteins (enzymes, receptors, transcription factors)(Stevenson and Hurst, 2007).

One of the first recognized properties of flavonoids is "veno-active", i.e. they have the capacity to reduce the permeability of blood capillaries and to reinforce their resistance.

Nowadays, the properties of polyphenols are widely studied in the medical field where they are recognized for their anti-viral, anti- bacterial, anti-tumor, anti-inflammatory, anti-allergic and anti-cancer activities. They also have positive actions on obesity, diabetes, Alzheimer's and Parkinson's diseases(Dangles and Dufour, 2008).

The biological activities of polyphenols have often been evaluated *In vitro* with purified proteins, cell extracts and whole cells in culture. The biological properties of the conjugated metabolites mainly present in blood and tissues have, on the other hand, been little studied due to the lack of commercial standards.

The significance of these biological effects in the field of human nutrition is still far from being established, especially since they almost always involve native forms or aglycones of polyphenols and not circulating conjugated forms. To make progress-in the *In vivo* demonstration of the health effects of polyphenols, a better understanding of the bioavailability of polyphenols (their fate after possible absorption through the intestinal wall) and a combination of relevant clinical studies is essential. The recent development of new tools and methods could lead to important advances in the coming years. This is particularly the case with nutrigenomics, which aims to identify genes whose expression is regulated (upwards or downwards) by food components. The difficulty then lies in the analysis and interpretation of these complex biological data(Nkhili, 2009).

I.5.1 Anti-inflammatory effects

Non-steroidal anti-inflammatory drugs (NSAIDs) are molecules with a very similar mode of action. They act by blocking the action of cyclooxygenase (COX), a protein involved in a cascade of reactions leading to the formation of prostaglandins involved in inflammation (redness, pain, etc.), fever, aggregation of blood platelets (at low doses only), and protection

of the stomach lining. COX exists in two forms, each with its own specificity: COX-1 is more involved in platelet aggregation and the stomach, while COX-2 is specific for inflammation and fever. They are called "non-steroidal" because their mode of action does not involve corticoids, the important hormones synthesised by the adrenal glands located at the upper pole of each kidney.

Under the action of cyclooxygenase and lipoxygenase, arachidonic acid is metabolized respectively into prostaglandins and leukotrienes thus inducing inflammatory phenomena. A study by Hong et al. (2001) and his group showed that certain polyphenols are capable of modifying the metabolism of arachidonic acid in platelets. The effects of quercetin and myricetin are dose-dependent. At high concentrations, they inhibit cyclooxygenase and lipoxygenase. However, at low concentrations, only lipoxygenase is affected. On the other hand, other flavonoids such as apigenin and chrysin act mainly on the activity of cyclooxygenase.

The phagocytosis that accompanies a viral or bacterial infection is followed by the production of reactive oxygen species by neutrophils, which will promote inflammation. Generally speaking, radical species, whatever their origin, can induce tissue damage, promote the aging process, and even cause certain pathologies such as cancer and atherosclerosis. It is interesting to note that many flavonoids are capable of countering this production of oxygen species by neutrophils (Limasset et al., 1993).

I.5.2. Antidiabetic

Diabetes is a chronic disease defined as a metabolic condition that occurs when the metabolic condition that occurs when the pancreas no longer produces enough insulin or the body does not use the insulin it does produce properly: the secretory and abnormalities in the action of insulin on the target tissues (muscle and adipose tissue) (muscle and adipose tissue) may be associated. Insulin is a hormone that regulates the concentration of sugar in the blood, its action is hypoglycaemic and in diabetes during diabetes, chronic hyperglycaemia sets in which will lead over time to serious the time to a serious damage of many organic systems and more particularly of the nerves and nerves and blood vessels, leading to the clinical complications of diabetes. clinical complications of diabetes

Simple phenolic acids have been shown to increase glucose uptake and glycogen synthesis, improve glucose and lipid profiles of certain diseases (obesity, cardiovascular diseases, DM, and its complication)(Vinayagam et al., 2016).

Flavonoids can also prevent the development of diabetes by inhibiting the enzyme aldose reductase. Ong and Khoo(2000) reported that myricetin has an effect hypoglycemic in

diabetic animals. The antioxidant activity of hydroxytyrosol protects pancreatic cells from damage and death. Treatment with resveratrol significantly decreases the level of glucosylated hemoglobin(Ahangarpour et al., 2019).

I.5.3 Antimicrobial activity

The antibacterial activity of catechins, considering flavan-3-ols, it was demonstrated that inhibited *In vitro* growth of several bacterial species, such as *Vibrio cholerae*, *Streptococcus mutans*, *Campilobacter jejuni*, *Clostridium perfringes*, and *Escherichia coli*(Borris, 1996).

Flavonols showed a remarkable activity against several Gram-positive bacteria, such as *Staphylococcus aureus*, *Lactobacillus acidophilus*, and *Actinomyces naeslundii* and Gram-negative bacteria, such as *Prevotella oralis*, *Prevotella melaninogenica*, *Porphyromonas gingivalis*, and *Fusobacterium nucleatum*(Cushnie et al., 2007).

More recently, it was demonstrated that some catechins, such as gallocatechin-3-gallate, epigallocatechin-3-gallate, catechin-3-gallate, and epicatechin-3-gallate, are active against some other food-borne pathogenic bacteria, such as *Bacillus cereus*. Most of these compounds were found to be more active than antibiotics, such as tetracycline or vancomycin, at comparable concentrations: this suggested that the tested catechins could exert a positive effect against gastrointestinal diseases(Friedman et al., 2006).

Recent investigations also pointed out the fungicidal activity of flavonols. It was shown that various types of bacterial and fungal dermatitis, had antifungal activity (*against Microsporum gypseum*, *Trichophyton mentagrophytes*, and *Trichophyton rubrum*), and the main responsible agents for this activity were identified as flavonols (galangin, izalpinin, and rhamoncitrin) (Agüero et al., 2010).

Besides antibacterial activity, proanthocyanidins showed antiviral effects against influenza A virus and type-1 herpes simplex virus (HSV). In this case the mechanism of action seems to consist in preventing the entry of the virus into the host cell, which is the first critical step in primary HSV-1 infection (Gescher et al., 2011).

The antimicrobial activity of hydrolysable tannins is well known. Ellagitannins show very interesting properties because they inhibit the growth of selected Gram negative intestinal bacteria (strains of *Salmonella*, *Staphylococcus*, *Helicobacter*, *E. coli*, *Clostridium*, *Campylobacter*, and *Bacillus*) (Puupponen-Pimiä et al., 2001).

Fist Part

Chapter II

Material and methods

II. Material and methods

In our study, we were interested on two Algerian plants namely *Rhamnus alaternus* and *Phillyrea angustifolia* which belong to the Rhamnaceae family and the Oleaceae, respectively.

II.1.1 Harvesting

The leaves of *Rhamnus alaternus* and *Phillyrea angustifolia* were collected in the region of Tighzert (Bejaia) (32 km from the west coast) during the flowering period in March 2019. The ecological characteristics of the harvest site of the two plants are grouped in the **Table I** below.

Table I: Ecological characteristics of the place where the plants are harvested.

Location Bioclimatic	Species	Latitude	longitude	Zone
Tighzert(Bejaia)	<i>P.angustifolia</i>	N36° 51' 01.05	E4° 52' 59.9330	Mediterranean
Tighzert(Bejaia)	<i>R.alaternus</i>	N36° 51' 01.05	E4° 52' 59.9330	Mediterranean

The site of the harvest is in mountainous wooded area, away from all sources of pollution. The choice of plant material used in our study is mainly based on:

- The abundance of the two species *P. angustifolia* and *R. alaternus* in the Bejaia region;
- Use in traditional medicine in Algeria.

II.1.2 Drying

After removing the stems and getting rid of the weeds, the leaves of the two harvested plants were dusted and rinsed with distilled water, then dried in an oven (WTC binder, Germany) at 40°C for 3 days.

The interest of drying is to reduce the humidity which favors the microbial fermentation of foliage and the development of moulds. Thus it prevents the action of polyphenol oxidases and glycosidases which degrade the phenolic compounds.

II.1.3 Crushing and Sieving

The dried plant material was shredded by an electric shredder (Severin Elektogerate GmbH, Germany) and then sieved using a 250 µm opening diameter sieve. The resulting powder is stored in labelled and closed glass bottles to protect the powder from moisture and mould attack.

II.2.Optimization of extraction conditions

II.2.1 Experimental model

In order to optimize the optimal extraction conditions of the phenolic compound content and the antioxidant activity of the extracts four two plants studied; 15-test experimental design with three central points was carried out using StatgraphicsCenturion XVI software (Statpoint Technologies, USA). Three independent variables the extraction time (30, 75, 120 min), the solvent concentration (percentage of ethanol) (%EtOH) (0, 50, 100%) and the ratio (mass of the powder in grams used in a volume of 15 mL of solvent) (g/15mL) (1, 1.5, 2 g/15 mL) were studied. Thus two responses, total polyphenol content (TPT) (mg EAG/g MS) and DPPH free radical scavenging ($\mu\text{g/mL}$) were determined (**Table II**).

The optimization of the extraction conditions is carried out using the response surface method (RSM) and the Box-Behnken mathematical scheme.

Table II: Experimental design used for the extraction of bioactive compounds from the two plants studied.

Test	Ratio (g/15ml)	Solvent (% Ethanol)	Time (min)
01	01	0	75
02	02	50	120
03	01	100	75
04	02	100	75
05	1,5	0	30
06^a	1,5	50	75
07	1,5	100	120
08^a	1,5	50	75
09	01	50	30
10	02	0	75
11	1,5	100	30
12	02	50	30
13	1,5	0	120
14	01	50	120
15^a	1,5	50	75

^a: Focal points of the experimental plant.

II.2.2. Application of the Box-Behnken (BB) plan

The optimization of the extraction method is carried out using the BB plan with three levels (-1,0,+1). This design was used to evaluate the most significant parameters on extraction and to find the optimal extraction conditions(Telli et al., 2010). In order to evaluate the best

conditions for total polyphenol extraction and antioxidant activity, three independent variables were chosen as relevant: ratio, percent solvent and extraction time, denoted as X1, X2 and X3, respectively (Table III).

Table III: Levels of the three selected parameters.

	-1	0	+1
X1 (g/15ml)	1	1,5	2
X2 (%)	0	50	100
X3 (min)	30	75	120

The Box-Behnken plan consists of 15 tests, each of which is repeated three times. The low, medium and high levels of each variable are denoted by -1, 0 and +1, respectively.

II.3. Extraction of phenolic compounds

The extraction of phenolic compounds from the plant matrix (the leaves of the plants studied) was done by Solid/Liquid Extraction method.

II.3.1. Procedure

The extraction of the bioactive compounds from *Phillyrea angustifolia* and *Rhamnus alaternus* was done by Solid/Liquid Extraction method. A quantity of powder of each plant studied was introduced into an Erlenmeyer flask containing 10 ml of extraction solvent. The resulting mixture was stirred for a specified time at room temperature under the conditions defined by the experimental design shown in Table II, then centrifuged at 60 rpm for 15 min and filtered. The recovered extract is stored in closed test tubes and kept in a freezer to prevent degradation of the extracts.

II.4. Determination of phenolic compounds

II.4.1. Principle

Folin-Ciocalteu's reagent consists of a mixture of phosphotungstic acid ($\text{H}_3\text{PW}_{12}\text{O}_{40}$) and phosphomolybdic acid ($\text{H}_3\text{PMO}_{12}\text{O}_{40}$). During oxidation, it is reduced to a mixture of tungsten blue oxide (W_8O_{23}) and molybdenum (MO_8O_{23}). The coloration produced is proportional to the amount of polyphenols present in the extract analysed (Ribereau-Gayon, 1968).

II.4.2. Method of operation

The determination of phenolic compounds for the different extracts of the two plants studied was carried out according to the method described by Nabet et al. (2019). 20 µl of each extract previously diluted to 1/10 is mixed with 1200 µl distilled water, then 100 µl Folin-ciocalteu reagent was added. After one minute of stirring, 300 µl of 20% sodium carbonate solution was added with 380 µl of distilled water. The mixture is incubated for two hours in the dark at room temperature. The content of total phenolic compounds is determined by referring to the calibration curve prepared with gallic acid (Appendix 2). The results are expressed in mg gallic acid Equivalent/g dry matter (mg GGE/g DM).

II.4.2. Determination of flavonoids

II.4.2.1. Principle

Flavonoids have a free hydroxyl (OH) group in position 5 which, together with the CO group, can give a coloured complex with aluminium chloride (AlCl₃). Flavonoids form yellowish complexes by chelation of metals (iron and aluminium). AlCl₃ forms a very stable complex with the hydroxide (OH) groups of phenols, this yellow complex absorbs visible light at a wavelength of 430 nm (Ribéreau-Gayon, 1968).

II.4.2.2. Operating procedure

The flavonoid content of extracts of the leaves of *R. alaternus* and *P. angustifolia* obtained under optimal extraction conditions with the experimental design was estimated by colorimetric determination according to the method described by Djeridane et al. (2006).

500 µl of the 2% aluminium chloride (AlCl₃) solution were added to the same volume (500 µl) of the extract. The absorbance was read at a wavelength of 430 nm, after a contact time of 15 minutes at room temperature. 2g of aluminium chloride were dissolved in 100 ml of methanol to prepare the 2 % aluminium chloride solution. A calibration curve (Appendix 3) with catechin (0.031 -1.0 mg/ml) was carried out to determine the flavonoid contents. The flavonoid results were expressed in mg quercetin equivalent/g dry matter (mg EQ/g DM).

II.4.3. Determination of condensed tannins

II.4.4.1. Principle

Tannins are polymers characterized by the presence of a sufficient number of hydroxyphenolic groups to allow more stable combinations with proteins and alkaloids. These

compounds are generally amorphous, soluble in water and insoluble in non-polar organic solvents. Tannins produce blue-black or greenish-brown precipitates. The intensity of the colour is proportional to the tannin content in the sample (Harbertson et al., 2002).

II.4.4.2. Operating procedure

The contents of condensed tannins in the studied extracts were determined using the method proposed by Škerget et al. (2005). 0.5 mL of the extract was mixed with 2 mL of butanol-HCl reagent (77 mg FeSO₄ is dissolved in 500 mL of butanol-HCl (2V:3V). The mixture was incubated at 95°C for 15 minutes and the absorbance was read at 530 nm.

The results are determined using the following formula using cyanidin as the standard.

$$\text{Condensed Tannin} = \left(\frac{(ABS) * Mw * 1000}{\epsilon * L} \right) * 1000 \text{ (mg Eq C/g MS)}.$$

With:

Mw: Molecular weight of cyanidine equal to 287.24 g/mol.

ϵ : Mole extinction coefficient of cyanidine equal to 34700 l. mol⁻¹.cm⁻¹.

L: width of the Cuvette (1cm).

Tannin contents are expressed in mg cyanidine equivalent per g dry matter (mg Eq C/ g MS).

II.5. Measurement of antioxidant activity

The estimation of the antioxidant activity of the extracts for the two plants studied is carried out using four different tests. The reducing power test, Non-enzymatic superoxide radical scavenging, ABTS[•] radical scavenging and the ammonium phosphomolybdate test were carried out only for the extracts of the two plants obtained under optimal extraction conditions.

II.5.1. DPPH free radical scavenging test

II.5.1.1. Principle

DPPH is a stable free radical that is electron or hydrogen accepting. The method is based on the reduction of the alcoholic solution of DPPH in the presence of a hydrogen-donating antioxidant and the formation of the non-radical form DPPH-H. The ability to reduce DPPH radicals is determined by the decrease in its absorbance at 517 nm, which is visually perceptible as a discoloration from purple to yellow (Gülçin et al., 2006).

II.5.1.2. Operating procedure

The antiradical power of extracts of *R. alaternus* and *P. angustifolia* on DPPH free radicals was determined according to the method reported by Brand-Williams et al. (1995). A volume of 1450 μl of DPPH prepared with methanol at a concentration of 6.10-5mM is added to 50 μl of the test extract (diluted 1:10). The mixture is incubated in the dark for 30 min at room temperature. The absorbance were read in 517nm.

II.5.2. Reducing power

II.5.2.1 Principle

Reducing power is the ability of the antioxidants in the extract to reduce ferric iron (Fe^{3+}) in the ferricyanide complex to ferrous iron (Fe^{2+}). The reduced form gives a green color proportional to the reducing power of the extract.

II.5.2.2. Procedure

The determination of the reducing power of the extracts of both plants is carried out according to the method described by Ferreira et al. (2007) In one tube, 1250 μl of potassium ferricyanide [$\text{K}_3\text{Fe}(\text{CN})_6$] at (1%) was added to the mixture of 1250 μl of phosphate buffer at (pH 6.6; 0.2 M) with 500 μl of the extract. The mixture was placed in a water bath at 50°C for 20 min, to which 10% trichloroacetic acid was added 1250 μl . 1250 μl of the mixture was removed, to which was then added 1250 μl of distilled water and 250 μl of 0.1% ferric chloride (FeCl_3). The absorbances were read at 700 nm using a UV-Vis spectrophotometer (Evolution 600, ThermoFisher Scientific, European Union).

II.5.3. Ammonium phosphomolybdate test

II.5.3.1 Principle

The ammonium phosphomolybdate test is a quantitative method for assessing total antioxidant capacity. It is based on the reduction of Mo^{6+} to Mo^{5+} with the formation of a green colored phosphate Mo^{5+} complex with maximum absorption at 695nm (Bougatef et al., 2009).

II.5.3.2. Procedure

The assay is performed according to the method described by Prieto et al. (1999). 100 μl of the plant extract obtained under optimal extraction conditions were added to 1000 μl of the mixture composed of (0.6 M sulphuric acid, 28 mM sodium phosphate and 4 mM ammonium

molybdate). After incubation for 90 min in a water bath at 95°C, the solutions obtained were cooled, and then the absorbances were measured at 695 nm. The total antioxidant capacity is expressed in milligram equivalent of gallic acid per gram of dry matter (mg EAG/g MS).

II.5.4 ABTS[•] radical scavenging

II.5.4.1 ABTS[•] radical scavenging Principle

The pre-formed radical monocation of 2,2'-azinobis-(3-ethylbenzothiazoline-6-sulfonic acid) (ABTS[•]) is generated by oxidation of ABTS with potassium persulfate (K₂S₂O₈). The oxidation of ABTS gives the solution a dark green coloration which suffers decolorization when in the presence of hydrogen-donating antioxidants, such as flavonoids, hydroxycinnamates, carotenoids, which cause the reduction of ABTS[•] (Re et al., 1999).

II.5.4.2 ABTS[•] radical scavenging

ABTS[•] radical scavenging was prepared according to Re et al. (1999). For this reason 5 mL of 7 mM aqueous ABTS solution was mixed with of potassium persulfate (K₂S₂O₈) (2,45 mM). The mixture was incubated in the dark for 16 h and diluted with methanol until the absorbance value at 744 nm equaled (0,750-0,800).

50 uL standard or sample + 250µL of the prepared ABTS radical solution was mixed with 50 uL standard or sample, the mixture was leaved the microplate in the dark for 20 min. then the absorbances were measured at 734 nm.

II.5.5. No enzymatic superoxide radical scavenging

II.5.5.1. Principle

The non-enzymatic phenazine methosulfate-nicotinamide adenine dinucleotide system (PMS/NADH) generates superoxide radicals, which reduce nitro blue tetrazolium (NBT) to a purple formazan. The plant extract, when added, will act as a scavenger of the superoxide radicals, competing with NBT preventing the color formation.

II.5.5.2. Procedure

Activity Superoxide radical scavenging activity is generally based on the anion radical which is associated with PMSNADH system. The measurement of superoxide scavenging activity of the is based on method. They are generated within PMSNADH systems by the oxidation of NADH and are assayed by the reduction of nitroblue tetrazolium (NBT).

Superoxide Radical Scavenging Activity (SRSA) For the non enzymatic system was performed, 75 μ l nitro blue tetrazolium (NBT, 0.2 mM) prepared in Phosphate buffer (20 mM, pH= 7.4) was added to 100 μ L of NADH (0.3 mM) for the mixture. 75 μ L of standard (0.0 – 0.2 mg/mL) or sample were add and then 50 μ L of phenazine methosulfate PMS 15 μ M The mixture was allowed to stand for 5 min and read at 560 nm.

II.6. Determination of antibacterial activity

Six bacterial strains were used to study antibacterial activities which are: *Salmonella enterica* CIP 813, *Bacillus cereus* 14579, *Escherichia coli* 25922, *Staphylococcus aureus* 29213, *Pseudomonas aeruginosa* 27883, *Klebsiella pneumoniae* 4352. These strains are kept in the refrigerator in screwed tubes containing the nutrient medium until they are revived.

II.6.1. Agar disc diffusion test

Antimicrobial activity was performed using the agar disc diffusion method described by Matuschek et al. (2014), which is a preliminary method for verifying and selecting extracts that have antimicrobial activity against the strains tested. This technique is based on the appearance of an inhibition zone on Mueller Hinton agar if the strain tested is sensitive to the extract.

II.6.2. Micro-dilution method

The minimum inhibitory concentration (MIC), which is defined as the lowest concentration of extract obtained under optimal conditions that inhibits the growth of microorganisms, was determined with the microdilution method according to NCCLS recommendations (NCCLS, 1999). The MIC values were determined for microbial strains that were sensitive to extractions in the agar disc diffusion test. All tests were performed with the Mueller Hinton (BMH) broth with Tween 80 added at a concentration of 0.5% (v/v). The bacterial strains were inoculated for 24 h at 37°C on Mueller Hinton agar (GMH) and 5x10⁵ microbial suspensions. CFU/mL was prepared in BMH, and this inoculum density was confirmed by the agar medium enumeration method. Five different dilutions (20 to 100 μ L/mL) in extracted were prepared and introduced at the microplate wells (96 wells). In each well 95 μ L of BMH, 5 μ L of inoculum and 100 μ L of each dilution of extracts have been introduced. The last well containing 195 μ L of BMH without extracts and 5 μ L of inoculum to the level of each column was used as a negative control. The final volume of each well of 200 μ L. The plates were covered with sterile lids and incubated at 37°C for 24 hours. The bacterial growth was

revealed by the presence of a white precipitate at the bottom from the well. All the tests were repeated three times.

II.7. Assessment *in vitro* of anti-inflammatory activity

II.7.1. Test of Inhibition BSA denaturation.

The inhibition of BSA denaturation test was used to evaluate the possibility anti inflammatory capacity of optimized extracts of *Rhamnus alaternus* and *Phillyrea angustifolia*. The reaction mixture was consists of test optimized extracts of *Rhamnus alaternus* and *Phillyrea angustifolia* with different concentrations and 2 mL of aqueous BSA solutions (1%). And then the mixture was incubated at 37 °C for 20 min, then a heat treatment at 60 °C for 20 min, the turbidity was measured at 660 nm after cooling and to express the percentage of protein denaturation the following equation was applied (Azeem et al., 2010).

$$\% \text{ Inhibition of BSA denaturation} = 100 \times (A_0 - A_1 / A_0)$$

Where :

- A_0 is the absorbance of control (heated BSA without extract) solution

- A_1 is the absorbance in the presence of plant extract.

II.7.2. Test of antiproteinase action

The test was performed according to Oyedapo and Famurewa.(1995). The reaction mixture (2 ml) was containing 0.06 mg trypsin, 1 ml 20 mM Tris HCl buffer (pH 7.4) and 1 ml test optimized extracts at different concentrations, the mixture was incubated for 20 min. Then the reaction was stopped by adding 2 volumes of 70% perchloric acid. The absorbance of the supernatant in the mixture was recorded at 210 nm after centrifugation . The buffer was used as white and the percentage of inhibition of the proteinase inhibitory activity was calculated as follows:

$$\% \text{ Inhibition} = 100 \times (A_0 - A_1 / A_0)$$

Where A_0 is the absorbance of control solution and A_1 is the absorbance in the presence of plant extract.

II.7.3. Membrane stabilization by hypotonicity induced hemolysis.

Preparation of Red Blood cells (RBCs) suspension. The Blood was collected from healthy human volunteer who has not taken any NSAIDs (Non Steroidal Anti-Inflammatory Drugs) for 2 weeks prior to the experiment and transferred to the centrifuge tubes. The tubes were centrifuged at 3000 rpm for 10min and were washed three times with equal volume of normal saline. The volume of blood was measured and re constituted as 10% v/v suspension with normal saline.

II.7.4. Hypotonicity induced hemolysis

Hemolytic activity was evaluated as described previously by Oyedapo and Famurewa. (1995). A volume of 5 mL of hypotonic PBS (10 mM, 50 mM NaCl, pH= 7.4) containing extracts at different concentrations was added to 0.5 mL of RBC suspension and then the samples were incubated for 10 min at 37 ° C and centrifuged at 3000 rpm for 10 min. The absorbance of the supernatant was then measured at 540 nm. The experiment was performed in triplicates for all the test samples. The percentage of hemolysis inhibition was calculated for each sample according to the following law:

$$\% \text{inhibition} = 100 \times (A_0 - A_1 / A_0)$$

Where A_0 is the absorbance of positive control solution and A_1 is the absorbance in the presence of plant extract.

II.7.5. hemolise assay

1 mL of RBC suspension, a volume of 1 mL of optimized extracts at increasing concentrations (0, 0.5, 1, 1.5, and 2 g/mL) was added. After 10 min of incubation at room temperature, the samples were centrifuged at 3000g for 10 min and the resulting supernatant was removed and used to evaluate their hemolytic activity using a spectrophotometer at 540 nm. RBC lysis in the presence of distilled water was considered as 100% hemolytic activity. Hemolysis in the presence of extracts was calculated relative to this control hemolysis (Pagano and Faggio, 2015; Pimentel, 2005).

$$\text{Hemolysis \%} = 100 \times (A_1 / A_0)$$

where A_0 was the absorbance of control (distilled water and erythrocyte without extract and A_1 the absorbance in the presence of plant extract.

II.8. Enzyme Inhibitory Activity

II.8.1. α -Amylase inhibitory activity

α -Amylase inhibitory activity was performed using the iodine/potassium iodide (IKI) method Zengin et al. (2014) with slight modifications. First, 25 μ L of sample solution at different concentrations in the range between 10 and 400 μ g/mL was mixed with α -amylase solution (50 μ L) in phosphate buffer (pH 6.9 with 6 mM sodium chloride) and then incubated for 10 min at 37 °C. After that, a starch solution (50 μ L, 0.1%) was added and incubated for 10 min. Finally, 25 μ L of HCl (1M) and 100 μ L IKI were added to each well in the 96-well microplate. Similarly, a blank was prepared by adding to the sample solution all reaction reagents except the enzyme (alpha-amylase) solution. The absorbance of both the sample and blank were read at 630 nm while the blank absorbance was subtracted from that of the sample. The pharmacological inhibitor, acarbose, was used as a positive control and the α -amylase inhibitory activity was calculated as follows:

$$\text{Activity inhibition (\%)} = \frac{A_{\text{control}} - A_{\text{sample}}}{A_{\text{control}}} \times 100$$

where A is the absorbance.

II.8.2. α -Glucosidase inhibitory activity

α -glucosidase inhibitory activity was performed according to the methodology described by Lordan et al. (2013). First, 50 μ L of sample solution (concentrations between 20 μ g/mL and 1000 μ g/mL) was mixed with 50 μ L of 5 mM p-nitrophenyl- α -d-glucopyranoside solution (in phosphate buffer) in a 96-well microplate. After 5 min of incubation at 37°C, phosphate buffer (100 μ L) containing 0.1 U/mL α -glucosidase was added to each well. Blank readings (without enzyme) were subtracted from each well and the results were compared to the control. The absorbance of the sample and blank were recorded at 405 nm and acarbose was used as the positive control. The activity of α -glucosidase was evaluated as follows:

$$\text{Activity inhibition (\%)} = \frac{A_{\text{control}} - A_{\text{sample}}}{A_{\text{control}}} \times 100$$

where A is the absorbance

Fist Part

Chapter III

Results and discussion



III. Results and discussion

III.1. Response surface methodology (RSM) experimental designs

III.1.1. Extraction optimization of total polyphenol content for *Rhamnus alaternus*

The results of the responses studied (TPC, DPPH) for the different tests proposed by the statistics software of the extract of *R. alaternus* are represented in the following **Table V**.

Table V. Experimental design and observed results for all investigated responses from *R. alaternus* (a: Central points of the experimental plant).

Test	Independent variables			Investigated responses	
	Time (min)	% (EtOH)	Ratio (g/10mL)	TPT (mgEAG/g MS)	DPPH(μ g EAG/mL)
1	75	0	1	32.7 \pm 0.02	9.40 \pm 0.01
2	120	50	2	62.3 \pm 0.05	83.2 \pm 0.06
3	75	100	1	59.1 \pm 0.6	38 \pm 0.06
4	75	100	2	30.4 \pm 0.03	41.1 \pm 0.02
5	30	0	1.5	48.6 \pm 0.04	19.7 \pm 0.03
6 ^a	75	50	1.5	61.1 \pm 0.23	72.6 \pm 0.06
7	120	100	1.5	28.4 \pm 0.01	47.1 \pm 0.05
8 ^a	75	50	1.5	54.6 \pm 0.06	74.5 \pm 0.06
9	30	50	1	60.7 \pm 0.4	53.6 \pm 0.9
10	75	0	2	24.6 \pm 0.03	22.3 \pm 0.04
11	30	100	1.5	32.3 \pm 0.02	36.4 \pm 0.01
12	30	50	2	48.9 \pm 0.1	73.3 \pm 0.1
13	120	0	1.5	24.9 \pm 0.05	24.8 \pm 0.06
14	120	50	1	63.1 \pm 0.09	63.90.09
15 ^a	75	50	1.5	57.2 \pm 0.03	76.2 \pm 0.7

highest total polyphenol content of the extract of *R. alaternus* is obtained at extraction time of 120 min, 50% ETOH and ratio of 1, with grade of 63.05 mg EAG/g MS. On the other hand, the lowest total polyphenol content is obtained in the extraction conditions: 75 min, 0% ETOH and a ratio of 2, with a value of 24.55 mg EAG/g MS.

According to the results of the process of optimization using Stat-graph software, a final model equation of the BOD dependence is as given.

Standardized Pareto charts are presented in **Fig. 3** statistically; the quadratic effect of the solvent has a significantly negative influence on the total polyphenol content of *R. alaternus*

extracts. On the other hand, the variables extraction time, solvent concentration and ratio had no effect significant on the polyphenol content of extracts of *R. alaternus*. The model ($R^2 = 81.77\%$) suggested a maximum value TPC of the extract of *R. alaternus*, with predict value is 69.24 mg EAG/g DM, obtained with optimal conditions of extraction are 30 min, 53% (EtOH%) and a ratio of 1.

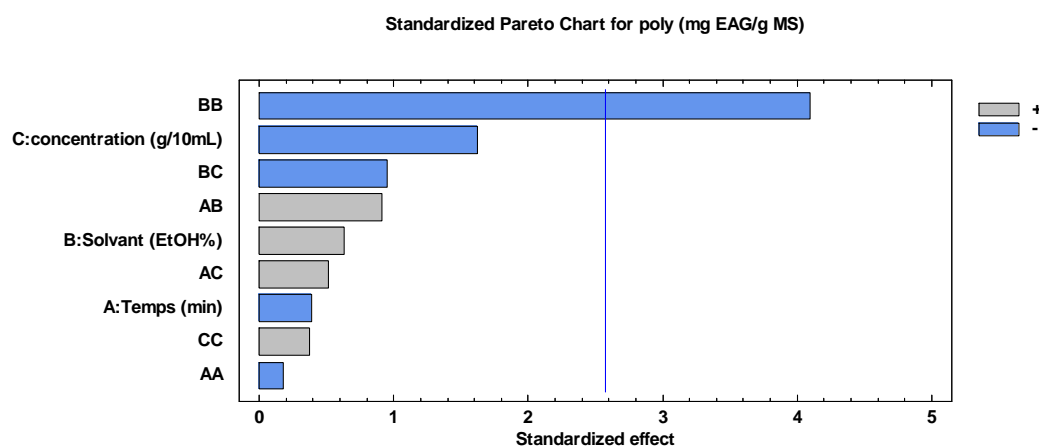


Figure 3. Standardized Pareto charts of *R. alaternus* for polyphenol (mg EAG/g DM)

Djeridane et al. (2007), found in their research a polyphenol content of 6 mg EAG/g MS for the ethanolic extract of the aerial part of *Rhamnus alaternus* harvested north of Laghouat, in Algeria. A similar study conducted by Ben Ammar et al. (2008), polyphenol content of 7 mg EAG/g of fresh material was found for the methanolic extract of the leaves of *R. alaternus* harvested in Tabarka in Tunisia.

Khettal et al. (2014), reported in their study that the ethanolic extract from the leaves of *R. alaternus* has a total polyphenol content of 150 ± 9.7 mg EAG/g dry extract. Furthermore, a content of 17.13 ± 0.09 mg EAG/g MS was obtained in the methanolic extract of *R. alaternus* (Moussi et al., 2015).

The polyphenol contents of the extract of *R. alaternus* reported in the literature are different from those obtained in our study (Table V). This difference can be explained by the method used, the extraction solvent, the harvest season or the geographical conditions of the plant.

III.1.2. Optimisation of the DPPH free radical scavenging effect

The highest effect scavenging radical DPPH of *R. alaternus* extracts is obtained at extraction time 120 min, 50% EtOH and a ratio of 2, with a grade of 81.85 μg EAG/mL. On the other hand, the lowest scavenging radical DPPH effect of the extracted from *R. alaternus* is obtained under the following extraction conditions: 75 min, 0 EtOH and a ratio of 1 with a content of 8.11 μg EAG/mL.

Standardized Pareto charts are presented in **Fig. 4** statistically; ethanol concentration (EtOH %) has the strongest significant positive effect on the antioxidant activity of *R. alaternus* extracts, followed by the ratio and the time of extraction which also have a significant positive effect. On the other hand, the quadratic effect of the solvent (EtOH %) shows a significant negative effect on the antioxidant of *R. alaternus* extracts.

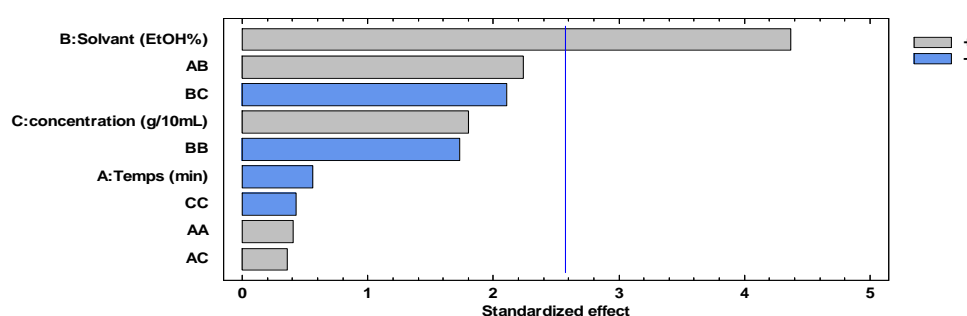


Figure 4. Standardized Pareto charts of *R. alaternus* for antioxidant activity DPPH (μg EAG/ml)

The model ($R^2 = 98.95\%$) proposes a maximum value for the antioxidant activity of *R. alaternus* extract which is 79.68 μg EAG/mL, with optimal extraction conditions of 120 min, 56% (EtOH%) and a ratio of 1.81.

Kosalec et al. (2013a), have shown that the DPPH free radical scavenging effect of *R. alaternus* extract is 78.7 ± 3.16 mg/g. A free radical scavenging effect of 34.7 μg of ascorbic acid/ml for the methanolic extract of *Rhamnus persica* was found in their study (Ashfaq et al., 2017). The latter results is half as high compared to the result obtained under optimal extraction conditions in our study.

Moreover, an inhibition percentage of $66.83 \pm 3.88\%$ of DPPH free radicals was obtained with the methanolic extract of the leaves of *Rhamnus alaternus* harvested in Adekar, Béjaïa (Moussi et al., 2015).

III.1.3. Optimization of multiple surface responses of *Rhamnus alaternus* extracts

Table VI shows the predicted results and the experimental results of the studied responses obtained under optimal conditions of extraction of the extract of *R. alaternus* by the conventional method which are: an extraction time of 83 min, a percentage of ethanol of 58% and a ratio of 1.2.

Table VI. Predicted and observed values of each individual response for the optimal *R. alaternus* with Optimum extraction conditions time of extraction 83 min, ethanol percentage of 58% and ratio of 1.2.

Response	Predicted	Observed	%RSD ^a
TPT (mg EAG/g MS)	63.05	70.36 ± 0.21	7.74
DPPH (µg/mL)s	67.29	69.49 ± 0.61	2.27

^a Relative standard deviation (RSD) between predicted and observed results, considering as observed results the average of three independent extracts obtained in the same conditions.

The model proposes a desirability factor of 0.90% (Figure 5) with a total polyphenol content of 63.05 mg EAG/g MS and a DPPH free radical scavenging effect of 67.29 µg EAG/mL. The experimental polyphenol content and DPPH radical trapping effect of the *R. alaternus* extract found were 70.36 mg EAG/g MS and 69.49 µg EAG/mL, respectively. These levels are close to those predicted by the statgraphics software (Table VI), therefore the proposed model is validated.

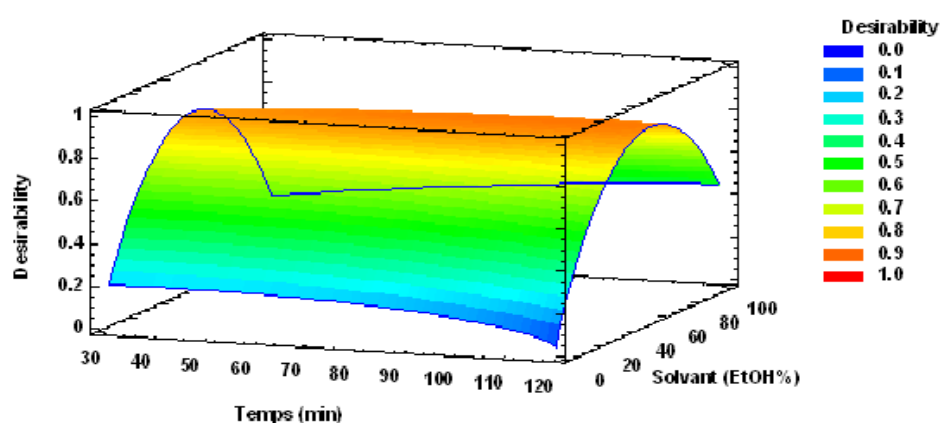


Figure 5. Three-dimensional diagram of the response surface for the effects of time and solvent on the desirability of the *R. alaternus* extract obtained by the method solid/liquid extraction.

III.2. *Phillyrea angustifolia*

III.2.1. Optimisation of the total polyphenol content of *P. angustifolia*

The results of the responses studied (TPT, DPPH) for the different tests proposed by the statgraphics software of the extract of *P. angustifolia* are represented in the **Table VII**.

Table VII. Experimental design and observed results for all investigated responses from *P. angustifolia*(a: Central points of the experimental plant).

Test	Independent variables			Investigated responses	
	Time (min)	% (EtOH)	Ratio (g/10mL)	TPT (mgEAG/g MS)	DPPH (μ g EAG/mL)
1	75	0	1	43.6 \pm 0.08	29.9 \pm 0.02
2	120	50	2	55.7 \pm 0.06	55.6 \pm 0.07
3	75	100	1	49.4 \pm 0.06	56.9 \pm 0.12
4	75	100	2	43.2 \pm 0.9	57.8 \pm 0.64
5	30	0	1.5	48.5 \pm 0.4	53.1 \pm 0.34
6 ^a	75	50	1.5	64.2 \pm 0.1	54.5 \pm 0.42
7	120	100	1.5	58.3 \pm 0.09	57.7 \pm 0.94
8 ^a	75	50	1.5	68.8 \pm 0.01	53.9 \pm 0.46
9	30	50	1	55.8 \pm 0.09	52.8 \pm 0.38
10	75	0	2	52 \pm 0.14	49.4 \pm 0.23
11	30	100	1.5	66.8 \pm 0.08	52.9 \pm 0.16
12	30	50	2	94 \pm 0.46	52.4 \pm 0.24
13	120	0	1.5	52.1 \pm 0.19	38.1 \pm 0.16
14	120	50	1	67.9 \pm 0.84	52.9 \pm 0.19
15 ^a	75	50	1.5	72.2 \pm 0.92	52.1 \pm 0.8

The highest total polyphenol content of *P. angustifolia* extract is obtained at an extraction time of 30 min, 50% EtOH and a ratio of 2, with a grade of 94.02 mg EAG/g MS. However, the lowest total polyphenol content is obtained in the extraction conditions: 75 min, 100% EtOH, a ratio of 2 and 75 min, 0% EtOH and a ratio of 1 with a value of 43 mg EAG/g MS

Standardized Pareto charts are presented in **Fig. 6** shows that the quadratic effect of the solvent has a significantly negative effect on the total polyphenol content of the *P. angustifolia* extracts obtained by the solid/liquid method. The variables extraction time, concentration in solvent and the ratio have no significant effect on the polyphenol content of

P. angustifolia extracts. Thus, there is an interaction between extraction time and the ratio (concentration of the powder).

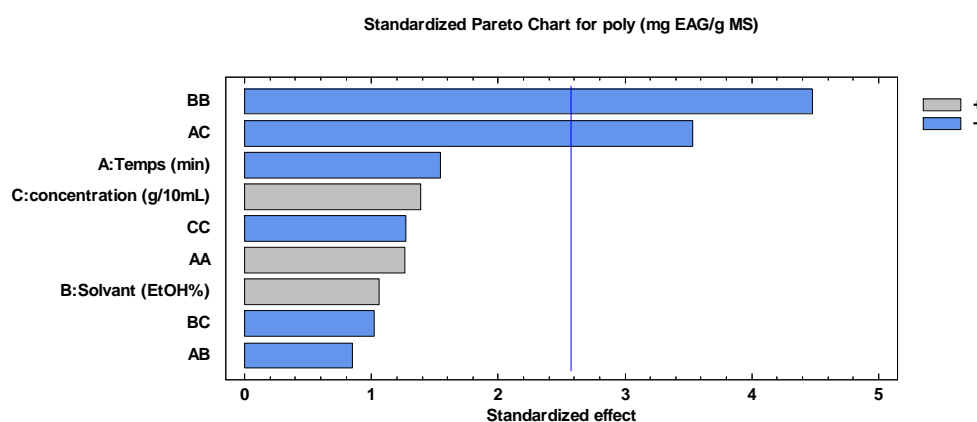


Figure 6. Standardized Pareto charts of *P. angustifolia* for polyphenol (mg EAG/g DM)

Indeed, when the ratio is 1 the increase in extraction time from 30 to 120 min only increases the total polyphenol content of *P. angustifolia* extracts by 55 at 75 mg EAG/g MS, respectively. Whereas, when the ratio is 2 the content of polyphenols is maximal at an extraction time of 30 min with a value of 89 mg EAG/g MS. Increasing the extraction time decreases the polyphenol content to achieve a minimum value of 55 mg EAG/g MS at an extraction time of 120 min (**Fig. 7**). The highest total polyphenol content of *P. angustifolia* extracts which is of 88.46 mg EAG/g MS, proposed by the model ($R^2 = 89.68\%$) with optimal conditions : extraction time = 30 min, 53% EtOH and a ratio of 2.

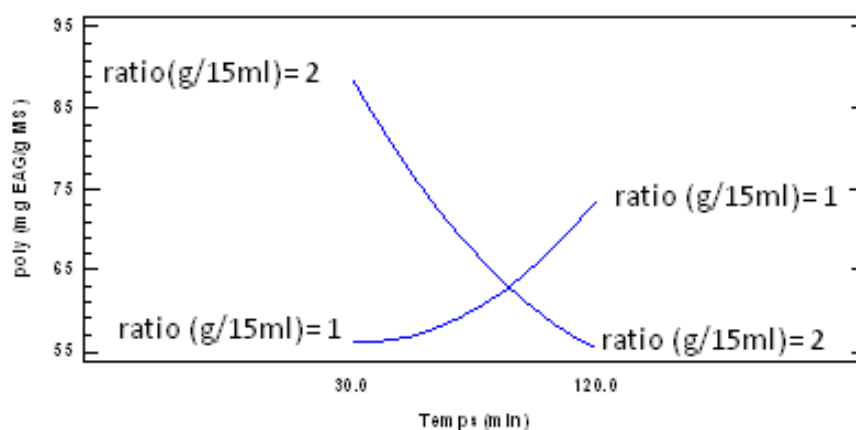


Figure 7. Interaction between the ratio and extraction time and their effect on the polyphenols of *P. angustifolia*.

The phenolic compound content of the methanolic extract of *P. latifolia* harvested in Turkey is 16,52 mg GGE/g of the fresh fruit (Ayranci and Erkan, 2013).

The result found by Mebirouk-Boudechiche et al. (2015b) for the species *P. angustifolia* harvested in Algeria shows that the total polyphenol content is 29,23 mg tannic acid equivalent/g DM. This is lower than that obtained in our study under optimal extraction conditions (79.40 mg GGE/g DM).

Several authors report that the polyphenol content varies with the variation of several parameters such as the extraction method, the species studied, the harvesting period, the part studied, etc.

III.2.2. Optimisation of the DPPH free radical scavenging effect

Based on the results of antioxidant activity grouped in the **Table VII**, the results of antioxidant activity as follows finds that the independent variables studied have little influence on activity antioxidant from extracts of *P. angustifolia*.

The strongest scavenging effect of the free radical DPPH is obtained at an extraction time at 75 min, 100% EtOH and a ratio of 2 with a grade of 56.49 μg EAG/mL. On the other hand, the lower free radical scavenging effect of DPPH free radical scavenging from *P. angustifolia* extracts is obtained under the following extraction conditions: 75 min, 0% EtOH and a ratio of 1 with a content of 28.63 μg EAG/mL.

Standardized Pareto charts are presented in **Fig. 8**, the only variable that has a significant positive influence on the antioxidant activity of *P. angustifolia* extracts is the concentration of the solvent (EtOH%). On the other hand, the two other variables: extraction time and the ratio have no significant effect on the antioxidant activity of *P. angustifolia* extracts.

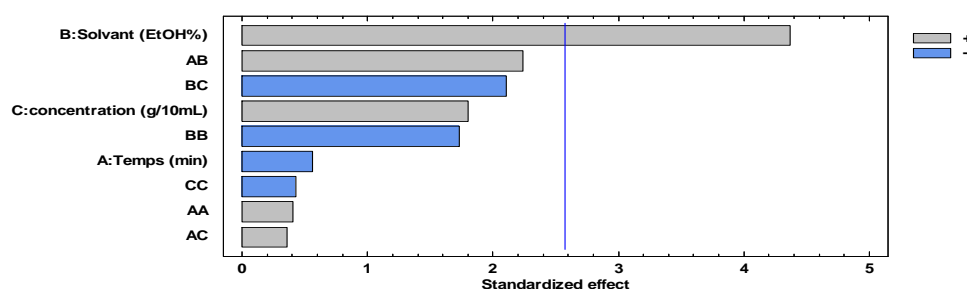


Figure 8. Standardized Pareto charts of *P. angustifolia*. for antioxidant activity DPPH (μg EAG/ml).

The model ($R^2 = 87.68\%$) proposes a maximum value of antioxidant activity of *P. angustifolia* extract which is 60.37 μg EAG/mL which is in optimal conditions of extraction are 120 min, 100% (EtOH%) and a ratio of 1.23.

Ayranci and Erkan. (2013), shows that the free-radical scavenging capacity DPPH (IC₅₀) of *P. latifolia* is $69.4 \pm 5.8 \mu\text{g/mL}$. In addition, a 90% DPPH free radical scavenging rate of the methanolic extract of *Olea europea* subsp maroccana of 90% was reported by Pavithra et al. (2013) for a concentration of 25 mg/ml.

III.2.3. Optimization of multi-surface responses of *P. angustifolia* extracts

At the level of **Table VIII** are grouped the predicted results and the experimental results of the studied responses obtained under optimal conditions of extraction of the extract of *Phillyrea angustifolia* by the conventional method which are: an extraction time of 30 min, a percentage of ethanol of 47% and a ratio of 2.

Table VIII: Predicted and observed values of each individual response for *P. angustifolia* the optimal with Optimum extraction conditions a time extraction time of 30 min, an ethanol percentage of 47% and a ratio of 2.

Response	Predicted	Observed	%RSD ^a
TPT (mg EAG/g MS)	88,22	$79,4 \pm 0.7$	7,44
DPP H ($\mu\text{g/mL}$)s	55,20	$63,72 \pm 0.2$	10,13

^a Relative standard deviation (RSD) between predicted and observed results, considering as observed results the average of three independent extracts obtained in the same conditions.

The model proposes a desirability factor of 0.92% (Figure 12) with a total polyphenol content (TPT) of 88.22 mg EAG/g MS and a DPPH free radical scavenging effect of 55.20 μg EAG/mL. The experimental results obtained are as follows: a polyphenol content of 79.40 mg EAG/g MS and an antioxidant activity (DPPH) of 63.72 $\mu\text{g/mL}$, the latter being close to those predicted by the software (Table VIII). Therefore, the model proposed by the statgraphics software for the optimization of TPT and DPPH free radical scavenging effect of *P. angustifolia* extract is validated.

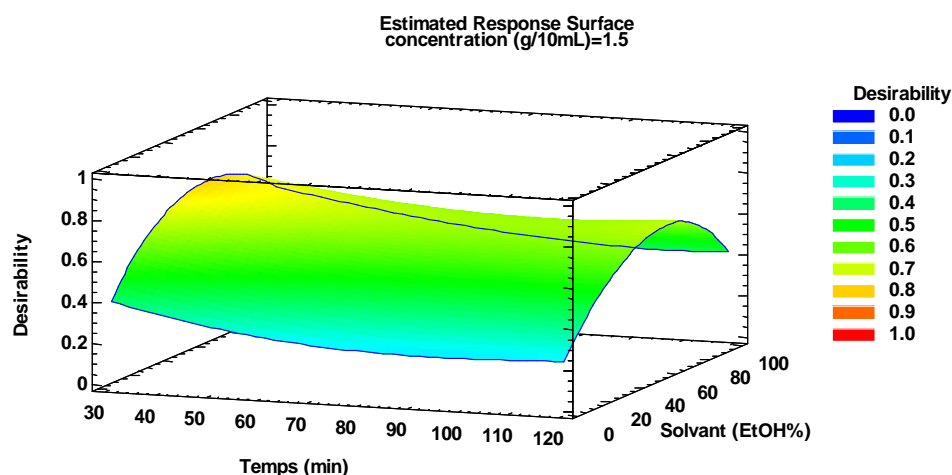


Figure 9. Three dimensional plots of surface response showing the interaction between the ethanol concentration and time of extraction on the overall desirability using *P. angustifolia*

III.3. Evaluation of antioxydants of extracts obtain under optimum condition

III.3.1. Flavonoid content

The results of the flavonoid contents of the extracts of the two plants tested are grouped in the Figure 10.

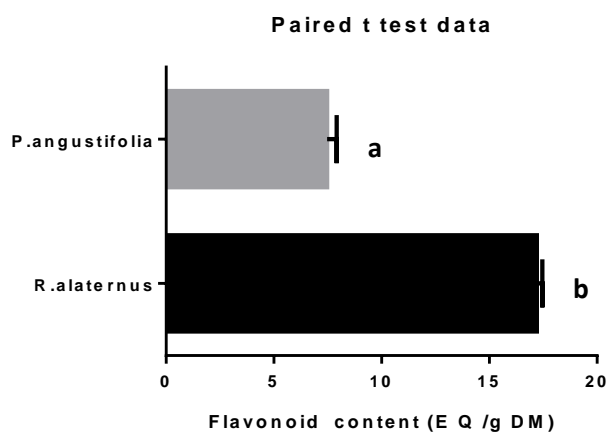


Figure 10. Flavonoid contents of the plants studied

Results with different letters ($a > b$) show a significant difference at $p \leq 0.05$.

The multiple comparison analysis student's t test shows that there is a significant difference between the flavonoid contents of the two plants studied.

The results indicate that the flavonoid content in the optimized extract of *R. alaternus* is higher than that of *P. angustifolia*, which is 7.04 ± 0.27 mg EQ/g DM.

Moussi et al.(2015), reported in their study a flavonoid content is 60.22 ± 5.76 mg EQ/g MS for the methanolic extract of *R. alaternus*. This is three and a half times higher than that obtained in our study for the same species.

Khettal et al. (2014), showed in their study that the flavonoid content (92 ± 14 mg E Q/g dry extract) of the ethanolic extract of *R. alaternus* is five times greater than that found in our study for the same species.

Tattini et al.(2005), reported the flavonoid content of 15.7 ± 1.5 nmol cm⁻² for *P. latifolia* leaf extract.

III.3.2. Condensed tannin contents

The results of the condensed tannin contents of the extracts of the two plants studied are grouped together in the Figure11.

The statistical study shows that there is a significant difference in tannin content between the two plants at $p \leq 0.05$.

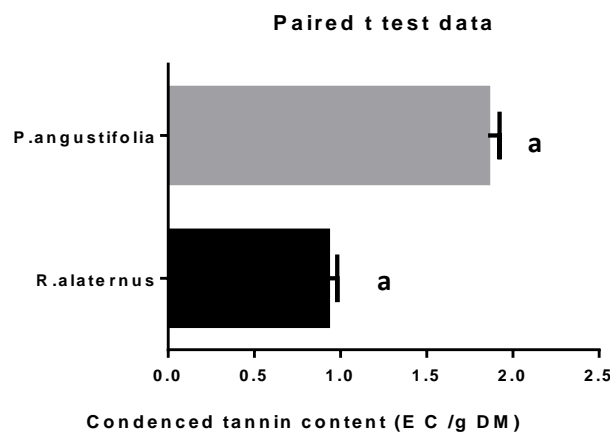


Figure 11. Condensed tannin contents of the plants studied

Results with different letters ($a > b$) show a significant difference at $p \leq 0.05$.

The multiple comparison analysis student's t test shows that there is no significant difference between Condensed tannin contents of the two plants studied

The result found by Mebirouk-Boudechiche et al (2014) for the *Phillyrea media* species collected in Algeria is 18 mg leucocyanidin equivalent/g MS.

The condensed tannin content of the methanolic extract of *R. alaternus* harvested in Tunisia is $14.72 \pm 0.38\%$ tannic acid (Ben Ammar et al., 2007)

III.4. Antioxidant activity of the plant extracts studied under optimized condition

III.4.1. Reducing power

The results of the reducing power of the extracts of the studied plants are represented in Figure 12.

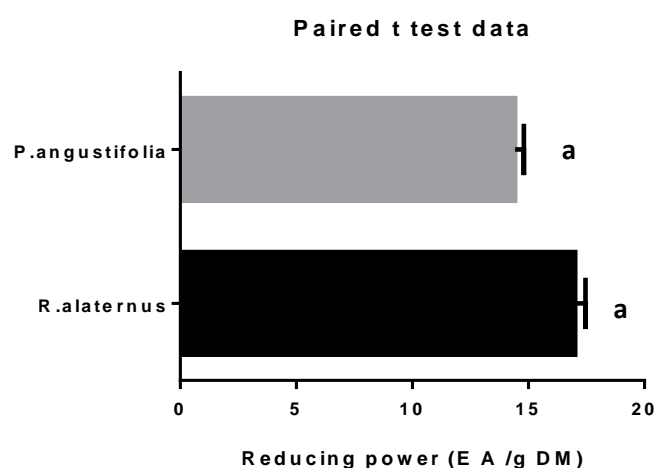


Figure 12. Reducing power test of the plant extracts studied

The multiple comparison analysis student's t test using GraphPad Prism 6 shows that there is no significant difference ($a > b$) between the levels of total antioxidant activity of the two plants studied at $p \leq 0.05$.

The reducing power results of the optimized extracts of the two plants tested show that they have a ferrous to ferric iron reducing capacity of 16.92 ± 0.22 and 14.69 ± 0.87 mg EAG/g MS for *R. alaternus* and *P. angustifolia*, respectively.

Kaempferol-3-O-isorhamnoside and rhamnocitrin-3-O-isorhamnoside isolated in *R. alaternus* extract have a reducing power of 33 and 36.8 mg Trolox equivalent/ml at a concentration of 1 mg/ml (Bhouri et al., 2012).

The extract of the flowers of *Jasminum grandiflorum* (Oleaceae) has a reducing power of 233 ± 64 ml Trolox/g (Dudonne et al., 2009).

III.4.2. Ammonium phosphomolybdate test

The results of the ammonium phosphomolybdate test that is used to determine the total antioxidant activity of the optimized extracts of the plants studied are shown in Figure 13.

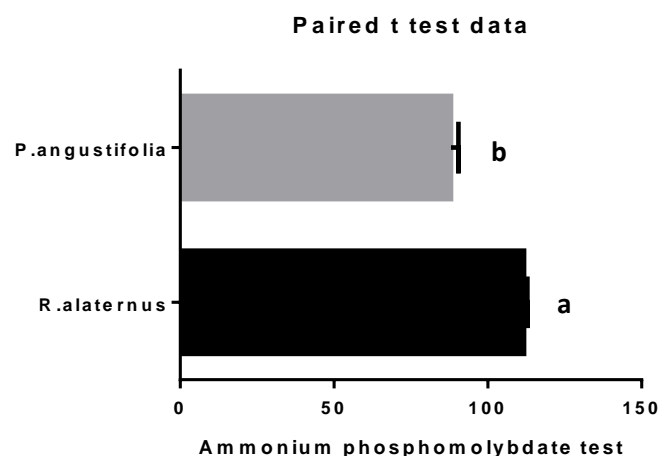


Figure 13. Ammonium phosphomolybdate test of the plant extracts studied.

Results with different letters ($a > b$) show a significant difference at $p \leq 0.05$

The multiple comparison analysis student's t test using GraphPad Prism 6 shows that there is a significant difference ($a > b$) between the levels of total antioxidant activity of the two plants studied at $p \leq 0.05$.

Extract from the leaves of *R. alaternus* obtained under optimal extraction conditions shows the highest total antioxidant activity which is 112.86 ± 4.2 mg EAG/g MS. This is greater than that of the optimized extract of *P. angustifolia* which is 85.84 ± 2.72 mg EAG/g MS.

Bourgou et al., 2008, reports that several flavonoids extract from several Medicinal plants have a significant contribution to total antioxidant activity. In the antioxidant activity of flavonoids depends on their structure and the substitution of the hydroxyl groups in these compounds. The essential condition for having a good radical scavenging effect is the presence of the 3',4' ortho-dihydroxy group on the cycle B and the 4-carbonyl group on cycle C. Thus, the presence of the double bond between the C2 and C3 in cycle C is responsible for the delocalization of electrons from cycle B, which increases antioxidant activity.

III.4.3. ABTS' radical scavenging

The results of ABTS' test that is used to determine the antioxidant activity of the optimized extracts of the plants studied are shown in **Figure 14**.

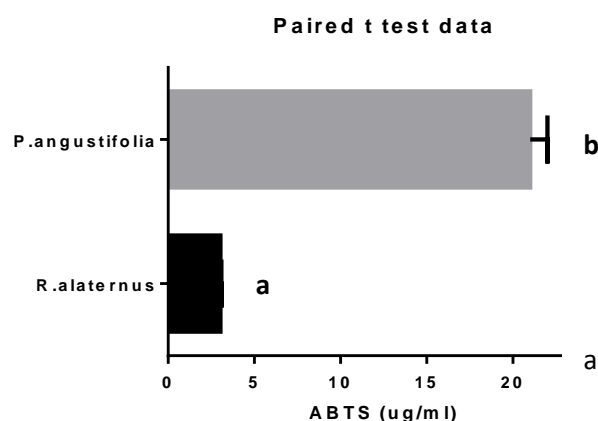


Figure 14. Test ABTS of the plant extracts studied.

Results with different letters ($a > b$) show a significant difference at $p \leq 0.05$

The multiple comparison analysis student's t test shows that there is a significant difference ($a > b$) between the levels of total antioxidant activity of the two plants studied at $p \leq 0.05$.

The strong trapping effect of $ABTS^+$ cations is obtained in the case of extract *R. alaternus*., followed by *P. angustifolia* extract with IC_{50} values 3 ± 0.02 and $22 \pm 0.1 \mu g / ml$ MS, respectively.

Bhouri et al.(2011), reported in their study that *R. alaternus* extract has the highest antioxidant activity (neutralization of the ABTS radical), IC_{50} value of $18.75 \mu g/ml$.

Ayranci and Erkan.(2013), reported in their study that fruit *P.latifolia* extract has the good activity (neutralization of the ABTS radical), IC_{50} value of $1.8 \mu g/ml$.

Our results are in concordance with what other researcher found.

The antioxidant activity studied can be attributed to the acids hydroxycinnamic acids present in this plant and in particular 5-caffeoylquinic acid. (chlorogenic acid). Indeed, AlGamdi et al.(2011) report that phenolic acids such as hydroxycinnamates, mainly 5-O-caffeoylquinic

acid are responsible for the antioxidant activity of the aqueous extract of the seeds of *Anastatica hierochuntica* (tea).

Hydroxycinnamoylquinic acid derivatives (3-caffeoylquinic acid, 5-caffeoylquinic acid, 4-caffeoylquinic acid, 3,4-di-O-caffeoylquinic acid, 3,5-di-O-caffeoylquinic acid and 4,5 di-O-caffeoylquinic acid) are the major compounds which help trap free radicals in the case of gardenia fruit extract (rosacea), these compounds are responsible for 73% of total radical scavenging(He et al., 2010).

III.4.4. No enzymatic superoxide radical scavenging

The results of test superoxide radical scavenging is used to determine the antioxidant activity of the optimized extracts of the plants studied are shown in **Figure 15**.

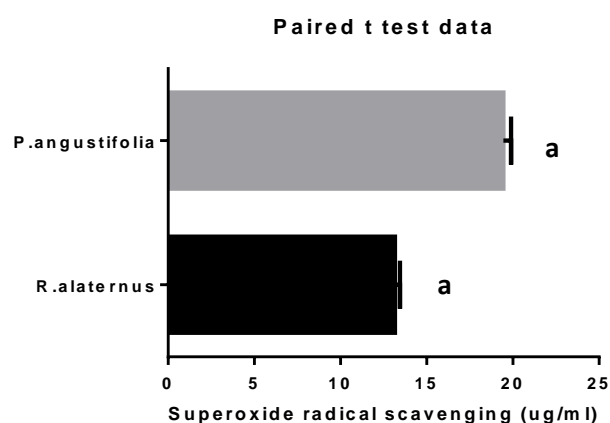


Figure 15. superoxide radical scavenging test of the plant extract studied

Results with different letters ($a > b$) show a significant difference at $p \leq 0.05$

The multiple comparison analysis student's test shows that there is no a significant difference ($a > b$) between the levels of total antioxidant activity of the two plants studied at $p \leq 0.05$.

Superoxide radical scavenging results of the optimized extracts of the two plants tested show that they have reducing capacity nitro blue tetrazolium (NBT) to a purple formazan, IC_{50} 13 ± 0.22 and 19 ± 0.87 mg EAG/g MS for *R. alaternus* and *P. angustifolia*, respectively.

Hsiao et al.(1996), in their study on *Rhamnus nakaharai* they show The effect of 5-100 /z M isotorachrysone on the reduction of cytochrome c by superoxide generated by xanthine plus xanthine oxidase.

The scavengers of nitric oxide compete with the oxygen, leading to reduced production of nitric oxide. In the PMS/NADH coupling reaction reduces NBT. The decrease of absorbance at 560 nm with antioxidants thus indicates the consumption of superoxide anion in the reaction mixture. The results were positive at the laboratory level and further work can be carried out to find out the exact constituent responsible for these activities by the process of modern analytical tools. Thus the plant can be a potential source for antioxidant property (Chakraborty, 2009).

III.5. Determination of antibacterial activity

The antibacterial activity of the two plant extracts tested is evaluated by measuring the diameters of the inhibition halos around the discs. The absence of halos results in the absence of activity and resistance of the tested bacteria. The diameter of the halos varies according to the strain tested, the nature and the dose of the active substance present in the extracts.

The scale for estimating antimicrobial activity is given by Bouharb et al.(2014). They classified the diameters of microbial growth inhibition zones as follows:

- $D < 8$ mm: non-susceptible bacteria;
- $9 < D < 14$ mm: susceptible bacteria;
- $15 < D < 19$ mm: highly susceptible bacteria;
- $D > 20$ mm: highly susceptible bacteria.

III.5.1. Sensitivity of the strains tested to antibiotics

The Gram+ bacterial strain (*Staphylococcus aureus* and *Bacillus cereus*) and Gram- (*Escherichia coli*, *Pseudomonas aeruginosa*, *Salmonella enterica* and *Klebsiella pneumoniae*) showed different sensitivities to the antibiotics tested: amoxicillin (amox), oxacillin (oxa), tetracycline (tet) and amikacin (ami).

S. aureus is highly sensitive to amoxicillin with an inhibition zone diameter of 45.25 mm, while it is less sensitive to tetracycline, oxacillin and amikacin with inhibition zone diameters of 30, 25.5 and 23.25 mm, respectively. In addition, the DZIs of the extracts of the two plants studied obtained from the same strain are very similar to those obtained with oxacillin and amikacin.

Pseudomonas aeruginosa is a Gram+; it is relatively resistant to certain antibiotics such as oxacillin and amikacin with DZIs of 6 and 9.25 mm, respectively. While it is highly sensitive to tetracycline and amoxicillin with DZIs of 34.25 and 38 mm, respectively.

Bacillus cereus showed decreasing sensitivity to the following antibiotics: tetracycline (37.75 mm), amikacin (27.5 mm), amoxicillin (24 mm) and oxacillin (23.75 mm).

Escherichia coli is a Gram- it is highly sensitive to the different antibiotics, tetracycline (31.5 mm), amikacin (27.25 mm) and amoxicillin (24.25 mm). It is resistant to oxacillin (6 mm).

Salmonella enterica is highly sensitive to amikacin (25.25 mm) and amoxicillin (23 mm), and slightly sensitive to tetracycline (8.5 mm).

Klebsiella pneumoniae is extremely sensitive to amoxicillin (40.5 mm) and tetracycline (32.25 mm), while it is resistant to oxacillin and amikacin.

The study by Venubabu Thati et al.(2010) on the effect of antibiotics on *S. aureus* showed DZIs of 15, 0, 14 and 22 mm with oxacillin (15 mm), amoxicillin (0 mm), amikacin (14 mm), tetracycline (22 mm), respectively.

A 25 mm DZI was found on *B. cereus* with the antibiotic tetracycline(Venubabu Thati et al., 2010). This result is lower than that found in our study on the same strain (37.75 mm). Furthermore, the DZI of the extract of *R. alaternus* on *B. cereus* is higher than those obtained with oxacillin and amoxicillin.

Three antibiotics (amikacin, tetracycline and amoxicillin) were tested on *S. aureus* and *E. coli*. The DZIs found were: 23 mm (amikacin), 7.5 mm (amoxicillin) and 25 mm (tetracycline), for *S. aureus*. In contrast, the DZIs found on *E. coli* are 10 mm (amoxicillin), 27 mm (amikacin), 25 mm (tetracycline)(Venubabu Thati et al., 2010).These results are lower than those obtained in our study for the two strains *Staphylococcus aureus* and *E. coli* .

III.5.2. Antibacterial activity of *P. angustifolia* and *R. alaternus* extracts

The results of the antibacterial activity of the extracts of the two tested plants obtained under optimal extraction conditions are grouped together in the Figure 16.

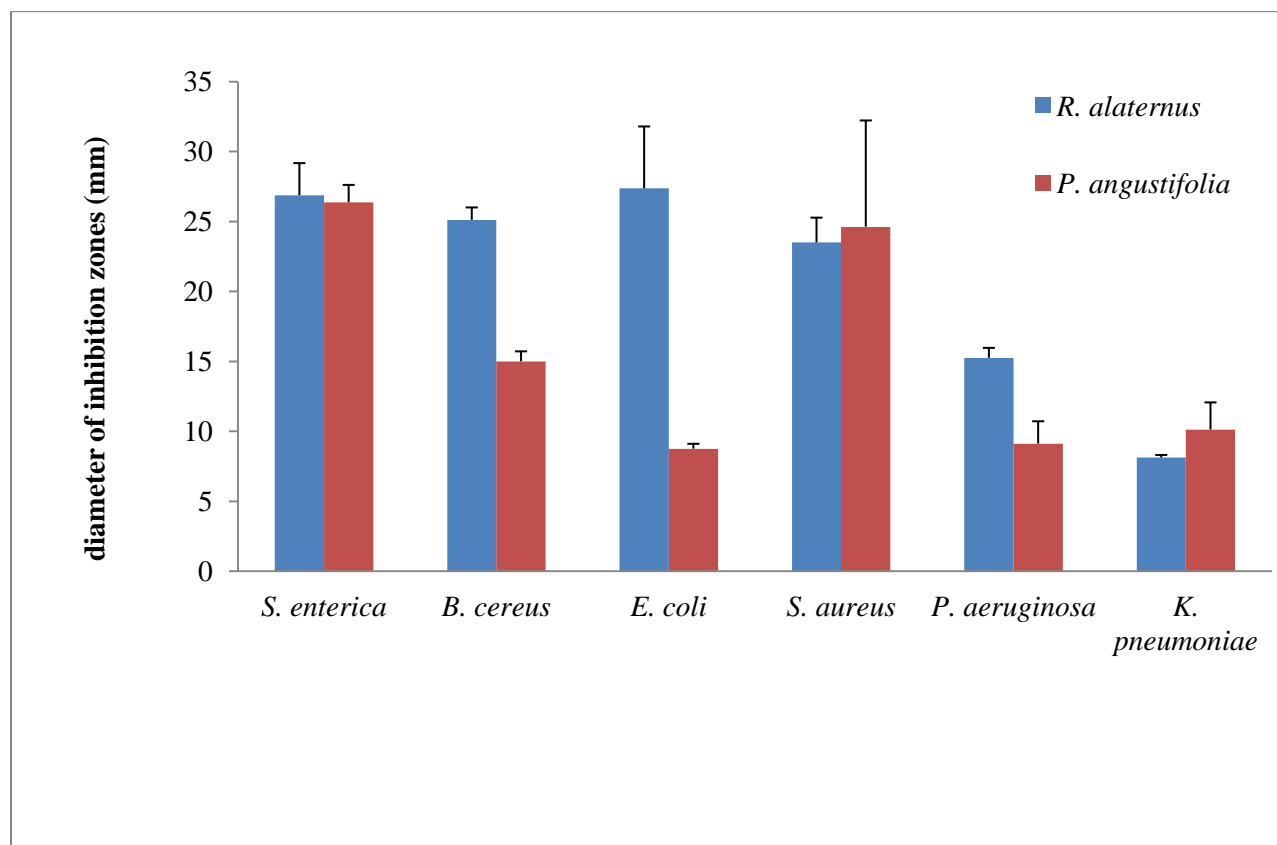


Figure 16. Antibacterial activity of *R. alaternus* and *P. angustifolia* extracts

The results obtained with the disc diffusion on agar method show that the optimized extracts of the two plants studied have a strong antibacterial activity against the majority of the strains tested with inhibition zone diameters (DZI) ranging from 8.12 to 27.37 mm.

The largest inhibition zone diameters are obtained with *R. alaternus* extract on the bacterial strains *E. coli*, *S. enterica*, *B. cereus* and *S. aureus* which are 27.37; 26.87; 25.12 and 23.5 mm, respectively.

The strain most resistant to *R. alaternus* extract is *K. pneumoniae* with a DZI of 8.12 mm. On the other hand, in the case of *P. angustifolia* extract, the strongest antibacterial activity is obtained on *S. enterica* and *S. aureus* strains with DZIs of 26.87 and 27.37 mm, respectively.

The strain most resistant to *P. angustifolia* extract is *E. coli* with a DZI of 8.75mm.

The extract of *R. alaternus* obtained under optimal extraction conditions (83 min, 58% EtOH and ratio of 1) had the strongest antibacterial effect on all strains tested except for *S. aureus* and *K. pneumoniae*.

A study carried out by Kosalec et al.(2013a) on the ethanolic extract of *Rhamnus alaternus* at a concentration of 20 mg/ml showed low activity on *Staphylococcus aureus* (12 mm), *Pseudomonas aeruginosa* (10 mm), *Escherichia coli* (10 mm). These results are lower than those obtained in our study for the same species.

Carranza et al.(2015) have shown the antibacterial effect of *Rhamnus californica* extract (1mg/ml) harvested in America on *Bacillus cereus* (10 mm), *Staphylococcus aureus* methicillin-resistant(MRSA) (10 mm), on the other hand, with no effect on *Staphylococcus aureus*, *Pseudomonas aeruginosa* and *Escherichia coli*.

Zeouk and Bekhti.(2020) found that the DZI of ethanolic extract from the leaves of *R. alaternus* obtained against two bacteria, *S. epidermidis* and *S. aureus* ATCC 29213, were 16 ± 1 mm and 25 ± 1 mm, respectively. The latter is consistent with that obtained in our study.

Malik.(2015) In their study show that *Olea europaea* and arugula extract were effective against the two Gram-positive strains (*Staphylococcus aureus*) but low activity was observed against the Gram- strain (*Bacillus cereus*).

A study conducted by Pavithra et al.(2013) on *Olea dioica* flower extract (50 mg/mL) showed low activity on *S. aureus* (14 mm), *B. cereus* (13 mm) and *E. coli* (11 mm). These results are lower than those obtained in our study with *P. angustifolia*.

The inhibitory effect of phenolic compounds on bacterial growth can be explained by several reasons. Among the hypothesis put forward, we can cite the chelation of metals such as iron which is necessary for microbial growth, the action on the membranes of microorganisms leading to the loss of its structural integrity and finally the action on bacterial metabolism (Clériveret et al., 1996).

III.5.3. Micro-dilution method minimal in (MIC)

The minimal inhibitory concentration (MIC) is the most common parameter used to evaluate the effect of an extract. It corresponds to the smallest concentration of antibiotic that inhibits the visible growth of the germ in 24H for rapidly multiplying bacteria (lack of increase in bacteria).

The results obtained with the microdilution method are represented as follows the table below:

Table IX: Antibacterial properties minimal inhibition concentration (MIC) of *Rhamnus alaternus* and *Phillyrea angustifolia* extracts.

Strains	<i>Rhamnus alaternus</i> (MIC)	<i>Phillyrea angustifolia</i> (MIC)
	($\mu\text{l /ml}$)	($\mu\text{l /ml}$)
<i>Salmonella enterica</i>	6.25 \pm 0.1	6.25 \pm 0.3
<i>Bacillus cereus</i>	2.01 \pm 0.06	6.25 \pm 0.12
<i>Escherichia coli</i>	6.25 \pm 0.19	16.25 \pm 0.5
<i>Staphylococcus aureus</i>	6.5 \pm 0.42	5.8 \pm 0.34
<i>Pseudomonas aeruginosa</i>	25.5 \pm 0.2	25.5 \pm 0.17
<i>Klebsiella pneumoniae</i>	25.5 \pm 0.8	23.5 \pm 0.6

This test was performed at five concentrations (20, 40, 60, 80 and 100 $\mu\text{l/ml}$) of each optimum extracts.

The IC₅₀CMI results showed that optimum extract of *Rhamnus alaternus* demonstrated antibacterial activity against six bacterial strains and the most susceptible is against *Bacillus cereus* IC 50 (2.01 \pm 0.06 $\mu\text{l/ml}$).

The IC₅₀CMI results showed that optimum extract of *Phillyrea angustifolia* demonstrated antibacterial activity against six bacterial strains and the signifying higher activity is observed against *Staphylococcus aureus* IC 50 (5.8 \pm 0.34 $\mu\text{l/ml}$).

To our knowledge, literature data reporting the antimicrobial potential of *R.alaternus* More specifically, based on the agar disc diffusion assay, methanolic extracts, Kosalec et al.(2013a) find in their research MIC value of 0.625 mg/mL. *R. alaternus* collected in Tunisia have shown *In vitro* antibacterial activity against *S. aureus*, *E. faecalis*, *E. coli*, *Salmonella enteritidis* and *Salmonella typhimurium* strains.

Cowan.(1999), has reported that the different classes of polyphenols, mainly the tannins and flavonoids can increase the toxicity of extracts towards the microorganisms. This toxicity depends on the site and the number of hydroxyl groups present on the phenolic compound. Furthermore, it is evident that the increase of Hydroxylation leads to an increase in toxicity.

The mechanism of the antimicrobial effects of polyphenols is undoubtedly very complex among the hypotheses put forward, the inhibition of nucleic acid synthesis, the alteration of the functions of the cytoplasmic membrane, the sequestration of substrates necessary for the microbial growth and inhibition of microbial energy metabolism (Jungkind et al., 2013).

III.6. Anti-inflammatory activities

III.6.1. Inhibition of BSA denaturation

Inflammation is reaction process in living tissue induced by inflammatory agents such as physical injury, microbial infections, and harmful chemical irritations. The response of cells to inflammation leads to certain pathological reactions characterized by redness, heat, swelling, and pain, or even physiological dysfunction. In general Inflammation is implicated in many diseases, including arthritis, stroke, and cancer (Ricciotti and FitzGerald, 2011). Protein denaturation leads to inflammatory response and various inflammatory diseases, including arthritis (Mizushima, 1966). According to Opie.(1962), tissue damage throughout life may be related to the denaturation of the cell's constituent proteins or intercellular material. Thus, the ability of a substance to inhibit protein denaturation means an apparent potential for anti-inflammatory activity. There are certain problems in using animals in experimental pharmacological research, such as ethical issues and the lack of rationale for their use when other suitable methods are available or could be investigated. For this purpose, in the present study the protein denaturation bioassay was selected for *In vitro* assessment of anti-inflammatory property of optimized extracts of two plants *R. alaternus* and *P. angustifolia*.

The capacity of different optimized extracts of *R. alaternus* and *P. angustifolia* to inhibit BSA denaturation which was ranging from $IC_{50} 250.27 \pm 0.98 \mu\text{g/mL}$ and $IC_{50} 73.03 \pm 0.04 \mu\text{g/mL}$ respectively, extracts had a good anti-denaturation activity of the BSA inhibition, in this assay *P. angustifolia* had therefore provided another evidence for its promising anti-inflammatory properties. In the current study, ibuprofen is used as the reference compound anticipated exerting optimally positive inhibition percentage. A statistical analysis had shown that there were significant differences ($P < 0.5$) between two plants, whereby the extract exhibited significant differences in multiple comparison analysis student's t test using GraphPad Prism 6.

In literature, the anti-inflammatory activity can be explained by the presence in the plants polyphenolic compounds such as hydrolysable tannins and flavonoids (Zarfeshany et al., 2014).

The major constituents of *R. alaternus*, polyphenolic compounds like flavonoids and phenolic acid (Ben Ammar et al., 2018). Polyphenols are well known natural products known to possess several notable biological properties. Flavonoids and their glycosides present in *Rhamnus prinoides* have shown inhibitory action of inflammation reducing the LPS-stimulated NO in Macrophage RAW 264.7 Cells and COX-2 inhibitory activity (Chen et al., 2020).

The major constituents of *P. angustifolia* polyphenolic compounds like tannins and flavonoids. Several studies shown that diet rich on phenolic compounds have significant anti-inflammatory effects, including inhibition of adhesion molecule, cytokine and chemokine gene expression; inhibition of platelet function; augmentation of endothelial nitric oxide release; suppression of smooth muscle activation; and other effects on proinflammatory factors such as endothelin and matrix metalloproteinases (Lee et al., 2006).

III.6.2. Proteinase Inhibitory Action

Proteinase leukocytes come from Neutrophils, they play an important role in tissue development damaged during inflammatory reactions and provide protection by proteinase inhibitors (Leelaprakash and Dass, 2011).

The capacity of different optimized extracts of *R. alaternus* and *P. angustifolia* to inhibit Proteinase Activity was ranging from IC_{50} 28.87 ± 1.87 ($\mu\text{g/ml}$) and IC_{50} 21.40 ± 0.18 ($\mu\text{g/ml}$) respectively. A statistical analysis had shown that there were no significant differences ($P < 0.05$) between two plants, whereby the extract exhibited significant differences in multiple comparison analysis student's t test (graphpad- prism 6). Naz et al. (2017) shown that the effect could be explained by the fact phenolic compound on anti-inflammatory as well as anti-proteinase inhibition activity. The exact mechanism can be explained that interaction of phenols compounds with site(s) distal from the trypsin active site; In agreement with earlier findings.

III.6.3. Anti-hemolytic activity

The erythrocyte hemolysis test has long been used since the human red blood cells (HRBC) are similar to the lysosomal enzyme membrane components.

Optimum extracts from *R. alaternus* and *P. angustifolia* exerted the best anti-hemolytic with an IC_{50} 142.4 ± 1 $\mu\text{g/ml}$ and 160.40 ± 4.48 $\mu\text{g/ml}$ respectively. We demonstrated that both of optimum extracts from *R. alaternus* and *P. angustifolia* at concentration range (100-500 $\mu\text{g/ml}$) protects the human erythrocyte membrane against lysis induced by hypotonic solution.

In the literature reports, several hypothetical mechanisms are proposed. We can cite some of them; polyphenols extracts could influence the surface area/volume ratio of the erythrocyte cells which could be induced by an expansion of membrane of the cell, and an interaction with membrane proteins (Shinde et al., 1999). This protective effect may be due to the ability of the extracts to modify the flow of calcium in the erythrocyte.

Omale and Okafor.(2008), reported that the effect of anti-inflammatory drugs including plants preparation on the stabilization of erythrocyte membrane exposed to hypotonic and heat that the effect could be due to the binding to proteins plasma, in particular membrane proteins, thus contributing either to the regulation of the intracellular water volume by controlling the movement of sodium and potassium ions through protein channels. In another study, have shown that flavonoids exhibit analgesic and anti-inflammatory effects as a result of their membrane stabilizing ability in various experimental models (Ranasinghe et al., 2012).

III.7. Cyto-toxicity activity

Cyto-toxicity activity is used on human erythrocytes to determine toxicity parameters for human use. This method assay is one tool that the pharmaceutical scientist may use as a guide to assess the safety and utility of a parenteral formulation (Pagano and Faggio, 2015).

The results showed that no hemolysis was induced by any of Optimum extracts from *R. alaternus* and *P. angustifolia* at all concentrations tested, no significant difference between the hemolysis percentages of the negative control and those obtained with the different concentrations of the optimum extracts. This results means that two extracts do not present any toxicity even at high concentration.

III.8. Enzymatic activity

III.8.1. α -Amylase Inhibition

In this study, we have investigated the potential antidiabetic effect of optimized extract for phenolic content as natural sources against α -amylase and α -glucosidase inhibitors for modulation of post-prandial hyperglycemia by decreasing meal-derived carbohydrate absorption.

An unexpected increase of glucose levels in blood causes hyperglycemia in type-2 diabetes patients due to hydrolysis of starch by pancreatic α -amylase and the consequent absorption of glucose by intestinal α -glucosidase. Thus, the strong inhibition of α -glucosidase and mild inhibition of pancreatic α -amylase is believed to be an effective strategy for type-2 diabetes management (Krentz and Bailey, 2005). The enzyme α -amylase breaks down long carbohydrate chains and α -glucosidase breaks down starch and disaccharides into glucose. These enzymes serve as major digestive enzymes and help in intestinal absorption. Importantly, α -amylase and α -glucosidase are potential targets in producing lead compounds for the management of diabetes (Rocchetti et al., 2019).

The inhibitory potencies of *R. alaternus* and *P. angustifolia* extracts on α -amylase and α -glucosidase activity are summarized in Table X.

Table X. Inhibitory activities of *Rhamnus alaternus* and *Phillyrea angustifolia* towards α -amylase and α -glucosidase

	α -Amylase (IC ₅₀ , μ g/mL)	α -Glucosidase(IC ₅₀ , μ g/mL)
<i>Rhamnus alaternus</i>	0.08 \pm 0.01	0.7 \pm 0.03
<i>Phillyrea angustifolia</i>	0,71 \pm 0,02	1.9 \pm 0.08
<i>Acarbose</i>	145.2 \pm 1.3	275.4 \pm 1.6

Values are means of three independent assays \pm SD

Acarbose showed the lowest IC₅₀, establishing its relative potency as α -Amylase inhibitor. Maximum inhibition was found to be 0.08 \pm 0.01, μ g/mL. *Rhamnus alaternus* showed a strong inhibition pattern against α -amylase activity, no significantly higher than *Phillyrea angustifolia*. few study has been done on inhibition α -Amylase of two species studied.

Ben Bacha et al.(2018), showed that methanolic extract of *Rhamnus frangula* leaves significantly inhibited α -glucosidase and α -amylase activities with 3.09 ± 0.15 and 45.86 ± 3.45 , respectively.

Uysal.(2020), demonstrated that the ethyl acetate extract exhibited the highest inhibitory effect for all tested of α -amylase, α -glucosidase and tyrosinase *Phillyrea latifolia*.

Many investigation shows that catechins may contribute to the inhibitory effects of the various extracts tested (Hara and Honda, 1990; Yilmazer-Musa et al., 2012). The structure of a polyphenol defines its binding affinity to the enzyme. For instance, the double bond between C2 and C3 of ring C in flavonoids increases the intensity of the electron cloud in ring C, which stabilizes the π - π conjugation between ring A (or B) with the aromatic ring of tryptophan in α -amylase (Zheng et al., 2020).

III.8.2. α -Glucosidase Inhibition

Compared to its strong inhibitory effect on α -glucosidase, acarbose was much less potent in inhibiting α -glucosidase (Figure 17). The IC_{50} values of acarbose for α -glucosidase activity were higher than those values for α -amylase. The highest inhibition α -Glucosidase tested (IC_{50} 0.7 μ g/mL) observed in *Rhamnus alaternus* extract. Interestingly, all extracts tested were much more potent inhibitors of α -glucosidase than acarbose (Table X).

Only few studies are reported inhibition α -Glucosidase of the two species studied.

The results of The enzyme inhibitory (α -glucosidase and α -amylase) potential of *Rhamnus petiolaris* fond by Rocchetti et al.(2019) is 0.58 ± 0.01 and 1.86 ± 0.01 μ g/ml respectively.

It has been found enzyme inhibitory effects of the members of the genus *Rhamnus*, the present findings seem to be consistent with other research (Bacha et al., 2018) which found the best amylase and glucosidase inhibitory effects for methanol extract of *Rhamnus frangula* leaves. Also, *Rhamnus lycioides* subsp. *oleoides* anthraquinone rich extract exerted a notable anti-acetylcholinesterase activities (Benamar et al., 2019a).

Dinda.(2019), in their study show that *phillyrea latifolia* has enzyme inhibitory (α -glucosidase and α -amylase) 0.43 and 1.73 μ g/ml. The enzyme inhibitory effect of studied extracts was related to total phenolic content.

Various mechanisms of action of medicinal plants with an effect on diabetes have been reported from studies of medicinal plants or their extracts used in the treatment of diabetes may act by different mechanisms:

 In terms of carbohydrate homeostasis

- Stimulate the secretion of insulin from the β cells and/or also induce their regeneration(Mukherjee et al., 2006).
- Action by the contribution of necessary elements (Cu^{++} , Mg^{++} , Ca^{++}) to the functioning of the cells, and also the revitalisation and/or hyperplasia of these cells(Mukherjee et al., 2006).
- Action on hepatic enzymes by stimulating and/or inhibition of Gluconeogenesis (El-Abhar and Schaalan, 2014).

 Intestinal level

- Modification of gene expression and the activity of hormones involved in digestion such as adiponectin, resistin, and incretin,
Inhibitory action on digestive enzymes such as α -amylase and α -glucosidases, reducing the breakdown of starch and oligosaccharides, therefore they act by slowing and reducing the absorption of glucose in the intestine,
- Inhibition of glucose transporters at the intestinal barrier, thus limiting intestinal glucose absorption, or by stimulation of glucose uptake by adipocytes or muscle cells (Chang et al., 2013; Ríos et al., 2015).

VI. Conclusion

The present study aims to optimize the extraction of phenolic compounds and the antioxidant activity of extracts from the leaves of *Phillyrea angustifolia* and *Rhamnus alaternus* obtained by the conventional extraction method using an experimental design with three variables and the study of two responses. Thus to evaluate the biological activity (antibacterial, anti-inflammatory activity, antioxidant activities and antidiabetic activity) of the extracts of the two plants studied.

The highest moisture content is obtained in the leaves of *R. alaternus*, which is $62.14 \pm 1.69\%$, and $48.88 \pm 0.69\%$ for *P. angustifolia*.

The crude extracts of *R. alaternus* and *P. angustifolia* are rich in carotenoids with contents of 93.74 and 79.74 mg β -carotene / 100 g, respectively.

The Box-Benken plan made it possible to identify the best parameters for having the highest content of total polyphenols and the highest scavenging effect of the free radical DPPH which are an extraction time of 83 min, an ethanol percentage of 58 % and a ratio of 1.2 for *R. alaternus* and an extraction time of 30 min, a percentage in ethanol of 47% and a ratio of for *P. angustifolia*.

The contents of total polyphenols and the scavenging effect of the free radical DPPH found, under optimal conditions are 79.40 mg EAG / g DM and 63.72 μ g EAG / mL, respectively in the case of *P. angustifolia* and 70.36 mg EAG / g MS and 69.49 μ g EAG / mL, respectively for the extract of *R. alaternus*.

The flavonoid content of the extract of *R. alaternus* (17.17 mg EQ / g DM) is higher than that of *P. angustifolia* which is 7.04 mg EQ / g DM.

Concerning the contents of condensed tannins, the plants studied have low contents, which are 1.86 and 0.98 mg EQ Cyanidine / g DM for *R. alaternus* and *P. angustifolia*, respectively.

The results of the reducing power test and the total antioxidant activity determined by the ammonium phosphomolybdate test of the extract of *R. alaternus* are 16.92 mg EAG / g MS and 112.86 mg EAG / g MS, respectively. On the other hand, a reducing power of 14.69 mg EAG / g MS and a total antioxidant activity of 85.84 mg EAG / g MS are obtained in the case of *P. angustifolia*

The strong trapping effect of ABTS⁺ cations is obtained in the case of extract *R. alaternus*., followed by *P. angustifolia* extract with IC₅₀ values 3 ± 0.02 and $22 \pm 0.1 \mu\text{g} / \text{ml MS}$, respectively.

Superoxide radical scavenging results of the optimized extracts of the two plants tested show that they have reducing capacity nitro blue tetrazolium (NBT) to a purple formazan.

The optimum extracts of the two plants studied shows antibacterial activity on all the strains tested. The strongest antibacterial activity is obtained with the extract of *R. alaternus* on *E.coli* and *S. enterica* with DZIs of 27.37 and 26.87 mm, respectively. Thus, the *K. pneumoniae* strain is resistant to the extract of *R. alaternus* with a DZI of 8.12 mm.

The optimal extracts obtain from two species was tested anti-inflammatory activity *In vitro* assessed with two tests (denaturation protein inhibition and antiproteinase) *P. angustifolia* exhibited a very interesting activities.

The optimized extract of *Rhamnus alaternus* has a good potential inhibition α -amylase and α -glucosidase.

In general we can say that the extracts of *R. alaternus* and *P. angustifolia* are an important source of phenolic compounds and have a good antioxidant potential thus a good antibacterial activities and can be used in the pharmaceutical industries against free radicals and in the food industry in order to extend the shelf life of food.

Fist Part

References

V. References

Abdelkrim, B., Khaled, K., Miloud, S., Imane, D., Kheira, A., 2015. Hepatoprotective effects of the decoction and macerated leaves of *Rhamnus alaternus* L. on rats exposed to carbon tetrachloride. *Journal of Pharmacognosy and Phytotherapy* 7, 253-262.

Afonso, A.F., Pereira, O.R., Valega, M., Silva, A.M.S., Cardoso, S.M., 2018. Metabolites and Biological Activities of *Thymus zygis*, *Thymus pulegioides*, and *Thymus fragrantissimus* Grown under Organic Cultivation. *Molecules* 23.

Agüero, M.a.B.n., Gonzalez, M., Lima, B., Svetaz, L., Sanchez, M., Zacchino, S., Feresin, G.E., Schmeda-Hirschmann, G., Palermo, J., Wunderlin, D., 2010. Argentinean propolis from *Zuccagnia punctata* Cav.(Caesalpinieae) exudates: phytochemical characterization and antifungal activity. *Journal of Agricultural and Food Chemistry* 58, 194-201.

Ahangarpour, A., Sayahi, M., Sayahi, M., 2019. The antidiabetic and antioxidant properties of some phenolic phytochemicals: A review study. *Diabetes & Metabolic Syndrome: Clinical Research & Reviews* 13, 854-857.

AlGamdi, N., Mullen, W., Crozier, A., 2011. Tea prepared from *Anastatica hirerochuntica* seeds contains a diversity of antioxidant flavonoids, chlorogenic acids and phenolic compounds. *Phytochemistry* 72, 248-254.

Ali Asgar, M., 2012. Anti-Diabetic Potential of Phenolic Compounds: A Review. *International Journal of Food Properties* 16, 91-103.

Amadeo, S., Benradia, I., David, G., Rereao, M., Tuheiava, A., Favro, P., VILHEM, S., Aminata, S., Fenni, A., Nguyen, N.L., 2020. Social Representations and Anthropo-Cultural Aspects of Mental Health in French Polynesia in the Survey" Mental Health in the General Population: Images and Realities".

Amirouche, R., Misset, M.-T., 2009. Flore spontanée d'Algérie : différenciation écogéographique des espèces et polyploïdie. *Cahiers Agricultures* 18, 474-480.

Ammar, H., Lopez, S., Gonzalez, J., 2005a. Assessment of the digestibility of some Mediterranean shrubs by in vitro techniques. *Animal feed science and technology* 119, 323-331.

Ammar, H., López, S., González, J.S., 2005b. Assessment of the digestibility of some Mediterranean shrubs by in vitro techniques. *Animal Feed Science and Technology* 119, 323-331.

Ammar, R.B., Bhouiri, W., Sghaier, M.B., Boubaker, J., Skandrani, I., Neffati, A., Bouhlel, I., Kilani, S., Mariotte, A.-M., Chekir-Ghedira, L., Dijoux-Franca, M.-G., Ghedira, K., 2009. Antioxidant and free radical-scavenging properties of three flavonoids isolated from the leaves of *Rhamnus alaternus* L. (Rhamnaceae) : A structure-activity relationship study. *Food Chemistry* 116, 258-264.

Ammar, R.B., Bouhlel, I., Valenti, K., Sghaier, M.B., Kilani, S., Mariotte, A.M., Dijoux-Franca, M.G., Laporte, F., Ghedira, K., Chekir-Ghedira, L., 2007. Transcriptional response of genes involved in cell defense system in human cells stressed by H₂O₂ and pre-treated with (Tunisian) *Rhamnus alaternus* extracts: combination with polyphenolic compounds and classic in vitro assays. *Chemico-biological interactions* 168, 171-183.

Ammar, R.B., Neffati, A., Skandrani, I., Sghaier, M.B., Bhouiri, W., Ghedira, K., Chekir-Ghedira, L., 2011. Anti-lipid peroxidation and induction of apoptosis in the erythroleukaemic cell line K562 by extracts from (Tunisian) *Rhamnus alaternus* L. (Rhamnaceae). *Natural product research* 25, 1047-1058.

Ammar, R.B., Sghaier, M.B., Boubaker, J., Bhouiri, W., Naffeti, A., Skandrani, I., Bouhlel, I., Kilani, S., Ghedira, K., Chekir-Ghedira, L., 2008. Antioxidant activity and inhibition of aflatoxin B1-, nifuroxazide-, and sodium azide-induced mutagenicity by extracts from *Rhamnus alaternus* L. *Chemico-biological interactions* 174, 1-10.

Ashfaq, K., Choudhary, B.A., Uzair, M., Qaisar, M.N., Hussain, S.N., Ghaffari, M.A., 2017. evaluation of alpha-glucosidase, urease inhibition and antioxidant potential of *Acacia jacquemontii* and *Rhamnus persica*. *indo American Journal of Pharmaceutical Sciences* 4, 3913-3918.

Assiliadis, C.V., 1999. Evolution et maintien de l'androdioécie Etude théorique et approches expérimentales chez *Phillyrea angustifolia* L., Université des Sciences et Technologies de Lille. Université de Lille 1, p. 142.

Aurand, J.-M., Tartian, A.C., Cotea, V.V., Niculaua, M., Zamfir, C.-I., Colibaba, C.L., Moroşanu, A.-M., 2017. The influence of the different techniques of maceration on the aromatic and phenolic profile of the Busuioacă de Bohotin wine. *BIO Web of Conferences* 9, 02032.

- Ayranci, E., Erkan, N., 2013. Radical scavenging capacity of methanolic *Phillyrea latifolia* L. extract: anthocyanin and phenolic acids composition of fruits. *Molecules* 18, 1798-1810.
- Azaizeh, H., Halahleh, F., Abbas, N., Markovics, A., Muklada, H., Ungar, E.D., Landau, S.Y., 2013. Polyphenols from *Pistacia lentiscus* and *Phillyrea latifolia* impair the exsheathment of gastro-intestinal nematode larvae. *Veterinary parasitology* 191, 44-50.
- Azeem, A.K., Dilip, C., Prasanth, S.S., Shahima, V.J.H., Sajeev, K., Naseera, C., 2010. Anti-inflammatory activity of the glandular extracts of *Thunus alalunga*. *Asian Pacific Journal of Tropical Medicine* 3, 794-796.
- Bacha, A.B., Jemel, I., Bhat, R.S., Onizi, M.A., 2018. Inhibitory effects of various solvent extracts from *Rhamnus frangula* leaves on some inflammatory and metabolic enzymes. *Cellular and Molecular Biology* 64, 55-62.
- Balasundram, N., Sundram, K., Samman, S., 2006. Phenolic compounds in plants and agri-industrial by-products: Antioxidant activity, occurrence, and potential uses. *Food Chemistry* 99, 191-203.
- Ben Ammar, R., Kilani, S., Bouhlel, I., Ezzi, L., Skandrani, I., Boubaker, J., Ben Sghaier, M., Naffeti, A., Mahmoud, A., Chekir-Ghedira, L., 2008. Antiproliferative, antioxidant, and antimutagenic activities of flavonoid-enriched extracts from (Tunisian) *Rhamnus alaternus* L.: combination with the phytochemical composition. *Drug and chemical toxicology* 31, 61-80.
- Ben Ammar, R., Miyamoto, T., Chekir-Ghedira, L., Ghedira, K., Lacaille-Dubois, M.-A., 2018. Isolation and identification of new anthraquinones from *Rhamnus alaternus* L and evaluation of their free radical scavenging activity. *Natural Product Research* 33, 280-286.
- Ben Ammar, R., Miyamoto, T., Chekir-Ghedira, L., Ghedira, K., Lacaille-Dubois, M.A., 2019. Isolation and identification of new anthraquinones from *Rhamnus alaternus* L and evaluation of their free radical scavenging activity. *Natural product research* 33, 280-286.
- Ben Bacha, A., Jemel, I., Bhat, R.S., Onizi, M.A., 2018. Inhibitory effects of various solvent extracts from *Rhamnus frangula* leaves on some inflammatory and metabolic enzymes. *Cellular and Molecular Biology* 64, 55.
- Benamar, H., Rarivoson, E., Tomassini, L., Frezza, C., Marouf, A., Bennaceur, M., Nicoletti, M., 2019a. Phytochemical profiles, antioxidant and anti-acetylcholinesterasic activities of the leaf extracts of *Rhamnus lycioides* subsp. *oleoides* (L.) Jahand. & Maire in different solvents. *Natural product research* 33, 1456-1462.

Benamar, H., Rarivoson, E., Tomassini, L., Frezza, C., Marouf, A., Bennaceur, M., Nicoletti, M., 2019b. Phytochemical profiles, antioxidant and anti-acetylcholinesterasic activities of the leaf extracts of *Rhamnus lycioides* subsp. *oleoides* (L.) Jahand. & Maire in different solvents. *Natural product research* 33, 1456-1462.

Benchiha, W., 2016. Phyto-écologie et étude biochimique des composants phénoliques (traitement in vivo contre hépatite) de *Rhamnus alaternus* L. des monts de Tessala wilaya de Sidi Bel Abbes.

Benchiha, W., Mahroug, S., Aoued, L., Bouterfas, K., 2015. Activité antihépatotoxique des extraits des feuilles de *Rhamnus alaternus* L. (Rhamnaceae). *Phytothérapie* 15, 10-15.

Benkiki, N., 2006. Etude phytochimique des plantes médicinales algériennes. Batna, Université El Hadj Lakhder. Faculté des sciences.

Bezerra, F.W.F., de Oliveira, M.S., Bezerra, P.N., Cunha, V.M.B., Silva, M.P., da Costa, W.A., Pinto, R.H.H., Cordeiro, R.M., da Cruz, J.N., Chaves Neto, A.M.J., Carvalho Junior, R.N., 2020. Extraction of bioactive compounds. 149-167.

Bezerra, M.A., Santelli, R.E., Oliveira, E.P., Villar, L.S., Escaleira, L.A., 2008. Response surface methodology (RSM) as a tool for optimization in analytical chemistry. *Talanta* 76, 965-977.

Bhourri, W., Boubaker, J., Kilani, S., Ghedira, K., Chekir-Ghedira, L., 2012. Flavonoids from *Rhamnus alaternus* L.(Rhamnaceae): Kaempferol 3-O- β -isorhamninoside and rhamnocitrin 3-O- β -isorhamninoside protect against DNA damage in human lymphoblastoid cell and enhance antioxidant activity. *South African Journal of Botany* 80, 57-62.

Bhourri, W., Sghaier, M.B., Kilani, S., Bouhlel, I., Dijoux-Franca, M.-G., Ghedira, K., Ghedira, L.C., 2011. Evaluation of antioxidant and antigenotoxic activity of two flavonoids from *Rhamnus alaternus* L.(Rhamnaceae): Kaempferol 3-O- β -isorhamninoside and rhamnocitrin 3-O- β -isorhamninoside. *Food and chemical toxicology* 49, 1167-1173.

Bohui, P.S.G., Adima, A.A., Niamké, F.B., N'Guessan, J.D., 2018. Etude comparative de trois méthodes d'extraction des flavonoïdes totaux à partir des feuilles de plantes médicinales : *Azadirachta indica* et *Psidium guajava*. *Journal de la Société Ouest-Africaine de Chimie* 046, 50 - 58.

Borris, R.P., 1996. Natural products research: perspectives from a major pharmaceutical company. *Journal of ethnopharmacology* 51, 29-38.

- Bougatef, A., Hajji, M., Balti, R., Lassoued, I., Triki-Ellouz, Y., Nasri, M., 2009. Antioxidant and free radical-scavenging activities of smooth hound (*Mustelus mustelus*) muscle protein hydrolysates obtained by gastrointestinal proteases. *Food chemistry* 114, 1198-1205.
- Bourgou, S., Ksouri, R., Bellila, A., Skandrani, I., Falleh, H., Marzouk, B., 2008. Phenolic composition and biological activities of Tunisian *Nigella sativa* L. shoots and roots. *Comptes Rendus Biologies* 331, 48-55.
- Boussahel, S., Dahamna, S., Ruberto, G., Siracusa, L., Harzallah, D., 2013. Phytochemical Study and Antioxidant Activities of Leaves Extracts from *Rhamnus alaternus* L. *Pharmacognosy Communications* 3, 46.
- Boussahel, S., Speciale, A., Dahamna, S., Amar, Y., Bonaccorsi, I., Cacciola, F., Cimino, F., Donato, P., Ferlazzo, G., Harzallah, D., Cristani, M., 2015. Flavonoid profile, antioxidant and cytotoxic activity of different extracts from Algerian *Rhamnus alaternus* L. bark. *Pharmacognosy magazine* 11, S102-109.
- Brand-Williams, W., Cuvelier, M.-E., Berset, C., 1995. Use of a free radical method to evaluate antioxidant activity. *LWT- Food science and Technology* 28, 25-30.
- Bravo, A., Anaconda, J.R., 2001. Metal complexes of the flavonoid quercetin: antibacterial properties. *Transition Metal Chemistry* 26, 20-23.
- Caravaca, F., Alguacil, M.M., Hernández, J.A., Roldán, A., 2005. Involvement of antioxidant enzyme and nitrate reductase activities during water stress and recovery of mycorrhizal *Myrtus communis* and *Phillyrea angustifolia* plants. *Plant Science* 169, 191-197.
- Carranza, M.G., Sevigny, M.B., Banerjee, D., Fox-Cubley, L., 2015. Antibacterial activity of native California medicinal plant extracts isolated from *Rhamnus californica* and *Umbellularia californica*. *Annals of clinical microbiology and antimicrobials* 14, 29.
- Chakraborty, G.S., 2009. Free radical scavenging activity of *Aesculus indica* leaves. *Int J Pharm Tech Res* 1, 524-526.
- Chang, F., He, X., Huang, Q., 2013. Effect of lauric acid on the V-amylose complex distribution and properties of swelled normal cornstarch granules. *Journal of Cereal Science* 58, 89-95.
- Chen, G., Li, X., Saleri, F., Guo, M., 2016. Analysis of Flavonoids in *Rhamnus davurica* and Its Antiproliferative Activities. *Molecules* 21.
- Chen, G.L., Munyao Mutie, F., Xu, Y.B., Saleri, F.D., Hu, G.W., Guo, M.Q., 2020. Antioxidant, Anti-inflammatory Activities and Polyphenol Profile of *Rhamnus prinoides*. *Pharmaceuticals* 13.

- Clérivet, A., Alami, I., Breton, F., Garcia, D., Sanier, C., 1996. Les composés phénoliques et la résistance des plantes aux agents pathogènes. *Acta Botanica Gallica* 143, 531-538.
- Cornelli, U., 2009. Antioxidant use in nutraceuticals. *Clinics in dermatology* 27, 175-194.
- Cowan, M.M., 1999. Plant products as antimicrobial agents. *Clinical microbiology reviews* 12, 564-582.
- Cushnie, T., Hamilton, V., Chapman, D., Taylor, P., Lamb, A., 2007. Aggregation of *Staphylococcus aureus* following treatment with the antibacterial flavonol galangin. *Journal of applied microbiology* 103, 1562-1567.
- D'Alessandro, L.G., 2013. Eco-procédés pour la récupération sélective d'antioxydants à partir d'*Aronia melanocarpa* et ses co-produits, Ecole Doctorale Sciences de la Matière, du Rayonnement et de l'Environnement. Université Lille 1 Sciences et Technologies, p. 169.
- Dahmoune, F., Boulekbache, L., Moussi, K., Aoun, O., Spigno, G., Madani, K., 2013. Valorization of *Citrus limon* residues for the recovery of antioxidants: evaluation and optimization of microwave and ultrasound application to solvent extraction. *Industrial Crops and Products* 50, 77-87.
- Damtoft, S., Franzky, H., Jensen, E.S.R., 1993. Biosynthesis of secoiridoid glucosides in Oleaceae. *Phytochemistry* 34, 1291-1129.
- Dangles, O., Dufour, C., 2008. Flavonoid-protein binding processes and their potential impact on human health. *Recent advances in polyphenol research* 1, 67-87.
- DellaGreca, M., Mancino, A., Previtera, L., Zarrelli, A., Zuppolini, S., 2011. Lignans from *Phillyrea angustifolia* L. *Phytochemistry Letters* 4, 118-121.
- Diaz, A.M., Abad, M.J., Fernandez, L., Recuero, C., Villaescusa, L., Silvan, A.M., Bermejo, P., 2000. In vitro anti-inflammatory activity of iridoids and triterpenoid compounds isolated from *Phillyrea latifolia* L. *Biological and Pharmaceutical bulletin* 23, 1307-1313.
- Dinda, B., 2019. Pharmacology of iridoids, Pharmacology and Applications of Naturally Occurring Iridoids. Springer, pp. 145-254.
- Djeridane, A., Yousfi, M., Nadjemi, B., Boutassouna, D., Stocker, P., Vidal, N., 2006. Antioxidant activity of some Algerian medicinal plants extracts containing phenolic compounds. *Food chemistry* 97, 654-660.

Djeridane, A., Yousfi, M., Nadjemi, B., Vidal, N., Lesgards, J., Stocker, P., 2007. Screening of some Algerian medicinal plants for the phenolic compounds and their antioxidant activity. *European Food Research and Technology* 224, 801-809.

Dommée, J.L.a.B., 1992. Is *Phillyrea angustifolia* L. (Oleaceae) an androdioecious species? *Botanical Journal of the Linnean Society* 108, 375-387.

Đorđević, T., Antov, M., 2017. Ultrasound assisted extraction in aqueous two-phase system for the integrated extraction and separation of antioxidants from wheat chaff. *Separation and Purification Technology* 182, 52-58.

Dudonne, S., Vitrac, X., Coutiere, P., Woillez, M., Mérillon, J.-M., 2009. Comparative study of antioxidant properties and total phenolic content of 30 plant extracts of industrial interest using DPPH, ABTS, FRAP, SOD, and ORAC assays. *Journal of agricultural and food chemistry* 57, 1768-1774.

El-Abhar, H.S., Schaalan, M.F., 2014. Phytotherapy in diabetes: Review on potential mechanistic perspectives. *World journal of diabetes* 5, 176.

Fernández, J.A., Balenzategui, L., Bañón, S., Franco, J.A., 2006. Induction of drought tolerance by paclobutrazol and irrigation deficit in *Phillyrea angustifolia* during the nursery period. *Scientia Horticulturae* 107, 277-283.

Ferreira, I.C., Baptista, P., Vilas-Boas, M., Barros, L., 2007. Free-radical scavenging capacity and reducing power of wild edible mushrooms from northeast Portugal: Individual cap and stipe activity. *Food chemistry* 100, 1511-1516.

Friedman, M., Henika, P.R., Levin, C.E., Mandrell, R.E., Kozukue, N., 2006. Antimicrobial activities of tea catechins and theaflavins and tea extracts against *Bacillus cereus*. *Journal of food protection* 69, 354-361.

Fromont, M.L., 1997. *Rhamnus alaternus*- environmental weed on motutapu and rangitoto island, auckland 36, 57-66.

Gajić, G., Djurdjević, L., Kostić, O., Jarić, S., Stevanović, B., Mitrović, M., Pavlović, P., 2020. Phytoremediation Potential, Photosynthetic and Antioxidant Response to Arsenic-Induced Stress of *Dactylis glomerata* L. Sown on Fly Ash Deposits. *Plants* 9, 657.

Gescher, K., Hensel, A., Hafezi, W., Derksen, A., Kühn, J., 2011. Oligomeric proanthocyanidins from *Rumex acetosa* L. inhibit the attachment of herpes simplex virus type-1. *Antiviral research* 89, 9-18.

Grenez, E.P., 2019. Phytothérapie - exemples de pathologies courantes à l'officine : Fatigue, Insomnie, Stress, Constipation, Rhume, Douleur et Inflammation, Faculté de Pharmacie de Lille. Université de Lille, Lille-France, p. 137.

Gucci, R., Lombardini, L., Tattini, M., 1997. Analysis of leaf water relations in leaves of two olive (*Olea europaea*) cultivars differing in tolerance to salinity. *Tree physiology* 17, 13-21. Guignard, J.-L., 2000. Biochimie végétale.

Gülçin, I., Mshvildadze, V., Gepdiremen, A., Elias, R., 2006. Screening of antiradical and antioxidant activity of monodesmosides and crude extract from *Leontice smirnowii tuber*. *Phytomedicine* 13, 343-351.

Halliwell, B., 1990. Review article how to characterize a biological antioxidant. *Hanwood Academic Publishers* 9, 1-32.

Halliwell, B., 1994. Free radicals and antioxidants: a personal view. *Nutrition reviews* 52, 253-265.

Halliwell, b., 1995. Antioxidant characterization methodology and mechanism. *Biochemical pharmacology* 49, 1341-1348.

Hamel, Sadou, Seridi, boukhdar, Boulemtafes, 2018a. Pratique traditionnelle d'utilisation des plantes médicinales dans la population de la péninsule de l'Edough (nord-est algérien). *Ethnopharmacologia* 59, 75-81.

Hamel, T., Sadou, S., Seridi, R., Boukhdar, S., Boulemtafes, A., 2018b. Pratique traditionnelle d'utilisation des plantes médicinales dans la population de la péninsule de l'edough (nord-est algérien). *Ethnopharmacologia* 59, 75-81.

Hara, Y., Honda, M., 1990. The inhibition of α -amylase by tea polyphenols. *Agricultural and Biological Chemistry* 54, 1939-1945.

Harbertson, J.F., Kennedy, J.A., Adams, D.O., 2002. Tannin in skins and seeds of *Cabernet Sauvignon*, *Syrah*, and *Pinot noir* berries during ripening. *American Journal of Enology and Viticulture* 53, 54-59.

Haslam, E., 1989. Plant polyphenols: vegetable tannins revisited. CUP Archive.

Hauenschild, F., Favre, A., Salazar, G.A., Muellner-Riehl, A.N., 2016. Analysis of the cosmopolitan *Buckthorn* genera *frangula* and *Rhamnus* s.l. supports the description of a new genus, *Ventia*. *Taxon* 65, 65-78.

He, W., Liu, X., Xu, H., Gong, Y., Yuan, F., Gao, Y., 2010. On-line HPLC-ABTS screening and HPLC-DAD-MS/MS identification of free radical scavengers in *Gardenia* (*Gardenia jasminoides Ellis*) fruit extracts. *Food chemistry* 123, 521-528.

Hong, J., Smith, T.J., Ho, C.-T., August, D.A., Yang, C.S., 2001. Effects of purified green and black tea polyphenols on cyclooxygenase-and lipoxygenase-dependent metabolism of arachidonic acid in human colon mucosa and colon tumor tissues. *Biochemical pharmacology* 62, 1175-1183.

Hsiao, G., Ko, F.-N., Lin, C.-N., Teng, C.-M., 1996. Antioxidant properties of isotorachrysone isolated from *Rhamnus nakaharai*. *Biochimica et Biophysica Acta (BBA)-Protein Structure and Molecular Enzymology* 1298, 119-130.

Huang, B., Chen, F., Shen, Y., Qian, K., Wang, Y., Sun, C., Zhao, X., Cui, B., Gao, F., Zeng, Z., 2018. Advances in targeted pesticides with environmentally responsive controlled release by nanotechnology. *Nanomaterials* 8, 102.

huang, D., ou, B., Prior, R.L., 2005. The Chemistry behind Antioxidant Capacity Assays. *Journal of agricultural and food chemistry* 53, 1841-1856.

IZZO, A.A., 1996. PAF and the digestive tract. A review. *Journal of pharmacy and pharmacology* 48, 1103-1111.

Janakat, S., Al-Merie, H., 2002. Evaluation of hepatoprotective effect of *Pistacia lentiscus*, *Phillyrea latifolia* and *Nicotiana glauca*. *Journal of Ethnopharmacology* 83, 135-138.

Jodoin, J., Demeule, M., Béliveau, R., 2002. Inhibition of the multidrug resistance P-glycoprotein activity by green tea polyphenols. *Biochimica et Biophysica Acta (BBA)-Molecular Cell Research* 1542, 149-159.

Jungkind, D.L., Mortensen, J.E., Fraimow, H.S., Calandra, G.B., 2013. Antimicrobial resistance: a crisis in health care. *Springer Science & Business Media*.

Khettal, B., Zaidi, A., Tacherfiout, M., Sobhi, W., 2014. P156: Effet des extraits de feuilles de *Rhamnus Alaternus* à activités antioxydant et antilipasique sur la masse corporelle et le métabolisme des lipides des souris nourries avec un régime enrichie en carbohydrates. *Nutrition Clinique et Métabolisme* 28, S149-S150.

Kosalec, I., Kremer, D., Locatelli, M., Epifano, F., Genovese, S., Carlucci, G., Randić, M., Končić, M.Z., 2013a. Anthraquinone profile, antioxidant and antimicrobial activity of bark extracts of *Rhamnus alaternus*, *R. fallax*, *R. intermedia* and *R. pumila*. *Food chemistry* 136, 335-341.

Kosalec, I., Kremer, D., Locatelli, M., Epifano, F., Genovese, S., Carlucci, G., Randic, M., Zovko Koncic, M., 2013b. Anthraquinone profile, antioxidant and antimicrobial activity

of bark extracts of *Rhamnus alaternus*, *R. fallax*, *R. intermedia* and *R. pumila*. *Food chemistry* 136, 335-341.

Krentz, A.J., Bailey, C.J., 2005. Oral antidiabetic agents. *Drugs* 65, 385-411.

Labieniec, M., Gabrylak, T., 2006. Study of interactions between phenolic compounds and H₂O₂ or Cu (II) ions in B14 Chinese hamster cells. *Cell biology international* 30, 761-768.

Lanza, A.M.D., Martínez, M.J., Matellano, L.F., Carretero, C.R., Castillo, L.V., Sen, A.M.S., Benito, P.B., 2001a. Lignan and phenylpropanoid glycosides from *Phillyrea latifolia* and their in vitro anti-inflammatory activity. *Planta medica* 67, 219-223.

Lanza, D., Martinez, Mattellano, Carretero, Castillo, sen, S., 2001b. Lignan and Phenyl propanoid glycosides from *Phillyrea latifolia* and their In vitro antiinflammatory activity. *Planta medica* 67, 219-223.

Lee, J.Y., Jang, Y.W., Kang, H.S., Moon, H., Sim, S.S., Kim, C.J., 2006. Anti-inflammatory action of phenolic compounds from *Gastrodia elata* root. *Archives of pharmacal research* 29, 849-858.

Leelaprakash, G., Dass, S.M., 2011. Invitro anti-inflammatory activity of methanol extract of *Enicostemma axillare*. *International Journal of Drug Development and Research* 3, 189-196.

Limasset, B., Le Doucen, C., Dore, J.-C., Ojasoo, T., Damon, M., De Paulet, A.C., 1993. Effects of flavonoids on the release of reactive oxygen species by stimulated human neutrophils: Multivariate analysis of structure-activity relationships (SAR). *Biochemical pharmacology* 46, 1257-1271.

Lordan, S., Smyth, T.J., Soler-Vila, A., Stanton, C., Ross, R.P., 2013. The α -amylase and α -glucosidase inhibitory effects of Irish seaweed extracts. *Food chemistry* 141, 2170-2176.

Lucchesi, M.-E., 2005. Extraction Sans Solvant Assistée par Micro-ondes Conception et Application à l'extraction des huiles essentielles, Faculté des Sciences et Technologies. Université de la Reunion p. 143.

Lucchesini, M., Mensuali-Sodi, A., 2004. Influence of medium composition and vessel ventilation on in vitro propagation of *Phillyrea latifolia* L. *Scientia Horticulturae* 100, 117-125.

Macheix, J.-J., Fleuriet, A., Jay-Allemand, C., 2005. Les composés phénoliques des végétaux: un exemple de métabolites secondaires d'importance économique. PPUR *presses polytechniques*.

- Malik, S.N., 2015. Antibacterial activity of olive (*Olea europaea*) leaves and arugula (*Eruca sativa*) seeds extract. *Int. J. Pharmacogn. Phytochem. Res* 7, 307-310.
- Martínez-Cruz, O., Paredes-López, O., 2014. Phytochemical profile and nutraceutical potential of chia seeds (*Salvia hispanica* L.) by ultra high performance liquid chromatography. *Journal of Chromatography A* 1346, 43-48.
- Mebirouk-Boudechiche, Cherif, Abidi, Bouzouraa, 2015a. Composition chimique et facteurs antinutritionnels de quelques feuilles de ligneux fourragers des zones humides du nord-est de l'Algérie. *Fourrages* 224, 321-328.
- Mebirouk-Boudechiche, L., Abidi, S., Cherif, M., Bouzouraa, I., 2015b. Digestibilité in vitro et cinétique de fermentation des feuilles de cinq arbustes fourragers du nord est algérien. *Revue Méditerranéenne Vétérinaire* 166, 11-12.
- Mizushima, Y., 1966. Screening test for antirheumatic drugs. *The Lancet* 288, 443.
- Moussi, K., Nayak, B., Perkins, L.B., Dahmoune, F., Madani, K., Chibane, M., 2015. HPLC-DAD profile of phenolic compounds and antioxidant activity of leaves extract of *Rhamnus alaternus* L. *Industrial Crops and Products* 74, 858-866.
- Mukherjee, P.K., Maiti, K., Mukherjee, K., Houghton, P.J., 2006. Leads from Indian medicinal plants with hypoglycemic potentials. *Journal of ethnopharmacology* 106, 1-28.
- Nabet, N., Gilbert-López, B., Madani, K., Herrero, M., Ibáñez, E., Mendiola, J.A., 2019. Optimization of microwave-assisted extraction recovery of bioactive compounds from *Origanum glandulosum* and *Thymus fontanesii*. *Industrial Crops and Products* 129, 395-404.
- Nagy, T.O., Solar, S., Sontag, G., Koenig, J., 2011. Identification of phenolic components in dried spices and influence of irradiation. *Food Chemistry* 128, 530-534.
- Naz, R., Ayub, H., Nawaz, S., Islam, Z.U., Yasmin, T., Bano, A., Wakeel, A., Zia, S., Roberts, T.H., 2017. Antimicrobial activity, toxicity and anti-inflammatory potential of methanolic extracts of four ethnomedicinal plant species from Punjab, Pakistan. *BMC complementary and alternative medicine* 17, 302.
- Nkhili, E.-z., 2009. Polyphénols de l'Alimentation : Extraction, Interactions avec les ions du Fer et du Cuivre, Oxydation et Pouvoir antioxydant, Génie de l'environnement. Université d'avignon et des pays de vaucluse p. 378.
- Omale, J., Okafor, P.N., 2008. Comparative antioxidant capacity, membrane stabilization, polyphenol composition and cytotoxicity of the leaf and stem of *Cissus multistriata*. *African Journal of Biotechnology* 7.

Opie, E.L., 1962. On the relation of necrosis and inflammation to denaturation of proteins. *Journal of Experimental Medicine* 115, 597-608.

Oyedapo, O.O., Famurewa, A.J., 1995. Antiprotease and Membrane Stabilizing Activities of Extracts of *Fagara Zanthoxyloides*, *Olex Subscorpioides* and *Tetrapleura Tetraptera*. *International Journal of Pharmacognosy* 33, 65-69.

Pagano, M., Faggio, C., 2015. The use of erythrocyte fragility to assess xenobiotic cytotoxicity. *Cell biochemistry and function* 33, 351-355.

Pavithra, G., Siddiqua, S., Naik, A.S., TR, P.K., Vinayaka, K., 2013. Antioxidant and antimicrobial activity of flowers of *Wendlandia thyrsoidea*, *Olea dioica*, *Lagerstroemia speciosa* and *Bombax malabaricum*. *Journal of Applied Pharmaceutical Science* 3, 114.

PENCHEV, P.I., 2010. Étude des procédés d'extraction et de purification de produits bioactifs à partir de de plantes par couplage de techniques séparatives à basses et hautes pressions, Institut National Polytechnique de Toulouse. Université de Toulouse p. 208.

Pieroni, A., Pachaly, P., Huang, Y., Van Poel, B., Vlietinck, A., 2000b. Studies on anti-complementary activity of extracts and isolated flavones from *Ligustrum vulgare* and *Phillyrea latifolia* leaves (Oleaceae). *Journal of ethnopharmacology* 70, 213-217.

Pimentel, D., 2005. 'Environmental and Economic Costs of the Application of Pesticides Primarily in the United States'. *Environment, Development and Sustainability* 7, 229-252.

Prieto, P., Pineda, M., Aguilar, M., 1999. Spectrophotometric quantitation of antioxidant capacity through the formation of a phosphomolybdenum complex: specific application to the determination of vitamin E. *Analytical biochemistry* 269, 337-341.

Puppo, A., 1992. Effect of flavonoids on hydroxyl radical formation by Fenton-type reactions; influence of the iron chelator. *Phytochemistry* 31, 85-88.

Puupponen-Pimiä, R., Nohynek, L., Meier, C., Kähkönen, M., Heinonen, M., Hopia, A., Oksman-Caldentey, K.M., 2001. Antimicrobial properties of phenolic compounds from berries. *Journal of applied microbiology* 90, 494-507.

Rajesh, E., Sankari, L.S., Malathi, L., Krupaa, J.R., 2015. Naturally occurring products in cancer therapy. *Journal of pharmacy & bioallied sciences* 7, S181.

Ranasinghe, P., Ranasinghe, P., Abeysekera, W.P., Premakumara, G.A., Perera, Y.S., Gurugama, P., Gunatilake, S.B., 2012. In vitro erythrocyte membrane stabilization properties of *Carica papaya* L. leaf extracts. *Pharmacognosy research* 4, 196-202.

Re, R., Pellegrini, N., Proteggente, A., Pannala, A., Yang, M., Rice-Evans, C., 1999. Antioxidant activity applying an improved ABTS radical cation decolorization assay. *Free radical biology and medicine* 26, 1231-1237.

Ribereau-Gayon, P., 1968. Notions generales sur les composes phenoliques, methodes generales d'etudes des composes phenoliques. Les composés phénoliques des végétaux.

Ribereau-Gayon, P., 1968. Les Composés phénoliques des végétaux: par Pascal Ribereau-Gayon. *Dunod*.

Ricciotti, E., FitzGerald, G.A., 2011. Prostaglandins and inflammation. *Arteriosclerosis, thrombosis, and vascular biology* 31, 986-1000.

Ríos, J.L., Francini, F., Schinella, G.R., 2015. Natural products for the treatment of type 2 diabetes mellitus. *Planta medica* 81.

Rocchetti, G., Miras-Moreno, M.B., Zengin, G., Senkardes, I., Sadeer, N.B., Mahomoodally, M.F., Lucini, L., 2019. UHPLC-QTOF-MS phytochemical profiling and in vitro biological properties of *Rhamnus petiolaris* (Rhamnaceae). *Industrial Crops and Products* 142, 111856.

Rodriguez-Amaya, D.B., 2001. A guide to carotenoid analysis in foods. ILSI press Washington.

Romani, A., Baldi, A., Mulinacci, N., Vincieri, E.E., Tattini, M., 1996a. Extraction and Identification Procedures of Polyphenolic Compounds and Carbohydrates in *Phillyrea* (*Phillyrea angustifolia* L.) Leaves. *Chromatographia* 42, 571-577.

Romani, A., Baldi, A., Mulinacci, N., Vincieri, F., Tattini, M., 1996b. Extraction and identification procedures of polyphenolic compounds and carbohydrates in *Phillyrea* (*Phillyrea angustifolia* L.) leaves. *Chromatographia* 42, 571-577.

Sacchi, K.L., 2005. A review of the effect of winemaking techniques on phenolic extraction in red wines. *American journal of enology and viticulture* v. 56, pp. 197-206-2005 v.2056 no.2003.

Sait, S., Hamri-Zeghichi, S., Boulekbache-Makhlouf, L., Madani, K., Rigou, P., Brighenti, V., Pio Prencipe, F., Benvenuti, S., Pellati, F., 2015. HPLC-UV/DAD and ESI-MS(n) analysis of flavonoids and antioxidant activity of an Algerian medicinal plant: *Paronychia argentea* Lam. *Journal of pharmaceutical and biomedical analysis* 111, 231-240.

Sakihama, Y., Cohen, M.F., Grace, S.C., Yamasaki, H., 2002. Plant phenolic antioxidant and prooxidant activities: phenolics-induced oxidative damage mediated by metals in plants. *Toxicology* 177, 67-80.

Sass-Kiss, A., Kiss, J., Milotay, P., Kerek, M., Toth-Markus, M., 2005. Differences in anthocyanin and carotenoid content of fruits and vegetables. *Food Research International* 38, 1023-1029.

Schubert, N., García-Mendoza, E., Pacheco-Ruiz, I., 2006. Carotenoid composition of marine red algae 1. *Journal of Phycology* 42, 1208-1216.

Shinde, U., Phadke, A., Nair, A., Mungantiwar, A., Dikshit, V., Saraf, M., 1999. Membrane stabilizing activity—a possible mechanism of action for the anti-inflammatory activity of *Cedrus deodara* wood oil. *Fitoterapia* 70, 251-257.

Silva, E., Rogez, H., Larondelle, Y., 2007. Optimization of extraction of phenolics from *Inga edulis* leaves using response surface methodology. *Separation and Purification Technology* 55, 381-387.

Škerget, M., Kotnik, P., Hadolin, M., Hraš, A.R., Simonič, M., Knez, Ž., 2005. Phenols, proanthocyanidins, flavones and flavonols in some plant materials and their antioxidant activities. *Food chemistry* 89, 191-198.

Stevenson, D., Hurst, R., 2007. Polyphenolic phytochemicals—just antioxidants or much more? *Cellular and Molecular Life Sciences* 64, 2900-2916.

Tattini, M., Guidi, L., Morassi-Bonzi, L., Pinelli, P., Remorini, D., Degl'Innocenti, E., Giordano, C., Massai, R., Agati, G., 2005. On the role of flavonoids in the integrated mechanisms of response of *Ligustrum vulgare* and *Phillyrea latifolia* to high solar radiation. *New Phytologist* 167, 457-470.

Telli, A., Mahboub, N., Boudjeneh, S., Siboukeur, O., Moulti-Mati, F., 2010. Optimisation des conditions d'extraction des polyphénols de dattes lyophilisées (*Phoenix dactylifera* L.) variété ghars. *Annales des sciences et technologie* 2, 107-114.

Tiwari, P., Pandey, R., Singh, R., Sharma, B., 2020. Role of Natural Products as Alternative of Synthetic Steroidal Drugs, *Advances in Pharmaceutical Biotechnology*. Springer, pp. 77-89.

Uysal, S., 2020. *Phillyrea latifolia* L.: Biological Properties Screening of Different Extracts. *Türk Doğa ve Fen Dergisi* 9, 74-78.

Shahani¹, N.F., Rahim Ahmadi¹, 2019. The Apoptotic Effects of *Rhamnus frangula* Skin Extract on MCF Cells, International Conference on BioMedical Sciences, Istanbul (Turkey).

- Venubabu Thati, A., Roy, S., Prasad, M.A., Shivannavar, C., Gaddad, S., 2010. Nanostructured zinc oxide enhances the activity of antibiotics against *Staphylococcus aureus*. *J. Biosci Tech* 1, 64-69.
- Vermerris, W., Nicholson, R., 2007. Phenolic compound biochemistry. *Springer Science & Business Media*.
- Vermerris, W., Nicholson, R., 2008. Isolation and identification of phenolic compounds, Phenolic compound biochemistry. *Springer*, pp. 151-196.
- Vinayagam, R., Jayachandran, M., Xu, B., 2016. Antidiabetic Effects of Simple Phenolic Acids: A Comprehensive Review. *Phytotherapy research* : PTR 30, 184-199.
- Wei, B.-L., Lu, C.-M., Tsao, L.-T., Wang, J.-P., Lin, C.-N., 2001. In vitro anti-inflammatory effects of quercetin 3-O-methyl ether and other constituents from *Rhamnus species*. *Planta medica* 67, 745-747.
- Yazici-Tutunis, S., Gurel-Gurevin, E., Ustunova, S., Demirci-Tansel, C., Mericli, F., 2016. Possible effects of *Phillyrea latifolia* on weight loss in rats fed a high-energy diet. *Pharmaceutical biology* 54, 1991-1997.
- Yilmazer-Musa, M., Griffith, A.M., Michels, A.J., Schneider, E., Frei, B., 2012. Grape seed and tea extracts and catechin 3-gallates are potent inhibitors of α -amylase and α -glucosidase activity. *Journal of agricultural and food chemistry* 60, 8924-8929.
- Zarfeshany, A., Asgary, S., Javanmard, S.H., 2014. Potent health effects of pomegranate. *Advanced biomedical research* 3, 100.
- Zengin, G., Sarikurkcu, C., Aktumsek, A., Ceylan, R., Ceylan, O., 2014. A comprehensive study on phytochemical characterization of *Haplophyllum myrtifolium* Boiss. endemic to Turkey and its inhibitory potential against key enzymes involved in Alzheimer, skin diseases and type II diabetes. *Industrial Crops and Products* 53, 244-251.
- Zeouk, I., Bekhti, K., 2020. A critical overview of the traditional, phytochemical and pharmacological aspects of *Rhamnus alaternus*: a Mediterranean shrub. *Oriental Pharmacy and Experimental Medicine*, 1-11.
- Zheng, Y., Liu, S., Xie, J., Chen, Y., Dong, R., Zhang, X., Liu, S., Xie, J., Hu, X., Yu, Q., 2020. Antioxidant, α -amylase and α -glucosidase inhibitory activities of bound polyphenols extracted from mung bean skin dietary fiber. *LWT* 132, 109943.

Second Part

Synthesis of alumina nanostructured and biological activities

Chapter I

Literature review

I.1. Generalities on Nanomaterials

There are many definitions of the term 'nanomaterial'. In October 2011, the European Commission proposed a definition for the term "nanomaterial" in a recommendation. A nanomaterial is a natural, accidentally formed or manufactured material containing free particles, either in aggregate or agglomerate form, of which at least one of the following is present at least 50 % of the particles in the numerical size distribution have one or more external dimensions between 1 nm and 100 nm.

This recommendation also states that any material is to be considered as falling within the above definition if it has a specific surface area in volume greater than ($60 \text{ m}^2/\text{cm}^3$).

According to ISO TS 80004-1; a nanomaterial is a material with at least one external dimension at the nanometer scale, i.e. including approximately between 1 and 100 nm or which has an internal or surface structure on the nanometer scale.

There are two main families of nanomaterials:

I.1.1. Nano-objects

They are materials with one, two or three external dimensions at the nanoscale, i.e. approximately 1 and 100 nm. Among the nano-objects, three categories can be distinguished (Moradi et al., 2019):

- a) **Nanoparticles**, which refer to nano-objects whose three external dimensions are on the nanometric scale: latex nanoparticles, latex oxide nanoparticles, and zinc, iron and cerium, alumina, titanium dioxide, calcium carbonate, etc.
Nanoparticles can be prepared from a variety of materials such as proteins, polysaccharides and synthetic polymers. The selection of matrix materials is dependent on many factors including : (a) size of nanoparticles required; (b) inherent properties of the drug, e.g., aqueous solubility and stability; (c) surface characteristics such as charge and permeability; (d) degree of biodegradability, biocompatibility and toxicity; (e) (Mohanraj and Chen, 2006);
- b) **Nanofibres, nanotubes, nanofilaments or nanosticks** that refer to nano-objects with two external dimensions at the scale of nanometric and the third dimension significantly larger (carbon nanotubes, polyester nanofibres, boron nanotubes, etc.). These terms are long-line nano-objects with a cross-section between 1 and a few tens of nm and a length between 500 and 10,000 nm (Christy et al., 2020);
- c) **Nano-sheets**, nano-plates or nano-wafers, which define nano-objects with an external dimension at the nanometric scale and both other dimensions are significantly larger

(clay nano-sheets, cadmium selenide nano-platelets, etc.). Nano-objects can be used as such in powder, liquid suspension or gel form(Wang and Arash, 2014).

I.1.2. Nanostructured materials

Nanostructured materials can be used to distinguish several families among which:

- a) **Aggregates and agglomerates of nano-objects**; Nano-objects can be presented either in individual form (i.e. in the form of particles primary) or in the form of aggregates or agglomerates with a size significantly greater than 50 nm(Wang and Arash, 2014).
- b) **Nanocomposites**, These materials are composed for all or part of nano-objects which give them improved or specific properties of the Nano-objects are embedded in a matrix or on a surface in order to provide a new functionality or to modify the existing one certain mechanical, magnetic, thermal properties, etc. Polymers filled with carbon nanotubes used in the equipment sector an example of nanocomposites are the use of nanocomposites in sports to improve their mechanical resistance and reduce their weight(Manias et al., 2001).
- c) **Nanoporous materials**, Silica aerogels are nanoporous materials with nanometric pore sizes excellent thermal insulation properties(Liang and Jiu-Lin, 2007).

Nanomaterials that are intentionally produced by man for specific applications and have specific properties are referred to as "nanomaterials" manufactured nanomaterials"

Some of these manufactured nanomaterials have already been produced for many years in large tonnages such as titanium dioxide, carbon black, alumina, calcium carbonate or amorphous silica. Other newer materials are manufactured in smaller quantities such as carbon nanotubes, quantum dots or dendrimers.

There are also unintentionally produced nanomaterials, sometimes called ultra-fine particles, produced by certain processes, such as thermal and mechanical emissions such as welding or thermal spray fumes, combustion engine emissions, etc.

Finally, natural ultra-fine particles are present in our environment, such as volcanic fumes or viruses. Because of their varied and often unprecedented properties, nanomaterials have very diverse potential and their uses open up multiple perspectives.

Nanomaterials thus enable incremental and breakthrough innovations in many sectors of activity such as health, automotive, construction, food processing and electronics(Khin et al., 2012).

I.2. Classification of Nanoparticles

The nanoparticles are generally classified into the organic, inorganic and carbon based. **2.1.**

I.2.1. Organic nanoparticles

Dendrimers, micelles, liposomes and ferritin, etc. are commonly known as the organic nanoparticles or polymers. These nanoparticles are biodegradable, non-toxic, and some particles such as micelles and liposomes have a hollow core, also known as nanocapsules and are sensitive to thermal and electromagnetic radiation such as heat and light. These unique characteristics make them an ideal choice for drug delivery. The drug carrying capacity, its stability and delivery systems, either entrapped drug or adsorbed drug system determine their field of applications and their efficiency apart from their normal characteristics such as the size, composition, surface morphology, etc. The organic nanoparticles are most widely used in the biomedical field for example drug delivery system as they are efficient and also can be injected on specific parts of the body that is also known as targeted drug delivery (Tiwari et al., 2008).

I.2.2. Inorganic nanoparticles

Inorganic nanoparticles are particles that are not made up of carbon. Metal and metal oxide based nanoparticles are generally categorised as inorganic nanoparticles.

I.2.3. Metal based

Nanoparticles that are synthesised from metals to nanometric sizes either by destructive or constructive methods are metal based nanoparticles. Almost all the metals can be synthesised into their nanoparticles (Salavati-Niasari et al., 2008). The commonly used metals for nanoparticle synthesis are aluminium (Al), cadmium (Cd), cobalt (Co), copper (Cu), gold (Au), iron (Fe), lead (Pb), silver (Ag) and zinc (Zn). The nanoparticles have distinctive properties such as sizes as low as 10 to 100 nm, surface characteristics like high surface area to volume ratio, pore size, surface charge and surface charge density, crystalline and amorphous structures, shapes like spherical and cylindrical and colour, reactivity and sensitivity to environmental factors such as air, moisture, heat and sunlight etc.

I.2.4. Metal oxides based.

The metal oxide based nanoparticles are synthesised to modify the properties of their respective metal based nanoparticles, for example nanoparticles of iron (Fe) instantly oxidises to iron oxide (Fe_2O_3) in the presence of oxygen at room temperature that increases its reactivity compared to iron nanoparticles. Metal oxide nanoparticles are synthesised mainly due to their increased reactivity and efficiency (Tai et al., 2007). The commonly synthesised are Aluminium oxide (Al_2O_3), Cerium oxide (CeO_2), Iron oxide (Fe_2O_3), Magnetite (Fe_3O_4), Silicon dioxide (SiO_2), Titanium oxide (TiO_2), Zinc oxide (ZnO). These nanoparticles have possess an exceptional properties when compared to their metal counterparts.

I.2.5. Carbon based

The nanoparticles made completely of carbon are known as carbon based (Bhaviripudi et al., 2007). They can be classified into fullerenes, graphene, carbon nano tubes (CNT), carbon nanofibers and carbon black and sometimes activated carbon in nano sizes.

I.3. Some application of nanomaterials

The passage of matter to nanometric dimensions reveals unexpected properties that are often totally different from those of the same materials on a micro or macroscopic scale, particularly in terms of mechanical resistance, chemical reactivity, electrical conductivity and fluorescence nanotechnologies therefore lead to the development of materials whose fundamental properties (chemical, mechanical, optical, biological, etc.) can be modified. For example, gold is totally inactive at the micrometric scale, whereas it becomes an excellent catalyst for chemical reactions when it takes on nanometric dimensions.

All the major families of materials are concerned: metals, ceramics, dielectrics, magnetic oxides, polymers, carbons, etc. Because of their varied and often unprecedented properties, nanomaterials have very diverse potentialities and their uses open up multiple perspectives.

Nanomaterials thus enable incremental and breakthrough innovations in many sectors of activity such as health, automotive, construction, food processing and electronics.

Table 1 - Examples of current applications of nanomaterials (INRS 2012):

Business sector	Examples of current and potential applications
Automotive, aeronautics and aerospace	Reinforced and lighter materials, exterior paints with a brighter colour effect, anti-scratch, anti-corrosion and dirt-repellent. Sensors optimising engine performance, ice detectors on aircraft wings, more durable and recyclable tyres. Diesel additives for better combustion...
Electronics and communication	High-density memory and miniaturised processors, solar cells, pocket-sized electronic library, ultra-fast computers, wireless technology, flat and flexible screens
Food and Agriculture	Active packaging, additives such as dyestuffs, anti-caking agents and innovative emulsifiers...
Chemistry and materials	Pigments, fillers, corrosion inhibitors, multifunctional catalysts, antibacterial and ultra-resistant coatings...
Construction	Self-cleaning and anti-pollution cements, anti-fouling glazing. Innovative paints, varnishes and glues...
Pharmaceuticals and health	Medicines and active agents, anti-allergenic medical adhesive surfaces, tailor-made medicines delivered specifically, biocompatible surfaces for implants. Innovative vaccines and imaging...
Cosmetics	Transparent sun creams, abrasive toothpaste, make-up from better hold...
Energy	New types of batteries, intelligent windows, insulating materials more efficient...
Environment and ecology	Reduction of carbon dioxide emissions, production of ultra-violet water from sea water, more efficient pesticides and fertilisers and less damaging...
Defence	Miniaturised monitoring systems, precise guidance systems, textiles light and protective self-repairing .

1.3.1. Nanoparticles for direct application to humans

The Nano register, presented above, is also concerned with substances in the nanoparticulate state for fields such as pharmacology and medicine. For these fields, the use of nanotechnologies implies the voluntary contact of nano-objects with the human organism,

which is a key factor in the development of new technologies which leads to slower development. However, nanomedicine has enormous potential in terms of targeted approaches (Santhosh and Ulrih, 2013).

With changing lifestyles and an ageing population, diseases such as neurological (Alzheimer's disease), hepatic (diabetes), cardiac (diabetes), and even more so the cancers, constitute growing public health problems. Currently, treatments have not yet been developed and nanotechnologies are a sure way forward to improve targeted therapy and early diagnosis of these diseases (Boisselier and Astruc, 2009).

I.4. Synthesis of nanoparticles

Nanoparticles can be synthesised using different approaches but essentially by bottom-up and top-down methods (Figure 1). Through the bottom-up approach nanoparticles are constructed atom by atom or molecule by molecule. In the large structure is gradually undersized, until it reaches a height that is nanometric dimensions after application of severe mechanical stress, shocks, etc. violent and strongly deformed. The two approaches tend to converge in terms of size of the synthesised particles. The bottom-up approach seems to be richer in the sense that it allows for the production of a greater diversity of architectures and often better control of the nanometric state (relatively monodisperse size and particle size distribution, positioning of the molecules, homogeneity of the products). For its part, although capable of larger productions, the top-down approach generally makes it possible to control the state of the nanometrically more delicate.

The British Standards Institute (BSI, 2005) lists no less than 29 commonly used approaches to the synthesis of manufacture in large quantities of nanoparticles. These approaches are classified into three main types of processes

- Physical processes (e.g. laser pyrolysis or plasma synthesis)
- Chemical processes (sol-gel techniques) (Leclerc, 2011).

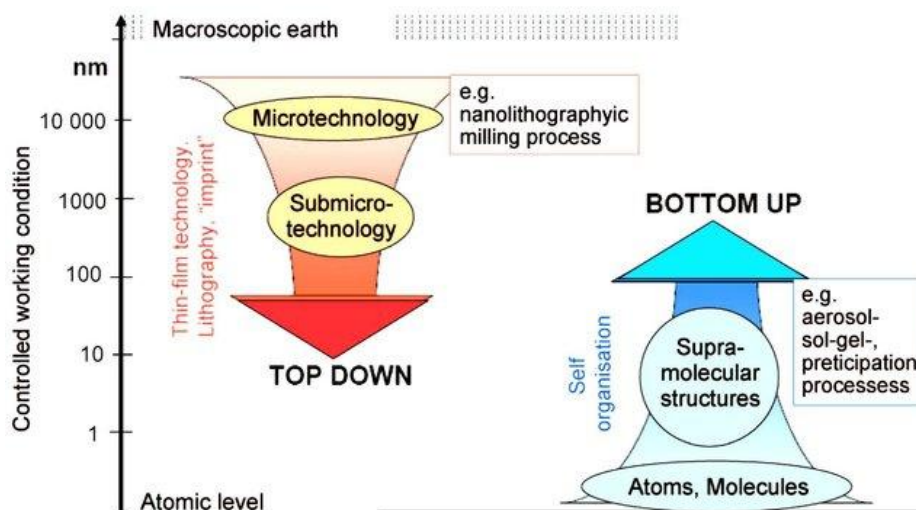


Figure 1. Nanoparticle production: top-down and bottom-up

I.5. Physical methods

I.5. 1. Evaporation/condensation

This method consists of evaporating a metal by heating and then condensing the metal vapour. in order to obtain nanopowders formed from dispersed nanometric particles. The difficulty of this technique is the absolute and homogeneous control of particles at the nanometric scale. The nanoparticles are obtained by very rapid cooling of metal vapour. This process allows the production of very large quantities of particles (Grover, 1966).

I.5. 2. Laser pyrolysis

Laser pyrolysis is a simple and efficient method for the synthesis of nanometric powders. It is based on the interaction between a CO₂ laser and a flow of reagents. The energy transfer causes a rapid rise in temperature. The "precursor" reagents are dissociated and a flame appears in which nanoparticles are formed, which then undergo a rapid drop in temperature or "quenching effect" at the flame exit. The powders are then entrained by a gas flow in a collection area. In most cases, this collection is done on dry powder (Lewis et al., 1984).

This method has many advantages: high chemical purity of the products, good physical and chemical homogeneity, fast quenching speed and good flexibility of use (Pirzada and Yadav, 1998).

I.5. 3. Aerosol method

An aerosol is a set of particles, solid or liquid, of a chemical substance given in suspension in a gaseous medium. The synthesis of nanoparticles can be obtained by oxidation in flames at very high temperatures or thermal plasma from gaseous precursors, or liquids brought in aerosol form (Nasibulin et al., 2005).

The formation of an aerosol does not require a large volume of liquid. The reaction time is very short and allows pure particles to be obtained with an interesting flow rate and yield. This process allows the production of several tons per year of titanium dioxide, silica, etc., which are used in the production of the raw materials or carbon black (McGraw, 1997).

I.6. Chemical methods

I.6.1. Sol-gel method

The sol-gel process makes it possible to produce an inorganic polymer by chemical reactions simple, at a temperature between 20 and 150°C. The synthesis is carried out from alcoholates of formula $M(OR)_n$ where M is a metal or silicon and R is an organic group alkyl C_nH_{2n+1} . This reaction takes place in two stages. Firstly, hydrolysis of the precursor and start of an alkyl group. This step can be catalysed by modifying the pH in the reaction medium. The dispersion is called the "soil". In a second step, it produces an inorganic polymerisation which results in the formation of the "gel". The "gel" is then dried in order to remove the aqueous phase with the help of an oven for example (Antonelli and Ying, 1995).

The advantage of this process is the existence of precursors for a large number of metals and nonmetals. They are either liquid or solid, and for the most part, soluble in common solvents aqueous or organic. This method allows a good control of the morphology of the nanoparticles obtained and the production of materials of greater homogeneity and purity at higher temperatures lower than conventional methods. On the other hand, one of the disadvantages remains the cost of precursors (Lee et al., 2010b).

I.6.2. Liposome production

The most classic way of preparing liposomes is the so-called hydration of a film. lipidic. This film is often obtained by evaporation of an organic solvent in which the lipids are dissolved. The hydration of this film then leads to the separation of bilayer fragments lipidic. The use of natural phospholipids makes it possible to create systems that mimic the biological membranes (Baker and Heriot, 2005).

I.6.3. Solvo-thermal and hydro-thermal methods

The solvo-thermal method makes it possible to produce a large number of materials: metals, ceramics, semiconductors and polymers. This process consists of using a solvent under high pressure (between 1 atm and 10,000 atm) and at a temperature of between 100 and 1000°C with autoclave. However, the main disadvantage of such a closed device is the thermal inertia of the reactor, which must resist the combined effect of temperature and pressure, and the variations resulting temperatures in the reaction medium. These limitations can be removed using a continuous device. A wide range of solvents with a high boiling temperature can be used. This solvo-thermal method ensures better control of size, shape and better quality of the crystals. When the solvent used is water, this is called the hydrothermal method. The temperature is then lower. Nanoparticles are generally very well crystallised and do not require any treatment(Nyankson et al., 2013).

I.7. Biological methods (Biosynthesis) of nanoparticles

Biosynthesis is presented as an alternative method to chemical and biological methods physical because these methods are often extremely expensive and non-environmental friendly due to the use of toxic, combustible, and hazardous chemicals, which may pose potential environmental and biological risk and high energy requirement. Efforts have therefore been made to synthesise nanoparticles at from biological materials in an aqueous medium. For example, plant extracts, bacteria, viruses, fungi microorganisms and proteins have been used to synthesise nanoparticles of various shapes and sizes(Awwad et al., 2013).

I.7.1. Biological Synthesis of Nanoparticles by Microorganisms

I.7.1.1. Biological Synthesis of Nanoparticles by Bacteria

Biological entities and inorganic materials have been in constant touch with each other ever since inception of life on the earth. Due to this regular interaction, life could sustain on this planet with a well-organized deposit of minerals. Recently scientists become more and more interested in the interaction between inorganic molecules and biological species. Microbial synthesis with rich biodiversity of microbes, using simple microbial cultivation, under cellular, biochemical and molecular mechanisms, the rate of synthesis and improvement in nanoparticle properties of can be achieved(Narayanan and Sakthivel, 2010). Microbial and metal interaction is well recognized in biotechnological processes, such as bioleaching,

biomineralization, biocorrosion, bioreduction and bioremediation (Narayanan and Sakthivel, 2010; Rajeshkumar et al., 2014). The properties of nanostructured mineral crystals and metallic nanoparticles produced by microbes are similar to chemically synthesized nano-materials (Gericke and Pinches, 2006). Many unicellular and multicellular organisms, such as bacteria (prokaryotes), fungi (eukaryotes) and viruses, produce either intracellular or extracellular inorganic materials (Thakkar et al., 2010). The formation of these inorganic materials to an extent can be manipulated for the shape and size by controlling the culture parameters. The mechanism of intracellular and extracellular production of nano-materials is different across varied microbes (Mandal et al., 2006). The intracellular mechanisms involve positive metal ions transportation into the cell wall by interaction with negative ions of the cell wall. Further, enzymes of cell wall reduce the metal ion into nanoparticles, and later, these nanoparticles diffuse across the cell wall of bacteria. In case of fungi, the extracellular production of nanoparticle is nitrate reductase-mediated synthesis in the presence of enzyme nitrate, which helps with bio-reduction of metal ions into nanoparticles (Hulkoti and Taranath, 2014).

1.7.1.2. Biological Synthesis of Nanoparticles by Fungal

Rational synthesis of nanoparticles by fungi holds advantages over the bacteria. Using fungi, it is possible to synthesize nanoparticles with nanoscale dimension and with more tolerable monodispersity in comparison with those synthesized by bacteria. Fungi have potential strategies for extracellular synthesis of nanoparticle for greater commercial viability. *Fusarium oxysporum* in the presence of aqueous AuCl_4^- ions with NADH-enzyme-mediated reaction releases reducing agents into the solution for the formation of gold nanoparticles. The synthesized nanoparticles show long-term stability in solution, due to the protein binding through linkage of cysteine and lysine residue. Because of this property, immobilization on matrices or thin-films for optoelectronic and nonlinear optical application is possible (Yong et al., 2002).

In comparison with other fungal species, *F. oxysporum* is capable of hydrolyzing never encountered metals and in the presence of K_2ZrF_6 aqueous solution, crystalline zirconia nanoparticles are formed. The fungus can also synthesize silica and titania nanoparticles in the presence of aqueous anionic complexes of Si and Ti, respectively. The fungal biological system possesses regenerative capability with eco-friendly and energy-conserving nature for large-scale synthesis of metal nanoparticles for possible commercial viability (Bansal et al.,

2005) *F. oxysporum* can carry out extracellular synthesis of Au–Ag nanoparticles at varying molar fraction when exposed to equimolar solution of AuCl_4 and AgNO_3 (Senapati et al., 2005), and in some cases it can also synthesize platinum nanoparticles through inter- and extracellular formation in the presence of hexachloroplatinic acid (H_2PtCl_6) (Riddin et al., 2006). Various bacteria, fungi and yeasts isolated from soil and metal-rich dump samples were used to manipulate the size and shape of gold nanoparticles by altering the pH and temperature during growth conditions. Two fungi, *Verticillium luteoalbum* and isolate 6–3 produced variety of nanoparticle shape by varying the pH, and with low operating temperature, the size of nanoparticle can be controlled (Rajeshkumar et al., 2014). *Aspergillus flavus* demonstrated synthesis of monodispersed silver nanoparticles with average particle size of 8.92 nm, and it also possessed ‘sil’ gene in plasmids for reduction of silver ions for large-scale production (Vigneshwaran et al., 2007). *C. versicolor*, a white-rot fungus, produced silver nanoparticles, via intra and extracellular mode in the absence of surfactants and linking agents. The silver nanoparticles synthesized by fungus in the presence of glucose as stabilizing agents had potential applications as water-soluble metallic catalysts for living cells (Sanghi and Verma, 2009).

I.7.1.3. Biological Synthesis of Nanoparticles by Yeast

The numerous publications have revealed that all yeast genera can accumulate different heavy metals. They have the ability to accumulate significant amounts of highly toxic metals. Enzymatic oxidation or reduction, sorption at the cell wall and in some cases consequent chelating with extracellular peptides or polysaccharides, controlled cell membrane transport of heavy metals towards or their active efflux from the cell are the different mechanisms developed by these species overcoming the toxic effects of heavy metals (Breierová et al., 2002). Stringent control of intracellular metal ions is required by yeast cells to avoid negative or lethal effects. Toxicity to the cells results due to over storage of essential metals ions or by the exposure of the cell to metals which do not have any biological significance such as mercury, lead or cadmium. The considerable variations in size, particle location, monodispersity and properties are due to different mechanisms employed by yeast strains of different genera for nanoparticle synthesis. Detoxification mechanisms in yeast cells is brought about by GSH (glutathione) and two groups of metal-binding ligands metallothioneins and phytochelatins (PC). In most of the yeast species studied, these molecules determine the mechanism for the formation of nanoparticles and stabilize the complexes. The capacity of

yeast cell to change the absorbed metal ions into complex polymer compounds that are not toxic to the cell is defined as resistance (Breierová et al., 2002).

I.7.2. Biological Synthesis of Nanoparticles by plant

(Mittal et al., 2013), reviewed that biomolecules present in plant extracts can be used to reduce metal ions to nanoparticles in a single-step green synthesis process. This biogenic reduction of metal ion to base metal is quite rapid, readily conducted at room temperature and pressure, and easily scaled up. Synthesis mediated by plant extracts is environmentally benign. The reducing agents involved include the various water soluble plant metabolites (e.g., alkaloids, phenolic compounds, and terpenoids) and coenzymes. Silver (Ag) and gold (Au) nanoparticles have been the particular focus of plant-based syntheses. Extracts of a diverse range of plant species have been successfully used in making nanoparticles. In addition to plant extracts, live plants can be used for the synthesis. The use of plant extracts for making metallic nanoparticles is inexpensive, easily scaled up, and environmentally benign. It is especially suited for making nanoparticles that must be free of toxic contaminants as required in therapeutic applications. The plant extract based synthesis can provide nanoparticles of a controlled size and morphology. In medicine, nanoparticles are being used as antimicrobial agents, for example, in bandages. Applications in targeted drug delivery and clinical diagnostics are developing.

I.7.3. Biological Synthesis of Nanoparticles by marine algae

There is a very little literature supporting the use of marine algae in nanoparticle synthesis. The brown seaweed *Sargassum wightii* is reportedly capable of synthesizing gold nanoparticles with a size ranging between 8 and 12 nm. An important potential benefit of the synthesis is that the nanoparticles are quite stable (Singaravelu et al., 2007). Another brown seaweed *Fucus vesiculosus* is reported to have an ability of gold biosorption and bio-reduction, as an environmental friendly process that can be used for recovering gold from dilute hydrometallurgical solutions and leachates of electronic scraps, and for the synthesis of gold nanoparticles of different size and shape (Mata et al., 2009). Similarly, the extracellular synthesis of silver nanoparticles by the brown seaweed *Sargassum wightii* and their antibacterial effects are registered (Govindaraju et al., 2009). In addition to antibacterial activity, the nanoparticles synthesized by seaweed extracts do have stabilizing effect on cotton fabrics (Sheeba and Thambidurai, 2009). *Fuoidan* is an algal polysaccharide, reported to

stabilize gold particles and this green synthesis using natural fucoidans will provide an alternative to chemical method. The red seaweed *Gelidiella acerosa* is reported to have the potential of synthesizing antifungal silver nanoparticles (Vivek et al., 2011). Recently, Rajesh et al.(2012). . have reported the synthesis of silver nanoparticles using *Ulva fasciata* extract as a reducing agent and this nanoparticles inhibited the growth of *Xanthomonas campestris* pv. *malvacearum*. In addition to seaweeds, microalgae such as diatoms (*Navicula atomus*, *Diadesmis gallica*) have the ability to synthesize gold nanoparticles, gold, and silica–gold bionanocomposites (Schröfel et al., 2011). The diatom *Stauroneis* sp. was used for the preparation of silicon–germanium nanocomposite and this method of nanocomposite preparation has great importance for possible future applications due to its accessibility, simplicity and effectiveness (Ali et al., 2011).

I.8. Generalities on Alumina (Al_2O_3)

Aluminium oxide is an amphoteric oxide of aluminium with the chemical formula Al_2O_3 . It is also commonly referred to as alumina or aloxite in the mining, ceramic materials science communities. It is produced by the Bayer process from bauxite. Its most significant use is in the production of aluminium metal, although it is also used as abrasive, due to its hardness, and as a refractory material due to its high melting point. Corundum is the most common naturally-occurring crystalline form of aluminium oxide. Much less-common rubies and sapphires are gem-quality forms of corundum with their characteristic colours due to trace impurities in the corundum structure. Rubies are given their characteristic deep red colour and their laser qualities by traces of the metallic element chromium. Sapphires are in different colours given by various other impurities, such as iron and titanium.

I.8.1. Properties of Alumina (Al_2O_3)

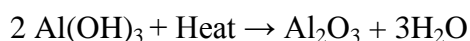
Aluminium oxide is an electrical insulator but has a relatively high thermal conductivity (40 W/m K). In its most commonly occurring crystalline form, called corundum or α -aluminium oxide, its hardness makes it suitable for use as an abrasive and as a component in cutting tools. Aluminium oxide is responsible for metallic aluminium's resistance to wearing. Metallic aluminium is very reactive with atmospheric oxygen, and a thin passivation layer of alumina quickly forms on any exposed aluminium surface. This layer protects the metal from further oxidation. The thickness and properties of this oxide layer can be enhanced using a process called anodising. A number of alloys, such as aluminium bronzes, exploit this property by including a proportion of aluminium in the alloy to enhance corrosion resistance. The alumina generated by anodising is typically amorphous, but discharge assisted oxidation processes such as plasma electrolytic oxidation result in a significant proportion of crystalline alumina in the coating, enhancing its hardness. Aluminium oxide was taken off the United States Environmental Protection Agency's chemicals lists in 1988.

Aluminium oxide, also known as alumina, is the main component of bauxite, the principal ore of aluminium. The largest manufacturers in the world of alumina are Alcoa, Alcan and Rusal. Companies which are specialized in the production of special aluminium oxides and aluminium hydroxides. The bauxite is made up of impure Al_2O_3 , Fe_2O_3 , and SiO_2 . Bauxite is purified by the Bayer process (Hind et al., 1999)



The Fe_2O_3 does not dissolve in the base. The SiO_2 dissolves as silicate Si(OH)_6^{2-} .

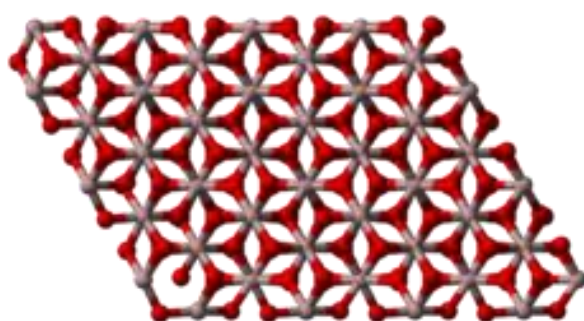
Upon filtering, Fe_2O_3 is removed. When the Bayer liquor is cooled, Al(OH)_3 precipitates, leaving the silicates in solution. The mixture is then calcined (heated strongly) to give aluminium oxide:



The alumina formed tends to be multi-phase, i.e. constituting several of the alumina phases rather than solely corundum. The production process can therefore be optimized to produce a tailored product. The type of phases present affects, for example, the solubility and pore structure of the alumina product which, in turn, affects the cost of aluminium production and pollution control.

I.8.1.1. Structure of Alumina (Al_2O_3)

The crystal system of corundum (α -Alumina) is a trigonal Bravais lattice with a space group R-3c, 2 formula units per unit cell of aluminium oxide, but is most commonly referred to a slightly distorted hexagonal close-packing of oxygen ions, or a larger hexagonal cell with 6 formula units, as we can observe in the Figure 1. Alumina has also other phases ($\gamma, \delta, \epsilon, \eta, \theta, \chi, \dots$), all corresponding to the Al_2O_3 formula, but the only one that its thermo stable is the α -Alumina. The electro negativity of alumina is 2, with a 63% of ionic character and



37% of covalent.

Figure 2: Scheme of the crystal structure of Al_2O_3 (Wikipedia:
https://en.wikipedia.org/wiki/Aluminium_oxide)

I.8.1.2. Electrical and chemical properties of Alumina (Al_2O_3)

Alumina has a very interesting combination of mechanical, electrical and chemical properties. Mechanically is very hard, resistant to abrasive wear and dimensional stable. Electrically it has high resistivity, good dielectric strength and low dielectric loss factor at high frequencies. It is inert against from chemicals, maintaining characteristics at high temperature (Peelen, 1977). The melting temperature is 2030–2050 °C, boiling temperature: 3500 °C, thermal conductivity “k” is 30.1 W/m.K, the lineal dilatation coefficient is $8.3 - 9 \times 10^{-6} \text{ }^\circ\text{C}$, thermal conductivity $10^{-10} - 10^{-12} (\Omega.\text{m})^{-1}$, the tensile strength is 380 GPa, Poisson coefficient of 0.26, hardness of 18-23 HV (GPa), ultimate strength of 200 - 345 MPa and a density of 3.97 g/cm³. The good properties of the elastic modulus and flexural strength at high temperatures can provide the increase of mechanical properties at higher temperatures for the elected alloy. Because of that we want to explore the potential application of Al_2O_3 in the reinforced alloys.

I.8.2. Aluminium oxide nanoparticles

Aluminium oxide nanoparticles have important applications in ceramic industry and can be used as an abrasive material, in heterogeneous catalysis, as an absorbent, a biomaterial and as reinforcements of metal–matrix composites (MMCs). In order to be used for effective discontinuous reinforcements in a continuous metal–matrix, Al_2O_3

Nanosized aluminium oxide (nanosized alumina) occurs in the form of spherical or nearly spherical nanoparticles, and in the form of oriented or undirected fibers.

particles have to fulfil certain structural and morphological requirements: small particle size and narrow size distribution, large surface area, spherical morphology and the absence of agglomerates. As far as the hot wall aerosol synthesis method (Spray Pyrolysis), as basic chemical route for obtaining advanced materials, is concerned, it offers several advantages in the preparation of well-defined oxide powders over conventional synthesis (Martin et al., 2008).

Reducing the sizes of low dimensional materials leads to dramatic increase in the portion of surface/interface atoms. The properties of a solid are essentially controlled by related surface/interface energies. Although such changes are believed to dominate behaviours of nanoscale structures, little experience or intuition for the expected phenomena, especially for the size-dependence of the energies and their practical implications, are modelled analytically. The classic thermodynamics as a powerful traditional theoretical tool is used to model

different bulk interface energies and the corresponding size dependences. During the modelling, an emphasis on size dependences of the interface energies is given, which is induced by size dependence of coherent energy of atoms within nanocrystals. It is found that solid–vapour interface energy, liquid–vapour interface energy, solid–liquid interface energy, and solid–solid interface energy of nanoparticles and thin films fall as their diameters or thickness decrease to several nanometres while the solid–vapour interface energy ratio between different facets is size-independent and equals to the corresponding bulk value. Predictions of the established analytic models without any free parameters, such as size and temperature, dependences of these four kinds of interface energies and related surface stress, correspond to experimental or other theoretical results. The established models are suitable for low dimensional materials with different dimensions and different chemical bond natures. Moreover, several related applications in the fields of nanophase transitions, nanocrystal growth, and self-diffusion of liquids are known (Jiang and Lu, 2008)

The major uses of special aluminium oxides are in refractories, ceramics, polishing and abrasive applications. Large tonnages are also used in the manufacture of zeolites, coating titania pigments, and as fire retardant /smoke suppressants. Alumina is a medium for chemical chromatography, available in basic (pH 9.5), acidic (pH 4.5 when in water) and neutral formulations. In lighting, GE developed "Lucalox" in 1961, a transparent alumina used in sodium vapor lamps.

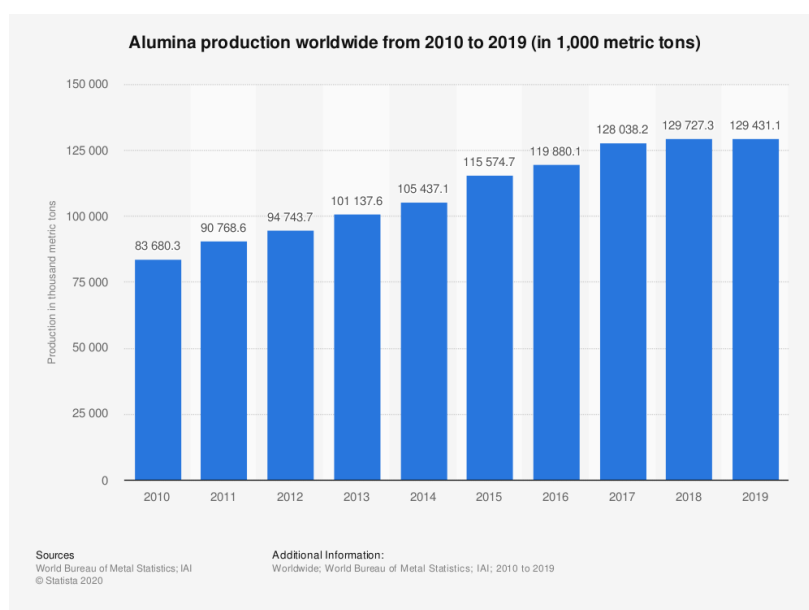


Figure 3. Alumina production worldwide from 2010 to 2019 (in 1,000 metric tons) (source: <https://www.statista.com/>)

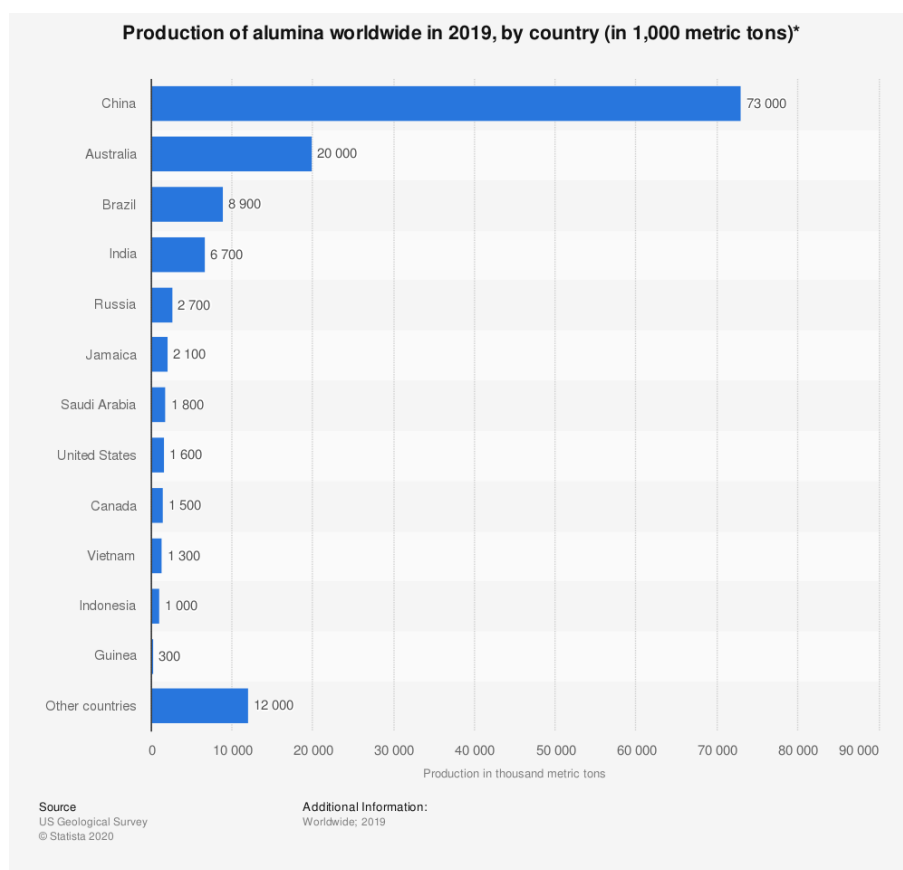


Figure 4. Alumina production worldwide in 2019, by country, (source: <https://www.statista.com/>)

The statistic in Figure 2 shows the total production of alumina (aluminum(III) oxide) worldwide, from 2010 to 2019. Alumina is the most commonly occurring of the aluminum oxides, and is refined to produce aluminum. In 2019, the global production of alumina amounted to 129.4 million metric tons (Martin et al., 2008).

Aluminium oxide is also used in preparation of coating suspensions in compact fluorescent lamps. Health and medical applications include it as a material in hip replacements. It is used in water filters (derived water treatment chemicals such as aluminium sulfate, aluminium chlorohydrate and sodium aluminate, are one of the few methods available to filter water-soluble fluorides out of water). It is also used in toothpaste formulations. Most pre-finished wood flooring now uses aluminium oxide as a hard protective coating. In 2004, developed technique for making a ceramic composed of aluminium oxide and rare earth elements to produce a strong glass called transparent alumina. Alumina can be grown as a coating on aluminium by anodizing or by plasma electrolytic oxidation. Its strength and abrasive characteristics are due to aluminium oxide's great hardness (position 9 on the Mohs scale of mineral hardness). It is widely used as a coarse or fine abrasive, including as a much less

expensive substitute for industrial diamond. Many types of sandpaper use aluminium oxide crystals. In addition, its low heat retention and low specific heat make it widely used in grinding operations, particularly cutoff tools. As the powdery abrasive mineral aloxite, it is a major component, along with silica, of the cue tip "chalk" used in billiards. Aluminium oxide powder is used in some CD/DVD polishing and scratch-repair kits. Its polishing qualities are also behind its use in toothpaste. Is also widely used in the fabrication of superconducting devices, particularly single electron transistors and superconducting quantum interference devices (SQUID), where it is used to form highly resistive quantum tunnelling barriers(Laachachi et al., 2009).

Nano- Al_2O_3 with small size, high activity and low melting temperature, it can be used for producing synthetic sapphire with the method of thermal melting techniques; the g-phase nano- Al_2O_3 with large surface area and high catalytic activity, it can be made into microporous spherical structure or honeycomb structure of catalytic materials. These kinds of structures can be excellent catalyst carriers. If used as industrial catalysts, they will be the main materials for petroleum refining, petrochemical and automotive exhaust purification. In addition, the g-phase nano- Al_2O_3 can be used as analytical reagent(Touzin et al., 2010).

Alumina nanoparticles have important applications in ceramic industry and can be used as an abrasive material, in heterogeneous catalysis, as an absorbent, a biomaterial and as reinforcements of metal–matrix composites (MMCs). Particles have to fulfil certain structural and morphological requirements: small particle size and narrow size distribution, large surface area, spherical morphology and the absence of agglomerates. As far as the hot wall aerosol synthesis method (Spray Pyrolysis), as basic chemical route for obtaining advanced materials, is concerned, it offers several advantages in the preparation of well-defined oxide powders over conventional synthesis(Martin et al., 2008). Alumina is also widely used in the fire retard, catalyst, insulator, surface protective coating, and composite materials (Lukić et al., 2009);(Touzin et al., 2010);(Keyvani et al., 2010).

I.8.3. Synthesis of Aluminium oxide nanoparticles

Aluminium oxide nanoparticles can be synthesized by many techniques including ball milling, sol-gel, pyrolysis, sputtering, hydrothermal, and laser ablation (Kavitha and Jayaram, 2006; Mirjalili et al., 2010; Qu et al., 2005; Reid et al., 2008). Among them, the laser ablation is a widely used technique for the synthesis of nanoparticles since it can be synthesized in gas, vacuum or liquid. This technique offers several advantages such as rapid and high purity

process compared with other methods (Kruusing, 2010). Furthermore, nanoparticles prepared by the laser ablation of materials in liquid are easier to be collected than those of in gas atmosphere.

In the recent years, Al_2O_3 nanoparticles were synthesized in liquid using a short pulse laser with the pulse width in the range of nanosecond (Liu et al., 2010; Yan et al., 2010). The synthesis of Al_2O_3 from Al powders using laser ablation in deionized water with a long pulsed Nd:YAG laser. The laser pulse widths adopted in this work were 2.5, 6, and 9.5 ms to obtain the output laser energies of 1, 3, and 5 J, respectively. The particle size and morphology of synthesized nanoparticles obtained at different laser energies were investigated by field emission scanning electron microscopy (FE-SEM). The optical property of synthesized nanoparticles was carried out using UV-visible spectroscopy. The structure of the synthesized nanoparticles was investigated using X-ray diffraction (XRD) technique (Piriyawong et al., 2012).

Out of all the methods, sol-gel method proved more helpful to obtain well shaped materials with designed texture and composition at low processing temperatures (Rajaeiyan and Bagheri-Mohagheghi, 2013). The literature survey reveals that Al_2O_3 was synthesized by sol-gel method using different precursor viz. aluminum triisopropylate in a hydrolysis system consisting of octanol and acetonitrile, aluminum nitrate in aqueous medium, aluminum secondary butoxide in an alcoholic medium (Liu et al., 2010; Mirjalili et al., 2010).

1.8.3. 1. Alumina Sol-Gel

The common solution-gelation route to aluminum oxides employs aluminum hydroxide or hydroxide-based material as the solid colloid, the second phase being water and/or an organic solvent. Aluminum hydroxide gels have traditionally been prepared by the neutralization of a concentrated aluminum salt solution; however, the strong interactions of the freshly precipitated alumina gels with ions from the precursors solutions makes it difficult to prepare these gels in pure form. To avoid this complication alumina gels may be prepared from the hydrolysis of aluminum alkoxides, $\text{Al}(\text{OR})_3$.



Although this method was originally reported in 1922, it was not until the 1970's that alumina aerogels were prepared, and transparent ceramic bodies were obtained by the pyrolysis of suitable alumina gels, that interest increased significantly. There have been several efforts to

improve the processing control of sol-gels (including development of environmentally benign routes), however, we proposed that without an understanding of the structure of these materials any further development was limited(Saha, 1994).

I.9. Some application of alumina nanoparticules

I.9.1. Antimicrobial activity of alumina oxide nanoparticles

Alumina nanoparticles are thermodynamically stable particles over a wide temperature range. They are corundum like structure with oxygen atoms adopting hexagonal close packing with alumina ions filling two thirds of the octahedral sites in the lattice(Sadiq et al., 2009) Murdock et al. (2008) have observed that the particle behaviour was also influenced by particle size, shape and surface charge. Nanoparticles tend to aggregate in hard water and seawater due to particle interaction with organic matter present in water. Aggregations of particle are also influenced by pH and salinity, which state the dispersion ability of particles in the suspension that lead to alter toxicity assessment. Before implementing toxicity studies certain important parameters have to be taken into consideration such as particle size, size distribution, morphology, composition, surface area, surface chemistry and particle reactivity in solution which need to be accurately characterized as prerequisites.

Bala et al.(2011), synthesized alumina-silver composite nanoparticles by a simple, reproducible, wet chemical method, with the surface of the oxides modified with oleic acid. Preliminary antibacterial studies performed using disc diffusion assays against *E. coli* DH5 α and *Staphylococcus epidermidis* NCIMB 12721 suggested that the composite nanomaterials have immense potential as antimicrobial agents. Some research group have carried out extensive studies on the antibacterial behaviour of these nanoparticles. The investigated of antibacterial effect of alumina towards *E. coli* and growth inhibition was studied at varying concentrations of alumina. To ascertain whether the antibacterial activity was due to particles in the broth or due to the specific interactions with bacterial cellular components, a growth reversibility study was performed. We observed a negligible dependence of growth rate with the concentration of the nanoparticles. The growth reversibility studies indicated a significant retardation in growth of recultured *E. coli* cells which had prior exposure to the nanoparticles. A decrease in the extracellular protein content after nanoparticle exposure was also observed as indicated by protein assays and FTIR studies. The results indicated that alumina nanoparticles had a mild inhibitory effect against *E. coli* at high concentrations upto 1000 $\mu\text{g/ml}$ (Sadiq et al., 2009).

In their study, Jiang et al.(2009), observed that dissolved metal ions were not present in a measurable quantity in the supernatant of the suspension thus ruling out the role of aluminum ions in nanoparticle mediated toxicity. They observed that the nanoparticles attached to the surface of the bacteria due to surface charge; bacterial surface was negative while alumina nanoparticles were positive at the pH studied.

Sadiq et al.(2009), They investigated the difference in toxic response of micron sized and nano sized alumina towards *Scenedesmus sp.* and *Chlorella sp.* A growth inhibitory effect of the nanoparticle was observed against both the species and an evident decrease in the chlorophyll content was also observed in the cells treated with nanoparticles. An interaction of the nanoparticles with the cell surface was suggested as the possible mechanism for the toxicity.

I.9.2. Use of alumina nanoparticles in potential clinical applications

I.9.2. 1. In membranes

Recently polyethersulfone/ aluminium oxide membranes with higher porosity have been developed for drug delivery applications(Maximous et al., 2009). Another notable study observed that the addition of alumina nanoparticles to PVDF membranes led to the effective improvement of the membrane performance. The study observed that with increased alumina concentrations, the water permeate fluxes, mechanical properties as well as the hydrophilicity increased(Yan et al., 2006)

I.9.2. 1. Drug delivery

Most of the drugs are delivered into the body predominantly using the oral or intravenous route. However other strategies need to be adopted to deliver drugs containing biological agents such as proteins and this is when nanoparticles come into play(Mukherjee et al., 2011). Alumina nanoparticles are also considered for drug delivery applications due to their potential scavenging behaviour. The scavenging property has been related to their ability to act as direct antioxidants, block ROS production and also cause a reduction in ROS production (Parveen et al., 2012).

I.9.2. 2. Use of alumina nanoparticles as insecticide powder

Nanostructured alumina (NSA), characterized by large aggregates of 40-60 nm particles with a large specific surface area $14 \text{ m}^2 \times \text{g}^{-1}$. Mimani and Patil.(2001), have recently discovered

as a contact insecticide. NSA is supposed to have a detrimental effect on insect water balance, similarly to microparticulate insecticidal inert dusts (IDs) in general (Stadler et al., 2012). The discovery of NSA's insecticidal activity opens new frontiers in pest management since the efficacy of NSA similar (Athanassiou et al., 2006) or greater than that obtained through some commercial diatomaceous earth (Stadler et al., 2010). Also, long term treatments with NSA at low concentrations (62.5 ppm) were more effective in reducing rice weevils, *Sitophilus oryzae* (L.) (Coleoptera Dryophthoridae), progeny than commercially available microparticulate IDs for different humidity levels (Stadler et al., 2012). Although dehydration appears to be the main cause of mortality. NSA particles dehydrate the insect by attaching to their cuticle via triboelectric forces and by surface area effect sorbs its wax layer. Along with their hydrophobic behavior, these abrasive particles also cause splits and scratches on insect bodies (Teodoro et al. (2017), Buteler et al. (2015)). Moreover, the striking differences observed in efficacy of insecticide dusts from different sources, among different insect species, and bioassay conditions (Athanassiou et al., 2016) mineral composition and type of formulation (Iatrou et al., 2010; Subramanyam and Roesli, 2000) suggest a complex action mechanism involving several phenomena. Thus, investigations in this direction are necessary in order to understand all the factors involved in IDs efficacy and to determine if nanoparticulate materials have analogous insecticide mechanism of action as microparticulate materials.

I.9.2. 3. Use nanoparticles in plant growth and development

Farmers used conventional chemicals for controlling pests and pathogens, which had a drastic impact on the environment as well as on the farmer's economy, because upon application 90% was lost as runoff or into the air (Thul and Sarangi, 2015). Release of pesticides and insecticides through a nano-scaled delivery system led to the application of these chemicals only when the need arises (Gruère et al., 2011).

Toxicity and accumulation of nanoparticles have led to the necessity to search for biodegradation pathways for nanoparticles and their impacts on living species, including the natural structures and functions as well as artificial biocenoses (Krysanov et al., 2010).

Use of nanoparticles is still a fresh and new approach, which needs further study and research for proper understanding and implementation of their properties for the betterment of food and crop as well as in other fields of science. Nanotechnology is a niche area which still needs

a thorough understanding, but it is sure to expand its boundaries, including agriculture and allied sectors, providing immense benefits.

Nanoparticles have gained demand in the agricultural and medical fields due to their unique physicochemical properties, including ability to penetrate, larger surface area and chemically active. With the increase in demand they have also become potential threats to the environment (Galhotra, 2010).

Plant transport pathways play a vital role in the entry of nanoparticles into plants as well as into the surrounding environment. They were transferred through protoplasts, intact plants and dissected organs (Wang et al., 2016). Nanoparticle entry into plant cells largely depends on the species of plant and the nanoparticle properties and is obstructed due to its cell wall (Singh et al., 2015). Entry through the plant cell wall occurs either through engulfing, endosome formation or through sieving mechanism. Entry of ENPs occurs either by way of organs and tissues above the ground level, i.e. stomata, hydathodes, cuticles, stigma and trichomes, or by the root tissues, as well as through junctions and injuries (Wang et al., 2016).

A plant cell wall has pores with diameters in the range of 5–20 nm. Usually, through the cell wall water molecule as well as solute accretion occurs, this is due to the porous polysaccharide fibre matrix of the cell wall (Tripathi et al., 2017).

Thus, for efficient entry into the plant cell wall, the size of the nanoparticles should be less than the cell wall pore diameter. The efficient passage of these nanoparticles through the pores enables them to extend towards the plasma membrane. The pore size of the cell wall can even be enlarged upon association with engineered nanoparticles, thereby favouring the uptake of nanoparticles (Nair et al., 2010). Plants grown in soil as well as on sand depicted no uptake or minimal uptake of nanoparticles.

Therefore plant cells are grown on growth medium for the uptake of nanoparticles.

The low or no uptake of nanoparticles by soil- and sand-grown plants is due to the adhesion of metal oxide nanoparticles (Singh et al., 2015). The growth medium varies with different types of nanoparticle uptake. The ion channels and carrier proteins which are embedded in the membrane also lead to the transport of nanoparticles across the membranes in the cell. Nanoparticle entry into the plant cells is therefore an active transport process which is regulated by various cellular mechanisms, including signal transfer, plasma membrane regulation and recycling (Tripathi et al., 2017). When applied on the surface of leaves,

the entry of nanoparticles is governed either by the stomatal openings, by the trichomes or by cuticular routes which accumulate and are then transported to the varying plant tissues, which is described as a top-down movement.

After penetration into the root's epidermal cell wall and membrane, the nanoparticles enter the vascular bundles through a series of steps. To achieve the crossing of nanoparticles into the cell membrane, it is necessary for the nanoparticles to undergo passive integration from the endodermal apoplast (Tripathi et al., 2017). The penetration into the seed coat occurs by uptake through parenchymatous spaces and is regulated by the aquaporins present in the seed, which thereby enhances liquid diffusion into the cotyledons (Wang et al., 2016). Entry of nanoparticles through the vascular system or lateral root sites occurs due to incomplete formation or breakdown of Casparian strips, respectively.

Second Part

Chapter II

Material and methods

II. Material and methods

II.1. Nanostructured alumina (NSA) preparation

NSA was prepared by the method described by Li et al.(2006) with little modifications. A preliminary solution was prepared by sol-gel method as follows: aluminium nitrate (0.5 M) and 1, 4-butandiol (50 mL) were gradually added to 200 mL 1:1 water-ethanol solution. Then the solution was placed on a hot plate at 40 °C for 30 min. citric acid (0.55 mL) dissolved in deionized water (40 mL), were added to the solution and continuously stirred until a colloidal solution was prepared. The obtained solution was heated in a water bath at 80 °C for 18 h to evaporate the solvent and then placed on a hot plate at 120 °C for 4 h until the viscosity and colour changed as the solution turned into a transparent stick gel. The obtained sol-gel precursors were then dried at 200 °C for 12 h in an oven and grinded into powders. Finally, the pale brown powder obtained after gel drying, was heated at 1000 °C for 1 h.

II.2. Characterization of NSA

The NSA obtained by sol-gel method was characterized by X-ray diffraction (XRD), Scanning Electron Microscopy (SEM) with Energy Dispersive X-Ray Analysis (EDX) microanalysis and Fourier Transform Infrared Spectroscopy (FT-IR spectroscopy) analyses.

The XRD analysis is one of the most widely used, empirical evidence to estimate the crystalline size of nanoparticles (Guczi et al., 2003; Lemine, 2009). The structure of NSA particles was investigated using a X'Pert Analytical type MPD multi-purpose X-ray diffraction system piloted by the X'Pert HighScore software (Malvern Panalytical Ltd, Malvern, UK) to display, treat, index, and match the diffraction data to known phases.

FT-IR spectroscopy analysis of NSA was carried out using a Irtaffinity-1 infrared spectrophotometer (Shimadzu, Kyoto, Japan) over the range of 4000 to 400 cm⁻¹. The analysis was carrying out at room temperature on KBr discs made up of 10 mg of NSA samples mixed in about 150 mg of ground KBr (IR grade, >99%). The powder was pressed into pellets (Ø = 10 mm) with low pressure (~1.5 psi) (Dablemont et al., 2008)

II.2.1. Scanning Electron Microscopy (SEM) with Energy Dispersive X-Ray Analysis (EDX) microanalysis

SEM-EDX microanalysis were performed on NSA to confirm their composition and on the leaves of the plants obtained from seeds treated with NSA to assess the contamination of the plants by NSA. For the NSA microanalysis, a little amount of the powder was adhered to a aluminium stub using carbon tape glued on both sides and were directly put on the stage

of the electron microscopy chamber. Five lectures of the elemental composition were performed on five different particles of the sample. As for the plant, five leaf samples (1 cm²) were cut from fresh leaves of *P. Vulgaris* var. “Piattelli” obtained from seeds treated or not treated with 240 mg NSA and grown as reported above. The samples were individually attached to aluminium stubs using carbon tape glued on both sides and were directly put on the stage of the electron microscopy chamber. Samples were then analysed using the environmental scanning electron microscopy (ESEM) (FEI Quanta 200, Netherlands). The elemental analysis was obtained by an energy-dispersive X-ray analysis (EDX) system performed in the ESEM chamber using a Bruker X-Flash 6/30 Detector. The chamber pressure and accelerating voltage were 130 Pa and 10 kV, respectively.

II.3. Insect rearing

Oryzaephilus surinamensis (L.), *Stegobium paniceum* (L.), and *Tribolium confusum* (du Val) were reared at room temperature, 65% Humidity, natural photoperiod, in PVC boxes (20 × 25 × 15 cm) containing chickpeas, beans, maize, and wheat grains and covered by a nylon net allowing air exchange. Adults mixed sex (about 7 days old) were used for the bioassays (Bougherra et al., 2015).

II.4. Insecticidal activity of NSA

The insecticidal efficacy was tested mixing the NSA with the beans at the doses of 0 (control), 25, 50, 100, 200, and 400 mg Kg⁻¹ of seeds. *Phaseolus vulgaris* L. var. “Piattelli” seeds were shaken manually for 10 minutes with each dose of NSA in a glass jar (750 mL) to achieve an even distribution in the entire seeds mass. Then, 10 unsexed adults of each insect species were added into each jar. The jars were placed in an incubator at 27±1°C, 60% RH and in the darkness. The mortality percentage was then determined after 3, 6, 9, 12, and 16 days. The insects were considered dead when no leg or antenna movements were observed visually after prodding them with a fine brush. Depending on the number of specimens available, five (*O. surinamensis* and *T. confusum*) or three (*S. paniceum*) replications for each NSA dose were performed.

*Oryzaephilus surinamensis**ibolium confusum**Stegobium paniceum*

II.5. Effects of NSA on *P. Vulgaris*

II.5.1. *In vitro* tests

Seeds of *P. vulgaris* var. “Piattelli” uniform in size were checked for their viability by suspending them in deionized water. The seeds were then surface sterilized in a 10% sodium hypochlorite solution for 10 minutes and rinsed through with deionized water several times. The NSA were dispersed in deionized water by ultrasonic vibration to obtain a concentration of 1.6 mg mL^{-1} and maintained in suspension by magnetic stirrer until use. A disc of Whatmann No. 1 filter paper was placed into a Petri dish (10×15mm) and 10 mL of the NSA suspension were added. Ten seeds were then transferred onto the filter paper and the Petri dish covered and sealed with tape. The Petri dish was then placed in an incubator for 5 days at $25 \pm 1^\circ\text{C}$ in darkness. Control seeds were treated with 5 ml of deionized water only. The germination of the seeds was checked daily and the Germination Percentage (GP) was calculated according to (Lombardi, 2019) by the following formula:

$$\text{GP} = (\text{germinated seeds} / \text{total seeds tested}) \times 100$$

P. vulgaris seedlings’ root and hypocotyl elongation was measured at the end of the trial. Five replications for treatment were performed.

II.5.2. *In pot* tests

The effects of NSA on plant growth were investigated by pot culture. A 1.6 mg mL^{-1} NSA solution was prepared as above reported. 150 mL (240 mg NSA) of the suspension were used to wet a sterilized filter paper disk (10 cm Ø). Seeds of *P. vulgaris* var. “Piattelli” were immersed in a 10% sodium hypochlorite solution for 10 min to ensure surface sterility, rinsed in deionised water and each seed was then wrapped in a sterilized filter paper charged with the NSA solution. The wrapped seeds were then sown in pots containing 800 ml of

substrate (Universal Toprak Virgoplant, Leroymerlin, Livorno, Italy). Three seeds were sown in each pot. As control, the seeds were wrapped in sterilized filter paper wetted by deionized water only. Three replications for each NSA treatment and the control (0 mg Kg^{-1}) were performed. The beans seedlings were grown for 7 days in a grow chamber at 25°C (day) and 23°C (night), with a 16:8 h light: dark photoperiod (photosynthetically active radiation intensity $280 \mu\text{E s}^{-1} \text{ m}^{-2}$) and $60 \pm 10\%$ relative humidity. After 14 days root and shoot elongation were measured.

II.6. Antifungal assay

II.6.1. Test organisms

The test fungal organisms used in this study (*Trichothecium roseum*, *Cladosporium herbarum*, *Penicillium chrysogenum*, *Alternaria alternata* and *Aspergillus niger*) were obtained from Section of Mycology and Plant Pathology, Department of Botany, University of Tizi ouzou

II.6.2. Spore germination assay

To evaluate the efficacy nanostructured of alumina on spore germination of some tested fungi, different concentrations, 0.1 mg/ml, 0.2 mg/ml, 0.3 mg/ml, 0.4 mg/ml and 0.5 mg/ml of NSA was prepared from the precipitated sample. Spore suspension with 1×10^3 conidia/ml was prepared in sterilized distilled water. Equal volume of spore suspension and the nanomaterials solutions were mixed in a test tube and then shaken. control spore suspension was mixed with equal volume of distilled water. A drop of the mixture (about 0.1 ml) was then placed in the cavity slide and these were incubated for $25 \pm 2^{\circ}\text{C}$. Three replicates were maintained for each treatment including the control. The slides were examined after 24 h by hand tally counts at different microscopic fields. Percent spore germination of each treatment was calculated by the formula given by Király et al.(1970).

$$\text{Percent spore germination} = \frac{\text{No.of spores germinated}}{\text{Tota no.of spores examined}} \times 100$$

$$\text{Inhibition of spore germination (\%)} = \frac{\text{Gc} \times \text{Gt}}{\text{Gc}} \times 100$$

Where Gc and Gt represent the mean number of germinated conidia in control and treated plates, respectively.

II.6.3. Agar well diffusion assay

The antifungal activity of nanostructured alumina was determined by agar well diffusion method as adopted by Perez et al.(1990). 7–8 days old fungal cultures grown on potato dextrose medium (PDA) medium were used to check the antifungal activity of synthesized nanostructured alumina. An aliquot of 0.02 ml of inoculum from each fungal pathogen was inoculated in 20 ml of PDA medium in culture tubes. The culture tubes were then homogenized between the hands and poured into 90 mm Petri plates. Different concentrations (0.10 mg/ml, 0.25 mg/ml and 0.50 mg/ml) of the nanostructured were prepared and added to respective wells. 0.1 mg/ml (20 µl/disc) was used as standard (Positive control). The effect of nanostructured alumina against the fungal pathogens were evaluated and compared with the standard used during the present study. The plates were then incubated at 25 ± 2 °C for 5 days. The antifungal activity was calculated by measuring the zone of inhibition by using standard scale.

II.7. Biosynthesis of alumina nanoarticles using *Rhamnus alaternus*

II.7. 1. Preparation of *Rhamnus alaternus* leaf extract

50 g fine grounded powders of *Rhamnus alaternus* was extracted under reflux conditions at 80 °C for 30 min in 500 mL double distilled water and centrifuged at 7000 rpm. The obtained extract then filtered and kept in refrigerator used as reducing and stabilizing agents.

II.7. 2. Synthesis of the alumina nanoarticles (Al₂O₃-Nps) using *Rhamnus alaternus* leaf extract

30 mL of aqueous plant extract and 100 mL of 0.05 M aqueous solution of Aluminium nitrate were mixed in 80 °C. Then the mixture centrifuged at 7000 rpm for 30 min, The mixture solution was then stirring at 100-150°C , and Finally , calcined at 1100 °C for about 3 h, Figure 05, Sutradhar et al. (2013).



Figure 5. Schematic representation of green synthesis of Al_2O_3 NPs

II.7.3 Characterization of synthesis of the alumina nanoarticles (Al_2O_3 -Nps) using *Rhamnus alaternus* leaf extract

The Al_2O_3 -Nps obtained by biosynthesis method was characterized by X-ray diffraction (XRD), Scanning Electron Microscopy (SEM) were describe below in synthesis of Nanostructured of alumina.(see page 102) characterization of NSA.

II.8. Data analysis

Univariate linear regression analysis was used to identify associations between the mortality of the insect pest species and the NSA dose. Differences in the insecticidal effect of NSA among the species were investigated by one-way between-groups univariate analysis of covariance (ANOVA) with the species as fixed factor. The NSA dose and the time of exposition were considered as covariates in the model and their effect was controlled in the analysis. The Abbott's formula was used to adjust the mortality percentage rates of the treatments on the basis of the controls' mortality. Post hoc comparisons were performed using Bonferroni corrections for multiple comparisons. The estimated marginal (EM) means of the insect pests' mortality are reported. Differences between plant germination, and plant growth data of NSA-treated and NSA-non-treated samples were analysed by student's t-test. Percentage data (insect mortality and seeds germination) were arcsine transformed prior to statistical analysis. All analyses were performed by SPSS 22.0 software (IBM SPSS Statistics, Armonk, and North Castle, New York, USA).

Second Part

Chapter III

Results and discussion

III. Results and discussions

III.1. Nanostuctured alumina-gel characterization

III.1.1. X-Ray diffraction (XRD)

The Scherrer method is used for calculating particle size gives an average value, the crystal sizes of the NSA were determined by means of an enhancement of crystallinity. XRD can measure nanocrystallites size; the fundamental mechanism for nanocrystallite size measurement can be explained as follows (Castellano, 1996).

The release from the foreground will be cancelled by the release from the 500 layer deep plan in the crystal, with a phase shift of $500.5\lambda_x$ similarly, if the distance for X-rays diffracted from the foreground is $1.00001\lambda_x$, the diffusion will be cancelled by an aircraft 50000 deep layers in the crystal. Bragg diffraction should only occur at the exact Bragg diffraction angle, producing an acute peak. However, if a particle is only 1 nm, then the blueprints had to cancel the diffusion of the initial shock wave. (such as the plane (hkl) with a diffracted distance of $1.0001\lambda_x$, this will be the plane 5000th plane and more) are not present (Baczanski et al., 2004). The diffraction peak will show the intensity at a θ lower and end at a θ higher than the Bragg angle. The size of the nanocrystallites causes the diffraction peak to widen. Conversely, the size of Dhkl crystallite can be estimated from the widening of the diffraction peak line:

$$D_{hkl} = \frac{Ssch \lambda}{B \cos \theta}$$

where:

- B is the full width at half maximum intensity,
- θ is the diffraction angle (in radians) of the considered diffraction peak, and
- SSch is Scherrer constant (~ 0.9).

Dried alumina-gel analysed using The X-ray diffractograms showed wide peaks corresponding to alumina nanoparticles (Figure 06).

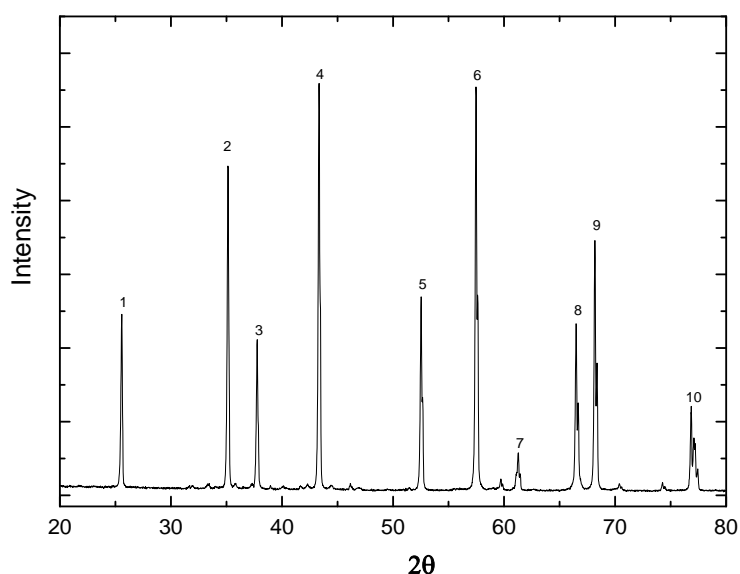


Figure 6. XRD spectra nanostructured alumina obtained after drying gel at 1000°C.

The average crystallite size of nanostructured alumina obtained was 56.9 nm. Broad peaks at 37°, 43°, and Sharp peaks of alumina proved its good crystallization (Sun et al., 2008). The data obtained were matched with the database of the Joint Committee on Powder Diffraction Standards (JCPDS), which confirmed with 80 % the crystalline structure of alumina in reference. The results of the XRD, shown in **Table II**, exhibited a well-resolved peaks, confirmed the polycrystalline and monophasic nature of the prepared material. The diffraction peaks provided a clear evidence of the formation of NSA with an average particle size of 56 nm.

Rogojan et al.(2011), demonstrate that crystallite sizes obtain from X-ray diffraction images for the alumina powders using sol-gel methods is 10.70 nm. The differences between two results can probably explained by measuring the angles and intensity of the diffracted rays, the symmetries of the crystal structure (space group) and a three-dimensional image of the electron density in the lattice. From this density, the average position of the atoms of the crystal forming the crystal pattern can be determined as well as the nature of these atoms, their chemical bonds, their thermal agitation.

Ates et al.(2015), reported and showed an amorphous structure with a small crystallization degree, for these purpose, the Debye-Scherrer equation was used to derive the crystallite size from the XRD data by determining the width of the 57.01° peak.

Another study on XRD patterns of Al_2O_3 NPs prepared at different laser fluences show that XRD pattern of alumina nanoparticles, prepared at 3.5 J/cm^2 , exhibited a single diffraction peak located at 32° corresponding to (220) plane which indexed to face centered cubic c- Al_2O_3 metastable phase according to JCPD# 29-0063, no peaks related to pure Al element or other metastable phases were found in XRD pattern indicating the complete transformation of Al into c- Al_2O_3 after laser ablation (Ismail et al., 2017).

Table II: X-ray diffraction (XRD) analysis of the nanostructured alumina.

Peak position ^a	B structure ^a	Crystallite size ^b
25.58	0.167	48.7
35.15	0.143	58.4
37.80	0.123	35.1
43.34	0.143	59.9
52.54	0.143	62.0
57.48	0.163	55.5
61.29	0.122	36.4
66.50	0.143	66.5
68.19	0.122	78.4
77.22	0.061	68.1

^a, 2θ Th; ^b, values are expressed in nm

III.1.2. Fourier Transform InfraRed spectroscopy analysis(FT-IR)

FT-IR spectroscopy is widely used for the analysis of nano-size metal oxides. Specific bands due to metal-oxygen bonds were recorded below 1000 cm^{-1} for these compounds.

The results of the FT-IR analysis are shown in Figure 07. The broad smooth absorption from 550 to 900 cm^{-1} reveals the formation of NSA. Significant spectroscopic strips at 1381, 1559, 1655, 1681 and 1736 cm^{-1} were identified as the absorption bands characteristic of H_2O and CO_2 . Peaks localized at 3400 and 3500 cm^{-1} were assigned to stretching vibration and deformation vibration of liaison O-H.

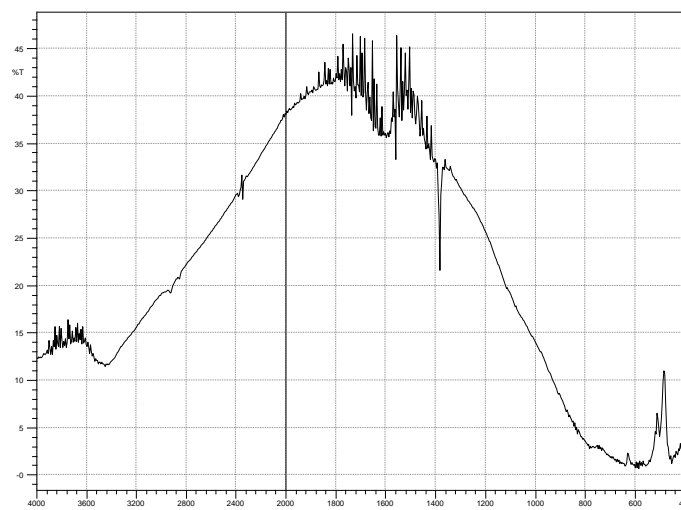


Figure 7. FTIR spectra of nanostructured alumina calcined at 1000 °C

The result of FTIR allowed to clarify the structure spectral relationships of the associated molecular vibrations, the resulting peak bands at 550 to 900 cm^{-1} can be attributed to the formation of alumina-oxygen.

A.Janbey et al.(2001) reported that IR spectra shows the strong absorption bands at 1600 cm^{-1} due to the various vibration made of triethanolamine the metal ions also the bands appearing at 1005 and 800 cm^{-1} could be attributed to the presence of nitrates ions and bands appeared in the region 700- 400 cm^{-1} could be the results of some trace amounts of metal oxides.

Several studies on the spectra of $\alpha\text{-Al}_2\text{O}_3$ shows band with a maximum of 454.2 cm^{-1} and a broad band with multiple peaks at 602.2, 644.3 and 729.1 cm^{-1} assigned to stretching and bending vibrations of Al-O were recorded. These were the most intense bands of the $\alpha\text{-Al}_2\text{O}_3$ FT-IR spectrum, with transmittance values between 22.7 and 37.2%. The peak of 1114.4 cm^{-1} may be assigned to Al-OH bending vibration (Manivasakan et al., 2011). Also, a few small bands were observed: the first with maxima at 1436.8 and 1384.7 cm^{-1} , the second with peaks at 1592.6 and 1630.6 cm^{-1} and the third with a large band at 3438.5 cm^{-1} . The transmittance values of these were small, which ranged from 69.1 to 79.8%. The band centered at 3438.5 cm^{-1} was assigned to O-H stretching vibration of adsorbed water, and those from 1630.6 to 1592.6 cm^{-1} were assigned to bending vibrations of H-O-H(Gondal et al., 2012). Bands with peaks at 1436.8 and 1384.7 cm^{-1} were assigned to carbon dioxide $\nu(\text{O-C-O})$ symmetric vibration in the forms of carbonate and bicarbonate, respectively. Because alumina is an amphoteric oxide it contains both basic and acidic sites: by carbon dioxide adsorption both carbonate and bicarbonate species, respectively, may be formed (Galhotra, 2010)

III.1.3. Energy Dispersive X-Ray (EDX) system coupled with Scanning Electron Microscopy (SEM)

III.1.3.1 . Nanostructured alumina structure

In order to observe the structure nanostructured alumina, EDX-system coupled with Scanning Electron Microscopy was carried out. It use also to determine the homogeneity and it's elemental distribution in the synthesize structure. High magnification image (Figure 08) reveals clearly that large particles are in fact agglomerates of much smaller particles and possess different shapes. The elemental analysis of nanostructured alumina by energy-dispersive X-ray analysis (EDX) of nanostructured alumina in order to elucidate the composition of nanostructured alumina they confirm the presence of constituent elements: Al, O and C with mass percentage 34.83%, 33.97% and 31.19%, respectively (**Table III**).

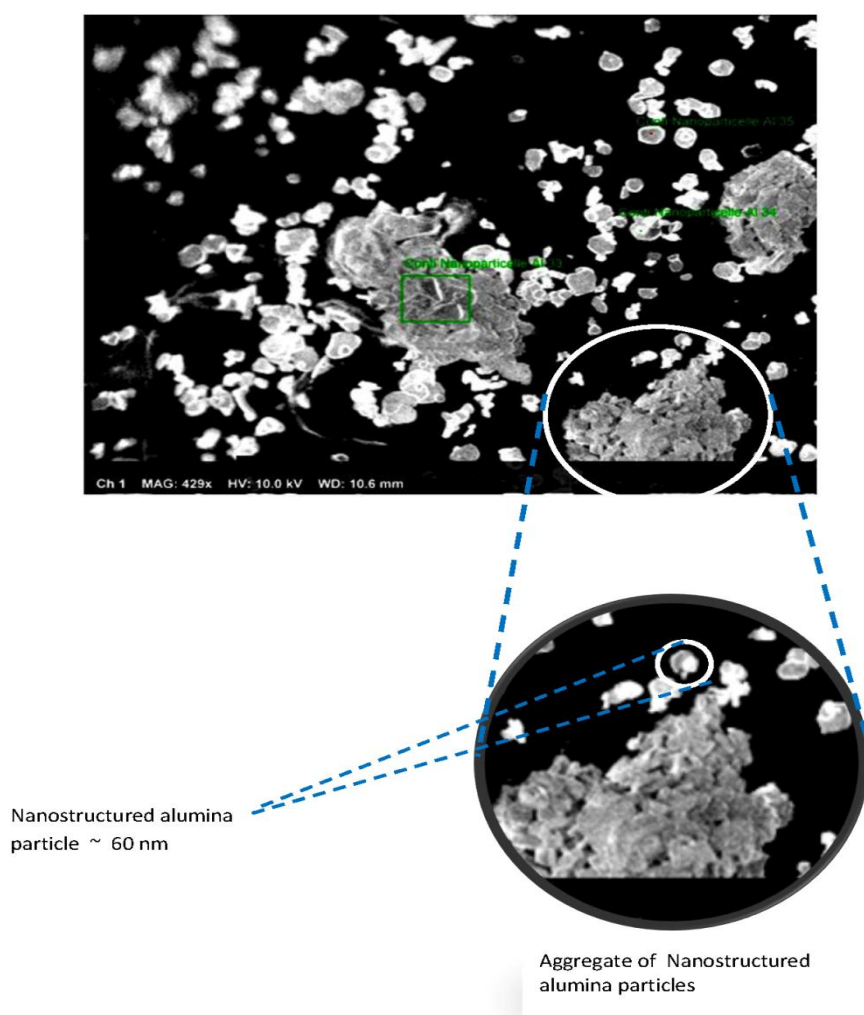
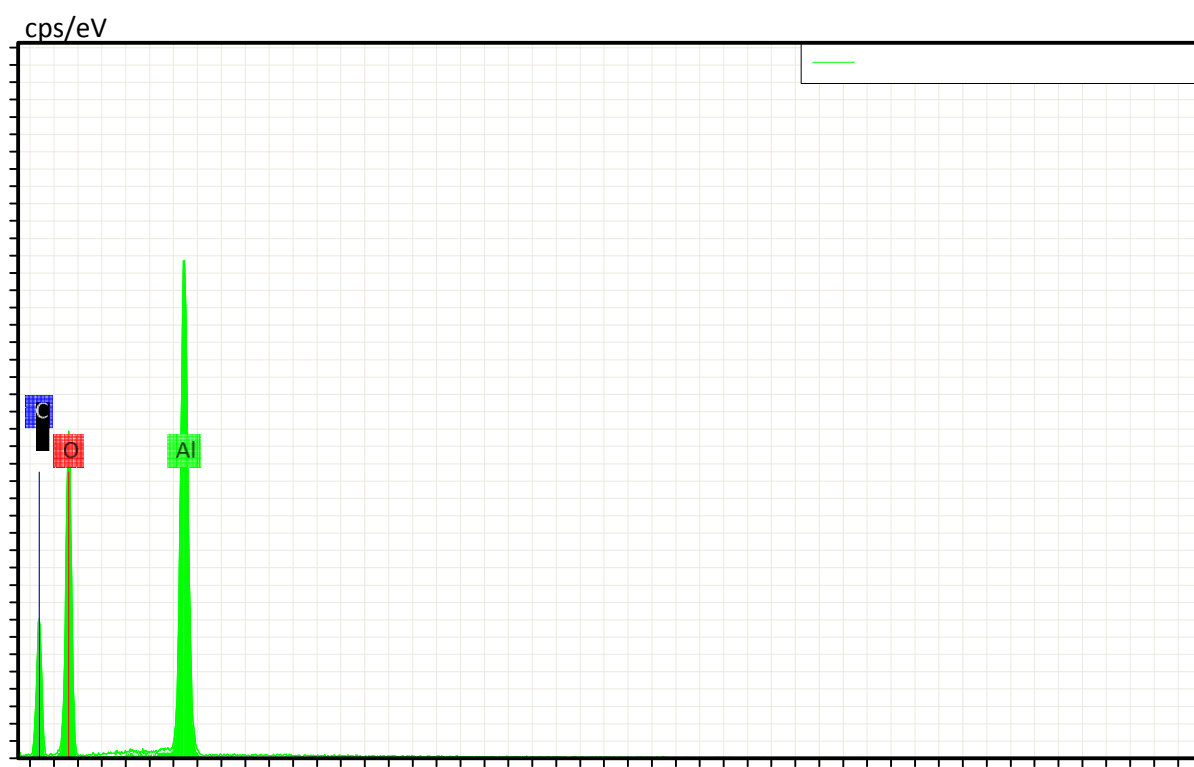


Figure 8. Scanning Electron Microscopy of nanostructured alumina

Table III: Miniral composition of nanostructured alumina

Element	atomic mass	Mass [%]	Mass Normal. [%]	abs. error [%] (1 sigma)	rel. error (1 sigma)
Oxygen	8 20292	31.77	34.83	5.32	12.87
Aluminium	13 42110	30.99	33.97	1.65	4.60
Carbon	6 7676	28.45	31.19	4.10	14.65

EDX spectrum shows (Figure 09) the typical absorption peak approximately at 10 keV due to surface Plasmon resonance. The presence of the elemental aluminium can be deduced from the EDX analysis, which also supports the XRD results. This indicates the reduction of aluminium ions to elemental alumina.

**Figure 9.** EDX spectrum of nanostructured alumina

III.1.3.2. Insecticidal effect of NSA

The toxicity assay of NSA showed a strong dose-effect relationship between NSA doses and insect mortality (*O. surinamensis*: $R = 0.684$; $F_{1,13} = 11.426$; $P = 17.535$; *S. paniceum*: $R = 0.952$; $F_{1,10} = 95.909$; $P \leq 0.001$; *T. confusum*: $R = 0.758$; $F_{1,13} = 48.987$; $P = 0.001$).) (Fig. 10A, 10B, 10C)

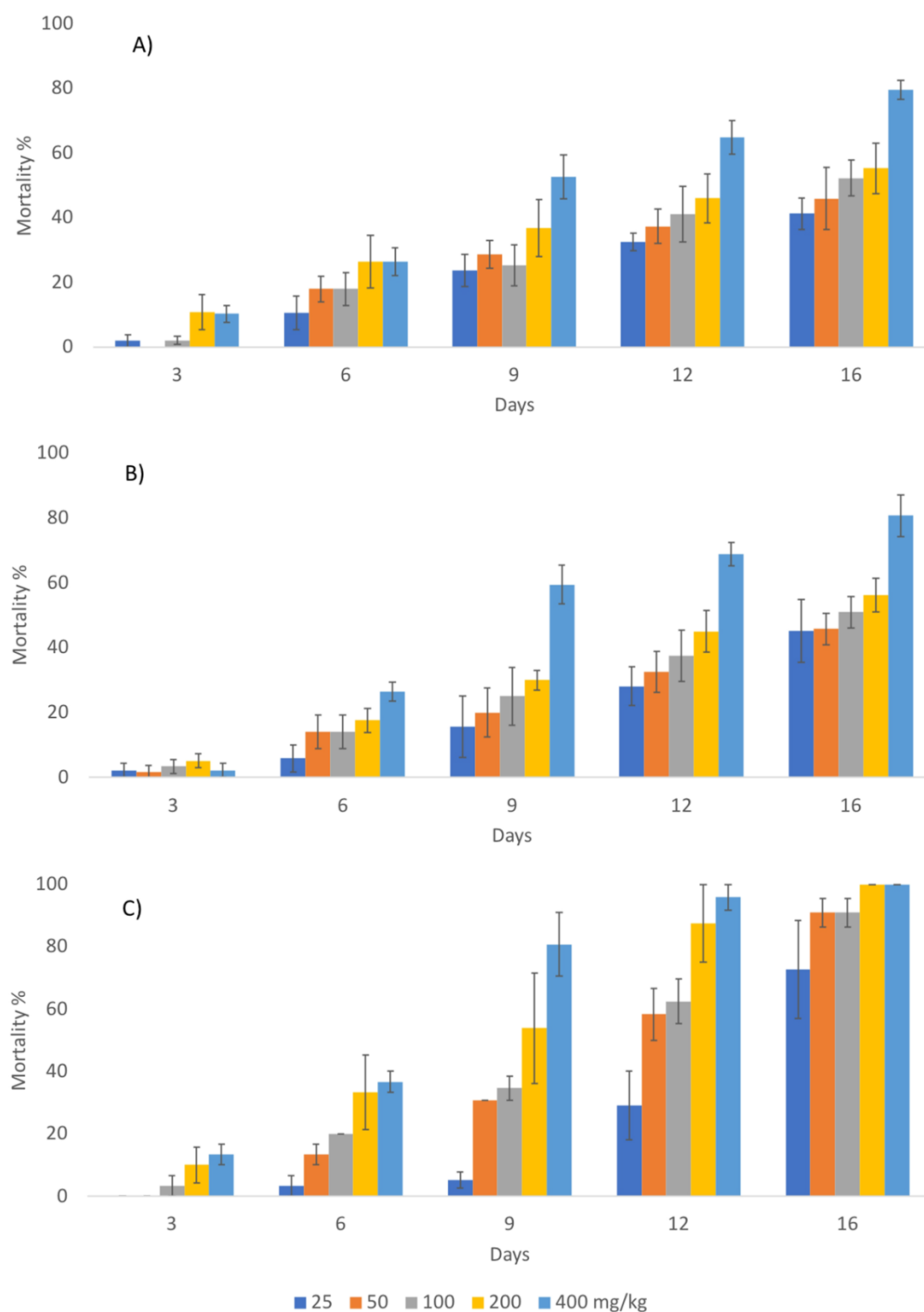


Figure 10. Mortality (%) (mean \pm SE) of *T. confusum*: (A) *O. surinamensis*; (B) *S. paniceum*; (C) adults fed on beans treated with nanostructured alumina (NSA) particles.

After sixteen days, the percentage of insect mortality at the highest NSA concentration tested (400 mg kg⁻¹) was 100.00% for *S. paniceum* followed by *O. surinamensis* (80.64%) and *T.*

confusum (79.41%). Repeated measures ANOVA showed a significant within-subjects effects of the time of exposition on mortality of the three specie after controlling for the effects of the NSA dose ($F_{3, 152} = 94.233$; $P < 0.001$; $\eta^2 = 0.623$) with a significant interaction of the time x dose ($F_{3, 152} = 14.991$; $P < 0.001$; $\eta^2 = 0.208$) and of the time x species ($F_{3, 152} = 6.587$; $P < 0.001$; $\eta^2 = 0.188$). The effect of the species (between-subject effect) was significant also ($F_{2, 57} = 12.689$; $P < 0.001$; $\eta^2 = 0.308$). The estimated marginal means (evaluated at NSA = 151.23 mg kg⁻¹) showed that the most susceptible species was *S. paniceum* (mean = 36.08%) followed by *T. confusum*, and *O. surinamensis* (mean = 28.55, and 23.04, respectively) (Table IV).

Table IV. Adjusted estimated marginal (EM) means on mortality of *Tribolium confusum*, *Oryzaephilus surinamensis*, and *Stegobium paniceum* exposed to nanostructured alumina

Species	Mean ^a ± SD	95% Confidence Interval	
		Lower bound	Upper bound
<i>T. confusum</i>	28.397 ± 1.116	26.201	30.593
<i>O. surinamensis</i>	23.298 ± 1.116	21.101	25.494
<i>S. paniceum</i>	35.928 ± 1.382	33.208	38.647

Data are expressed as mean mortality percentage ± standard error. ^a

Covariates (dose and time of exposure) are evaluated at the following values:

NSA = 297.54 mg kg⁻¹, Time = 9.20 d.

Pairwise comparisons of EM means showed that *S. paniceum* was significantly more susceptible to NSA than the other two insect species (Table VI).

Median lethal concentration (LC₅₀) values calculated by Probit analysis were 61.53, 14.87, and 127.17 mg Kg⁻¹ for *O. surinamensis*, *S. paniceum*, and *T. confusum*, respectively (Table III), consistently with the RM-ANOVA. RMP analysis showed that, *S. paniceum* was significantly more susceptible to NSA than *O. surinamensis* (*S. paniceum* vs *O. surinamensis* RMP = 0.242; 95% CI: 0.034-0.770) and *T. confusum* (*S. paniceum* vs *T. confusum* RMP = 0.117; 95% CI: 0.010-0.403).

Table V: Toxicity of nanostructured alumina against adult *Oryzaephilus surinamensis*, *Stegobium paniceum* and *Tribolium confusum*

Species	LC ^a	Intercept	P
<i>O. surinamensis</i>	0.44(0.23-1.02)	1.186	< 0.001
<i>S. paniceum</i>	1.10(0.60-10.70)	-0.138	0.544
<i>T. confusum</i>	127.17(60.24-305.92)	-0.978	0.001

^a, Concentration of the NSA that kills 50% of the exposed insects.

Data are expressed as mg Kg⁻¹; in bracket, confidence interval.

Pearson goodness of fit test: $\chi^2 = 3.379$; df = 11; $P = 0.985$.

The toxicity bioassay showed the NSA is able to exert a significant insecticidal activity against the main seeds pests *O. surinamensis*, *S. paniceum*, and *T. confusum*. According to our results, the most susceptible species to the NSA was *S. paniceum*, while *O. surinamensis* resulted the most resistant one. Although no previous studies are available on the effects of NSA on the species tested in this work, in line with our results Stadler et al.(2010) reported 100% mortality of the stored grain pests *Rhyzoperta dominica* (Coleoptera: Bostrichidae) and *Sitophilus oryzae* (Coleoptera: Curculionidae) adults in wheat treated with 1000 mg kg⁻¹ of NSA dust after 9 days of exposure and about 95% mortality after only 3 days of exposure. A high effectiveness of NSA was observed also by Goswami et al.(2010) with about 90% of mortality of *S. oryzae* and *Tribolium castaneum* (Coleoptera: Tenebrionidae) exposed for 7 days to 2000 mg kg⁻¹ of hydrophilic NSA. Similarly, NSA produced by combustion of glycine and aluminium nitrate caused more than 94% mortality of *S. oryzae* adults after 15 days of exposure applied on wheat at doses ranging from 62.5 to 1000 mg kg⁻¹ (Stadler et al., 2012). Nevertheless, the efficacy of this NSA for control of *R. dominica* adults resulted in lower overall mortality levels than for *S. oryzae*. Similar results were obtained when three novel NSA dusts, based on chemical solution methods, were applied on wheat for control of *R. dominica* and *S. oryzae*. Buteler et al.(2015) and Teodoro et al.(2017) obtained a LC₅₀ of 79.91 mg kg⁻¹ after 39 days of exposition with a LT₅₀ of 23.82 days when tested at 500 mg kg⁻¹ for NSA against *S. oryzae*. The insecticidal effect of the NSA could be probably due to the electrically charged particles resulting by the oxidation of aluminium. Alumina electrically charged particles, showing interaction between dipole-dipole promote the formation of aggregates that stick firmly to the insect cuticle wax layer and generated electric charges resulting by triboelectric effect (Pimentel, 2005). In addition,

according to Stadler et al.(2017) the toxic effect of the NSA, similarly to those of other insecticidal dust such as diatomaceous earth should be due to the absorption by NSA of the epicuticular lipids, causing the insect death by dehydration. The insecticidal effect should also depend on NSA physical characteristics, (i.e. particle size, particle morphology) and on other biotic and abiotic factors such as target species, and relative humidity (Buteler et al., 2015).

III.1.3.3. Effects of NSA on growth and germination of *P. Vulgaris*

The initial stages of growth and development of plants begins with seed germination, leading to elongation of roots and emergence of shoot. Depending on the concentration and on the plant species, nanoparticles have varying effects on seed germination. Metal oxide nanoparticles and carbon-based nanoparticles exhibit diversifying effects on seed germination, root elongation and shoot growth. Scientists have shown through their experiments that different nanoparticles augment both positive and negative effects upon different plant species. Upon exposure to metal oxide nanoparticles, the effect on seed germination as well as elongation can be inhibitory, neutral or promoting.

In our study the NSA treatment of the beans show not affect the *P. vulgaris* on germination ($t_8 = 1.159$, $P = 0.192$) the seedlings' root and hypocotyl elongation ($t_8 = 1.074$, $P = 0.341$; $t_8 = 1.159$, $P = 0.280$, respectively. (Table VI)

Table VI: Effect of nanostructured alumina (NSA) on seed germination and radicle and shoot elongation of *Pheseolus vulgaris* seedling.

	Control	NSA
Seed Germination ^a	7.60 ± 0.60	6.00 ± 0.95
Ipocotyle ^b	30.12 ± 7.71	18.00 ± 7.06
Root ^b	5.20 ± 0.78 ^a	10.68 ± 5.04 ^b

^a, % germination seed; ^b, cm control seed not treated with NSA, data are expressed as means ± standard error

Table VII: Effects of nanostructured alumina (NSA) on plant of *Phaseolus vulgaris* in pot culture

	<i>Control</i>	<i>NSA</i>
First internod ^a	2.59 ± 2.13	2.13 ±0.39
Second internod ^a	5.76 ± 0.79	5.75 ±0.66
Third internod ^a	6.70 ± 1.00	7.37 ±0.50
Fourth internod ^a	0.67 ± 0.66a	6.93 ±1.25b
Shoot (total) ^a	15.07±1.20a	22.76±2.25b
Leaves area ^b	56.93 ± 3.15	64.13 ± 1.72
Stoma density ^c	15.58 ± 0.36	13.25 ± 0.88
Root ^a	12.61±1.91	14.08±1.28

^a, cm; ^b, cm²; ^c, No. stoma cm⁻². Data are expressed as means ± standard error. Different letters indicate significant difference between treatments (t-test, P< 0.05).

No negative effect on the beans plants was observed also in pot culture. Nanoparticles with the emerging advancement have shown varying beneficial effects upon plants.

After 14 days from the seedlings emergence no differences were recorded for the leaves area, stoma density, and root length ($t_4 = 2.008$; $P = 0.115$; $t_4 = 2.456$; $P = 0.070$; $t_4 = 0.640$; $P = 0.557$, respectively). On the contrary, we observed a positive effect of the NSA on the shoot growth ($t_4 = 2.974$; $P = 0.041$) with the treated plants that were about 66% higher than the non-treated plants (Table VII).

We observed no significant effect of NSA on plant germination, seedlings elongation and plant growth, we observed any aluminate contamination on the surface of the *P. vulgaris* leaves. Nanoparticles can penetrate into the plant through the stomatal openings or the bases of trichomes and then transferred to various tissue (Fernández and Eichert, 2009). Previous studies showed that nanoparticles whose diameter is less than the pore diameter can reach the plasmatic membrane and cross it with incorporated transport carrier proteins or through ionic channels interfering with metabolic processes (Jia et al., 2005) and reaching mitochondria or nucleoli in both plant and insect tissues (Yasur and Rani, 2013). For this reason, it is important to assess the phytotoxicity of nanomaterials. Lee et al. (2010a) evaluated the effect of four metal oxide nanoparticles, aluminium oxide (nAl₂O₃), silicon dioxide (nSiO₂), magnetite (nFe₃O₄), and zinc oxide (nZnO), on the development of *Arabidopsis thaliana* (L.) Heynh (Brassicaceae) (seed germination, root elongation, and number of leaves) and, in

accordance with our results, found that aluminium oxide nanoparticles were no toxic whereas they observed a toxic effect of the other three metal oxide nanoparticles. The absence of effect of aluminium oxide nanoparticles on seed germination and root growth was also observed by Lin and Xing.(2007) who showed that the nanoparticles have no adverse effects on *California red* beans, while (Mahajan et al., 2011) observed a positive effect on seedlings growth of *Vigna radiata* (L.) Wilczek, and *Cicer arietinum* L. (Fabaceae) after a treatment by ZnO nanoparticles. In this experiment, the only effect of the NSA we observed was the increase of shoot growth in the treated plants that were about 66% higher than the non-treated ones (length of the shoot 15.07 ± 1.20 cm for the control and 22.76 ± 2.25 cm for NSA treatment). In line with our results, Khodakovskaya et al. (2009), observed that nanostructured carbon determines an increase on tomato plants seed germination and the plant growth and, according to the authors, such a positive effect of the nanoparticles could be due to their ability to penetrate the seed coat and enhance the water uptake.

III.1.3.4. SEM coupled with EDX of leaves *Pheseolus vulgaris* treated with Nanostructured alumina

The SEM image and EDX spectrum of leaves *Pheseolus vulgaris* treated with Nanostructured alumina are shown in Figure 11 and Figure 12. The EDX analysis confirms the mineral element contents present in *Pheseolus vulgaris* leaves treated with nanostructured alumina. The area number 36 showed mineral contents percentages as follow 67% oxygen, 24% carbon, silicon 7%, 0.24% calcium and 0.22% of potassium, while mineral contents percentages of 66% oxygen 33% carbon and 0.21% potassium (Figure 10).

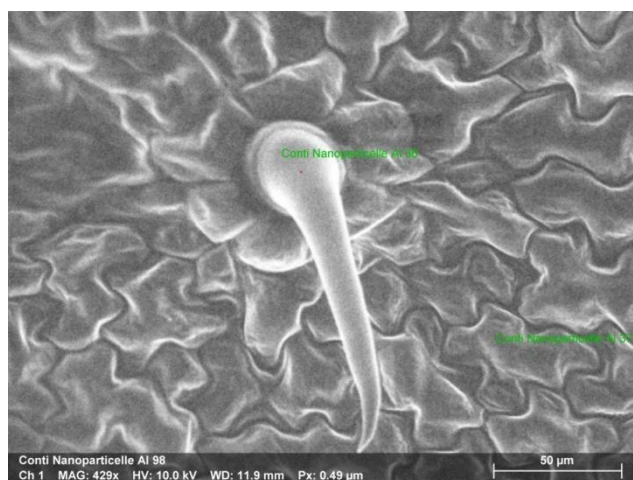


Figure 11. SEM image of *Pheseolus vulgaris* leave treated with nano structured alumina.

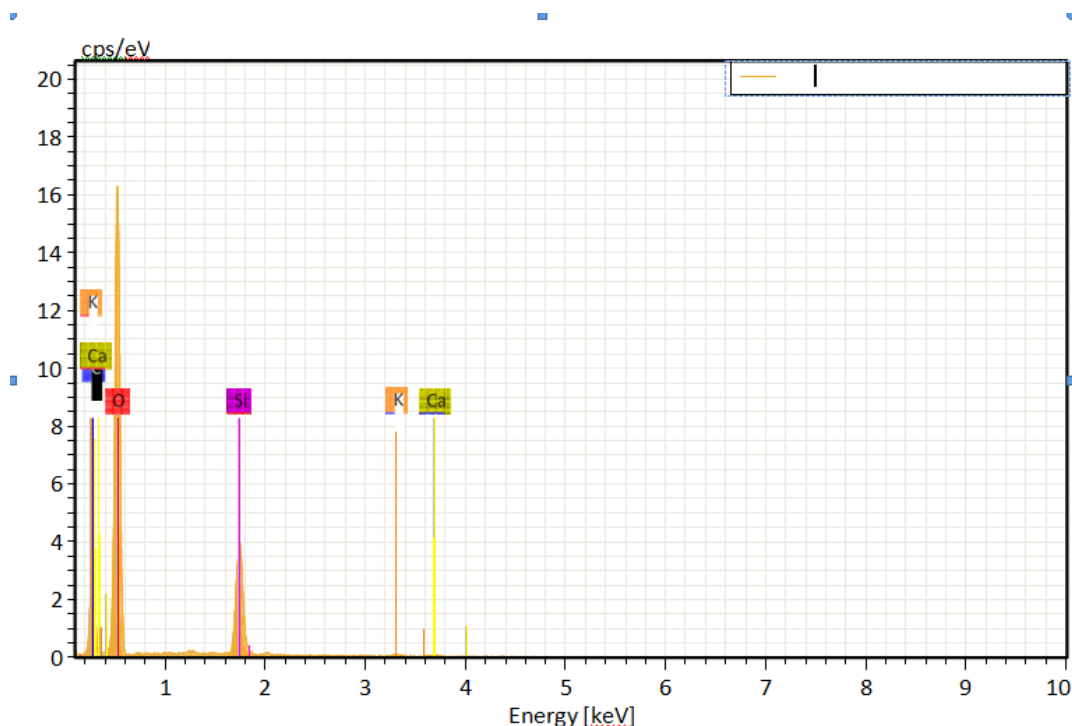


Figure 12. EDX spectrum of *Pheseolus vulgaris* leave treated with nanostructured alumina.

After 14 days of germination period, the *Pheseolus vulgaris* leaves treated with nanostructured alumina were analyzed by EDX-system. The result showed that alumina used in insecticidal activity was not present at the surface the leave (Figure 12). In Previous investigation, Santos. (2013), has demonstrated that different nanoparticles bestow a different effect on plants as every particle interacts with plants in a different pattern, including alteration in morphology as well as physiology. The chemical composition, reactivity, size and other properties of these nanoparticles determine its function upon interaction with plants, which can be positive or negative. Nanoparticles have been found to accumulate in plants and the surrounding environment, as plants bear large size, higher leaf area and are immobile in nature, rendering them highly susceptible to exposure from varied nanoparticles present in the environ (Dietz and Herth, 2011). The size of nanoparticles contributes to the contamination of the surrounding environment, depicting distinctive physicochemical characteristics, such as high surface area, energy and surface confinement, resulting in alteration in environmental behaviour and increasing toxicity drastically, compared to their bulk components. The surface properties are the main reason for toxicity of ENPs (Engineered Nano-Particles), which can be inhibited using surface functioning (Geisler-Lee et al., 2012). The absence of NSA in leaves can be explain, *Pheseolus vulgaris* can effectively decide the fate of nanoparticles and their environmental transport by aggregating them into their biomass (Anjum et al., 2013).

III.1.4. Antifungal assay

III.1.4.1. Effect of different concentrations of nanostructured alumina on the spore germination of some fungal pathogens

Nanostructured alumina effect of on spore germination results are represented in Table VIII.

Table VIII: Effect of nanostructured alumina on spore germination of different fungi.

Fungal pathogen	0.0 mg/ml	0.1 mg/ml	0.2 mg/ml	0.3 mg/ml	0.4 mg/ml	0.5 mg/ml
<i>T. roseum</i>	19±0.1	15.33±0.2 (19.31)	12.67±0.1 (33.31)	9.33±0.58 (50.9)	6.33±0.1 (66.68)	2.33±0.5 (87.73)
<i>C. herbarum</i>	17±0.2	15.67±0.01 (16.08)	12±0.9 (29.41)	9.33±0.58 (45.12)	5.33±0.5 (68.64)	2.67±0.3 (84.42)
<i>P. chrysogenum</i>	20±0.6	17.96±0.3 (10.2)	15±0.1 (25)	12.33±0.52 (40)	7.67±0.6 (61.65)	4±0.6 (80)
<i>A. alternata</i>	20±0.5	17.69±0.2 (11.55)	15±0.1 (25)	12.45±0.2 (37.75)	9.33±0.58 (53.35)	5.76±0.58 (71.2)
<i>A. niger</i>	19.6±0.1	17±0.1 (13.27)	13±0.3 (33.67)	9.67±0.9 (50.66)	6.33±0.8 (67.70)	3.33±0.9 (83.01)

Values are represented as mean ± SD.

Figures in parenthesis indicate the inhibition in spore germination (%).

The different concentration of nanostructured alumina tested at different concentrations (0.1 mg/ml, 0.2 mg/ml, 0.3 mg/ml, 0.4 mg/ml, 0.5 mg/ml) brought about significant inhibition of spore germination of all the tested fungal pathogens. However, inhibition in spore germination increases with the increase in concentration of the NSA. The maximum inhibition in spore germination was found by highest concentration of NSA (0.5 mg/ml) against *Trichothecium roseum* (87.73%) followed by *Cladosporium herbarum* (84.42%), *Aspergillus niger* (83.01%), *Penicillium chrysogenum* (80%), and least effective against *Alternaria alternata* (71.2%) at same concentration.

The results show clearly that nanostructured alumina tested at different concentrations in the present study caused significant inhibition in the spore germination and radial growth of all the tested fungal pathogens. The highest concentration was found more effective followed by the lower concentrations, also reported that the highest concentration of MgO, FeO and ZnO

nanoparticles as most effective than the lower concentrations(Wani and Shah, 2012) reported that antimycotic activity of MgO and ZnO nanoparticles against *Alternaria alternata*, *Fusarium oxysporum*, *Rhizopus stolonifer* and *Mucor plumbeus*. Nanoparticles due to their small size and large area to volume ratio show significant differences in properties not seen in the same material in their bulk forms(Issa et al., 2013; Khan et al., 2019).It can be due to their unique physiochemical, biological properties these NP's are used in pharmaceutical products, medical diagnostic imaging and medical treatment protocols (Khan et al., 2019).

III.1.4.2. Agar well diffusion assay

Antifungal activity of nanostructured alumina was also recorded by measuring the zone of inhibition for different fungal pathogens. All the concentrations showed significant zone on the inhibition against all the selected fungal pathogens. Highest zone of inhibition was shown by the highest concentration of nanostructured alumina (Table VIII, Figure 12). The maximum zone of inhibition was shown against *Penicillium chrysogenum* (28.67 ± 1.53 mm), followed by *Aspergillus niger* (27.33 ± 1.15 mm), *Trichothecium roseum* (25.67 ± 2.52 mm), *Alternaria alternata* (22.33 ± 3.83 mm) and *Cladosporium herbarum* (20.00 ± 1.00 mm) .

Table XI : Zone of inhibition by nanostructured alumina against different fungi.

Fungal pathogen	Activity index			
	0.1 mg/ml	0.25 mg/ml	0.5 mg/ml	Standard fungicides
<i>Trichothecium roseum</i>	$12.67 \pm 1.15a$	18.00 ± 1.73	25.67 ± 2.52	30.33 ± 2.52
<i>Cladosporium herbarum</i>	10.33 ± 0.58	15.00 ± 1.00	20.00 ± 1.00	26.00 ± 2.00
<i>Pencillium chrysogenum</i>	18.00 ± 1.00	23.33 ± 1.15	28.67 ± 1.53	34.33 ± 1.53
<i>Alternaria alternata</i>	15.67 ± 2.08	16.33 ± 3.51	22.33 ± 3.83	34.33 ± 0.58
<i>Aspergillus niger</i>	19.33 ± 1.53	24.67 ± 1.53	27.33 ± 1.15	34.00 ± 2.00

The presence of inhibition zone on culture media clearly indicates the biocidal activity of nanostructured alumin . The extent of inhibition depends on the concentration of nanoparticles and also fungal spore concentration. In another work Abdeen et al.(2013), reported that nanostructured alumina posses promising antimicrobial activity against several human pathogens. Wu et al.(2018) Studied the antifungal activity of green synthesized silver nanoparticles against *Cladosporium cladosporoides* and *Aspergillus niger* reported that NP's have effective biocidal properties even at low concentrations. Nehra et al.(2018), reported the antifungal and antibacterial activity of iron oxide nanoparticles against *Aspergillus niger*, *Fusarium solani*, *Escherichia coli*, *Bacillus subtilis* and *Candida albicans*. They also reported that iron oxide NP's can be used as effective antimicrobial agents. The mechanism of the antimicrobial activity of nanoparticles is due to their small size and larger surface area to volume ratio which effectively covers the microorganism and reduces oxygen supply for respiration.

Zakharova et al.(2015), reported that the antimicrobial activity of iron nanoparticules is due formation of reactive oxygen species (ROS) that cause damage to proteins and DNA in microorganisms by oxidative stress. Mohamed et al.(2015), also reported that iron nanoparticule cause oxidative stress by ROS generation and Fenton reaction. Since iron is strong reducing agent, it induces the decomposition of functional groups in membrane proteins and lipopolysaccharides. Iron nano also cause oxidation by intracellular oxygen leading to oxidative damage via Fenton reaction. These NP's penetrate through disrupted membranes causing further damage and death of cells(Lee et al., 2008).

III.1.5. Biosynthesis alumina nanoparticules(Al_2O_3 NPs) using extract of *Rhamnus alaternus*

Nowadays, several methods have been successfully used to fabricate the Al_2O_3 NPs, however, they have some demerits such as the higher cost of the method and not being eco-benevolent since they make lots of pollution in the ecosystem because of using perilous solvents and toxic reducing agent to overcome these disadvantages, green chemistry approaches have been employed for the fabrication of Al_2O_3 -NPs which are sustainable, less energy-intensive, eco-accommodating and increase the efficiency of the methods.

In this study, the green synthesis of the Al_2O_3 -NPs with aqueous *R.alaternus* leaf extract as reducing agent and efficient stabilizer was focused to convert Al ions to Al NPs.The

stabilization of Al_2O_3 NPs is dependent on biomolecules such as amino acids, enzymes, proteins, steroids, phenols, tannins, sugar and flavonoids, which are already present in the plant extracts having medicinal importance and are eco-benign (Ghotekar, 2019b; Sorbiun et al., 2018). The main principle in the green chemistry approaches is that the phytoconstituents are present in the plant parts serve the dual role of a natural reducing agent and a NP stabilizer (Duraismy, 2018b; Manikandan et al., 2019; Sutradhar et al., 2013). The various parts of plant such as leaves, seed fruit and flower are used to fabricate Al_2O_3 NPs in different morphologies and sizes by biological approaches. The aqua soluble heterocyclic constituents are mainly accountable for formation and stabilization of nanoparticles (Ghotekar, 2019a).

X-ray Diffraction (XRD) is used to determine the particle size, and every crystal structure and exact phase identification of Al_2O_3 -NPs.

The Scherrer method is used for calculating particle size gives From 19 to 69 (Table XI). Broad peaks at , and Sharp peaks Al_2O_3 NPs of proved its good crystallization(Sun et al., 2008).

The data obtained were matched with the database of the Joint Committee on Powder Diffraction Standards (JCPDS), which confirmed with 79 %, the crystalline structure of alumina in reference. The results of the XRD analysis (**Table X**) consisting in well-resolved peaks The X-ray diffraction peaks at $37,78^\circ$, $44,87^\circ$, and $66,532^\circ$ were assigned as (111), (200), and (220) lattice planes which are in good agreement with those of the standard pure Al_2O_3 nanoparticles (JCPDS No. 004-0787) (fig.12) , confirmed the polycrystalline and monophasic nature of the prepared material. The diffraction peaks provided a clear evidence of the formation of Al_2O_3 NPs with an average particle size of 37 nm.

Table X: X-ray diffraction (XRD) analysis of the Al₂O₃ NPs using extract of *Rhamnus alaternus*

No.	Peak pos. [°2Th]	B struct. [°2Th]	Crystallite size [nm]
1	25,603	0,117	69,6
2	31,281	0,335	24,7
3	32,824	0,201	41,3
4	35,184	0,167	49,8
5	36,667	0,24	34,9
6	37,787	0,184	45,6
7	39,92	0,401	21,1
8	43,381	0,184	46,5
9	44,87	0,401	21,4
10	47,729	0,335	26,0
11	50,746	0,401	21,9
12	57,511	0,224	40,4
13	59,739	0,286	32,1
14	63,368	0,49	19,1
15	66,532	0,163	58,2
16	67,552	0,387	24,7
17	68,188	0,184	52,3
18	76,905	0,204	49,7

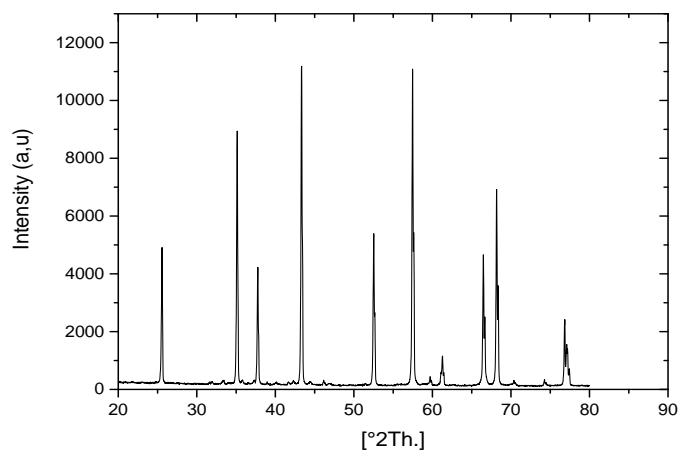


Figure 13. XRD spectra of the Al_2O_3 NPs using extract of *Rhamnus alaternus*

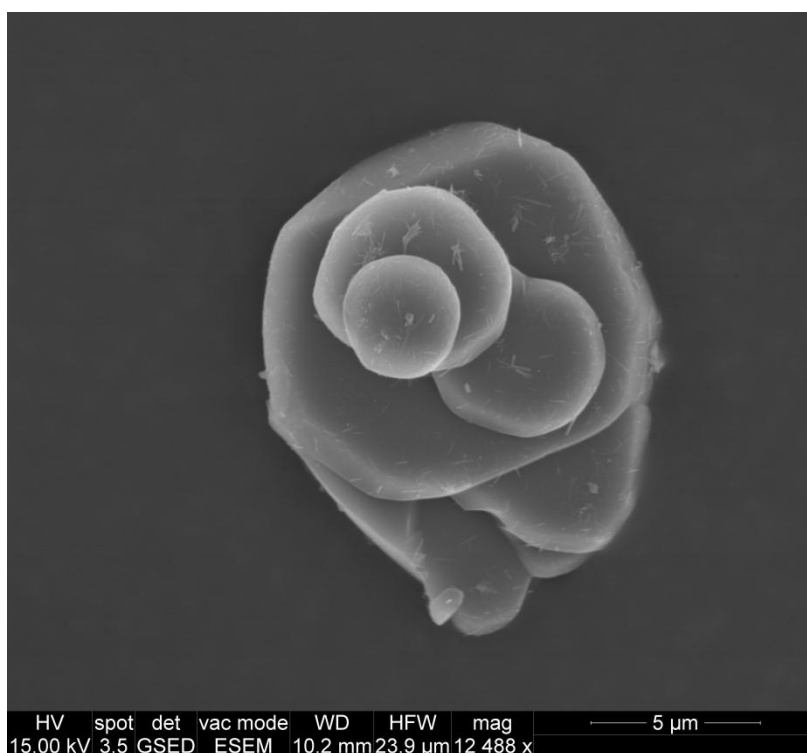


Figure 14. Scanning Electron Microscopy image spherical agglomeration alumina nanostructured using *Rhamnus alaternus* extract

According to Jalal et al.(2016) in their study on synthesis of alumina nanoparticles using lemongrass leaf extract as coupling and stabilizing agents, they found the XRD pattern shows the characteristic diffraction peaks of phase α -alumina ($\alpha\text{-Al}_2\text{O}_3$) at 2θ angles corresponds (012), (104), (110), (113), (024), (116), (214) and (300) indicate that $\alpha\text{-Al}_2\text{O}_3$ was the

dominant phase when calcinated above 1100 °C (JCPDS card no. 42-1468). The estimated average size of synthesized Al₂O₃ NPs was 34.5 nm.

Another study on XRD patterns of Al₂O₃NPs using *Prunus* and *yedoensis* leaf extracts. The size of the pH = 7 Al₂O₃ NPs are spherical and hexagonal shape and the size ranges between 50–100 nm (Manikandan et al., 2019).

Green Synthesis of Aluminium Oxide Nanoparticles by using *Aerva Lanta* and *Terminalia Chebula* Extracts. Analysis of the X-ray diffraction data revealed the average size of the Al-NPs as 70 nm. The AlNP were found to be spherical agglomeration in shape in case of *Aerva lanta* leaves extract with a size of 50–70 nm and to be spherical shaped in case of *Terminalia chebula* seed extract with an average size of 50–100 nm (Duraismy, 2018a). **Figure 15** shows the SEM images of Al₂O₃NP using *Rhamnus alaternus* extract, and the results indicate the formation of spherical shaped nanoparticles.

IV. Conclusion of the second part

Nanotechnology has a huge potential to develop alternative pest control strategy and lower risk insecticidal molecules. In this study we showed that alumina nanoparticles synthesized by sol-gel method could be a new effective protective agent that can be used to control the infestations of insect pests during the seeds storage.

The percentage of insect mortality at the highest NSA concentration tested was $100.00 \pm 0.00\%$ for *S. paniceum* followed by *T. confusum* ($79.41 \pm 2.94\%$), and *O. surinamensis* ($80.64 \pm 6.45\%$).

The toxicity bioassay showed the NSA is able to exert a significant insecticidal activity against the main seeds pests *O. surinamensis*, *S. paniceum*, and *T. confusum*.

The NSA treatment of the beans did not affect the *P. vulgaris* germination ($t_8 = 1.159$, $P=0.192$) nor the seedlings' root and hypocotyl elongation ($t_8 = 1.074$, $P = 0.341$; $t_8 = 1.159$, $P = 0.280$, respectively).

The efficacy of NSA against three species the absence of negative effects on seed germination and plant growth indicate that NSA can be a valid alternative to the chemical synthetic insecticides used for seeds coating. However, further studies are needed to evaluate the efficacy of various NSA seed treatments under a wide range of field conditions.

The NSA shows antifungal activity against *Trichothecium roseum*, *Cladosporium herbarum*, *Penicillium chrysogenum*, *Alternaria alternata*, *Aspergillus niger* strains tested also inhibition of spore germination.

Green Synthesis of Alumina Nanoparticles by using *Rhamnus alaternus* Extracts analysis the X-ray diffraction data revealed the average size of the Al-NPs as 37 nm. The Al₂O₃NP were found to be spherical agglomeration in shape with a size of (19–69 nm).

Global Conclusion and outlook

V. Global Conclusion and outlook

In the first part of this thesis, two plants *Rhamnus alaternus* and *Phillyrea angustifolia* they have been chosen in order to find new ways of application in the medical and pharmaceutical field as well as in the food and cosmetic field.

The objective of this work was to adopt scientific bases for the validation of certain biological properties attributed to these medicinal plants, chosen on the basis of their traditional use. In this study, the optimised extracts of these plants seem to be of real and potential interest in the treatment of inflammation, and the prevention of the spread of diseases against the effects of oxidative stress, preventing diabetes and inhibiting the growth of certain micro-organisms.

In the second part of this these, the work presented allows to widen the knowledge on the mode of action of nanostructured alumina and to propose a new strategy to control insect pests of stored products. The approaches in terms of methodology developed here constitute a first step in the development of an effective phytosanitary formulation which could be used in the fight against insects and microorganisms.

At the outset of the present study, it would be interesting to carry out a more in-depth study to isolate, purify and identify the molecules responsible for the previous activities, by studying the mechanisms of action on the inflammatory mediators, the enzymes involved in the production of ROS and on antioxidant systems *In vivo*. It would be of great interest to study the antibacterial activity of the extracts against bacterial strains that are resistant to conventional antibiotics and to broaden the scope of the study of the fractions of the extracts and volatile oils of the plant.

In order to be as close as possible to the real conditions of use, it would be interesting to optimise the nanoparticle process and to develop alternative strategies must be able to adapt to the treatment conditions traditionally used in agriculture. Studies will therefore be needed to assess the best application process for this type of formulation (e.g. spraying, nebulisation, etc...). This part will require the establishment of a partnership with phytosanitary industries specialised in this field. It is important to note that the development of such a strategy must be accompanied by ecotoxicological tests on non-target organisms such as bees.

It would be interesting to explore the synthesis of Nanostructured alumina by the green method using plant extracts. it would be preferable to evaluate their biological activities. Especially is considered to be a non-toxic, inexpensive, simple and not dangerous to nature.

V. References

A.Janbey, K.Paati, R., Tahir, S., Pramanik, P., 2001. A new chemical route for the synthesis of nano-crystalline, *Journal of the European Ceramic Society*, 2285-2289.

Abdeen, S., Isaac, R.R., Geo, S., Sornalekshmi, S., Rose, A., Praseetha, P., 2013. Evaluation of Antimicrobial Activity of Biosynthesized Iron and Silver Nanoparticles Using the Fungi *Fusarium Oxysporum* and Actinomycetes sp. on Human Pathogens. *Nano Biomedicine & Engineering* 5.

Ali, D.M., Divya, C., Gunasekaran, M., Thajuddin, N., 2011. Biosynthesis and characterization of silicon-germanium oxide nanocomposite by diatom. *Digest J. Nanomaterial biostructures* 6, 117-120.

Anjum, N.A., Gill, S.S., Duarte, A.C., Pereira, E., Ahmad, I., 2013. Silver nanoparticles in soil-plant systems. *Journal of Nanoparticle Research* 15, 1896.

Antonelli, D.M., Ying, J.Y., 1995. Synthesis of hexagonally packed mesoporous TiO₂ by a modified sol-gel method. *Angewandte Chemie International Edition in English* 34, 2014-2017.

Ates, M., Demir, V., Arslan, Z., Daniels, J., Farah, I.O., Bogatu, C., 2015. Evaluation of alpha and gamma aluminum oxide nanoparticle accumulation, toxicity, and depuration in *Artemia salina* larvae. *Environmental toxicology* 30, 109-118.

Athanassiou, C.G., Kavallieratos, N.G., Chiriloaie, A., Vassilakos, T.N., Fatu, V., Drosu, S., Ciobanu, M., Dudoiu, R., 2016. Insecticidal efficacy of natural diatomaceous earth deposits from Greece and Romania against four stored grain beetles: the effect of temperature and relative humidity. *Bulletin of Insectology* 69, 25-34.

Athanassiou, E.K., Grass, R.N., Stark, W.J., 2006. Large-scale production of carbon-coated copper nanoparticles for sensor applications. *Nanotechnology* 17, 1668.

Awwad, A.M., Salem, N.M., Abdeen, A.O., 2013. Green synthesis of silver nanoparticles using carob leaf extract and its antibacterial activity. *International journal of Industrial chemistry* 4, 29.

Baczanski, A., Braham, C., Seiler, W., Shiraki, N., 2004. Multi-reflection method and grazing incidence geometry used for stress measurement by X-ray diffraction. *Surface and Coatings Technology* 182, 43-54.

Baker, M.T., Heriot, W.A., 2005. Method and apparatus for liposome production. Google Patents.

- Bala, T., Armstrong, G., Laffir, F., Thornton, R., 2011. Titania–silver and alumina–silver composite nanoparticles: Novel, versatile synthesis, reaction mechanism and potential antimicrobial application. *Journal of colloid and interface science* 356, 395-403.
- Bansal, V., Rautaray, D., Bharde, A., Ahire, K., Sanyal, A., Ahmad, A., Sastry, M., 2005. Fungus-mediated biosynthesis of silica and titania particles. *Journal of Materials Chemistry* 15, 2583-2589.
- Bhaviripudi, S., Mile, E., Steiner, S.A., Zare, A.T., Dresselhaus, M.S., Belcher, A.M., Kong, J., 2007. CVD synthesis of single-walled carbon nanotubes from gold nanoparticle catalysts. *Journal of the American Chemical Society* 129, 1516-1517.
- Boisselier, E., Astruc, D., 2009. Gold nanoparticles in nanomedicine: preparations, imaging, diagnostics, therapies and toxicity. *Chemical society reviews* 38, 1759-1782.
- Bougherra, H.H., Bedini, S., Flamini, G., Cosci, F., Belhamel, K., Conti, B., 2015. *Pistacia lentiscus* essential oil has repellent effect against three major insect pests of pasta. *Industrial Crops and Products* 63, 249-255.
- Breierová, E., Vajcziková, I., Sasinková, V., Stratilová, E., Fišera, M., Gregor, T., Šajbidor, J., 2002. Biosorption of cadmium ions by different yeast species. *Zeitschrift für Naturforschung C* 57, 634-639.
- Buteler, M., Sofie, S.W., Weaver, D.K., Driscoll, D., Muretta, J., Stadler, T., 2015. Development of nanoalumina dust as insecticide against *Sitophilus oryzae* and *Rhyzopertha dominica*. *International Journal of Pest Management* 61, 80-89.
- Castellano, A.C., 1996. Insight into biosciences from synchrotron radiation. *Giugno* 5, 3-9.
- Christy, P.N., Basha, S.K., Kumari, V.S., Bashir, A., Maaza, M., Kaviyarasu, K., Arasu, M.V., Al-Dhabi, N.A., Ignacimuthu, S., 2020. Biopolymeric nanocomposite scaffolds for bone tissue engineering applications–A review. *Journal of Drug Delivery Science and Technology* 55, 101452.
- Dablemont, C., Lang, P., Mangeney, C., Piquemal, J.-Y., Petkov, V., Herbst, F., Viau, G., 2008. FTIR and XPS study of Pt nanoparticle functionalization and interaction with alumina. *Langmuir* 24, 5832-5841.
- Dietz, K.-J., Herth, S., 2011. Plant nanotoxicology. *Trends in plant science* 16, 582-589.
- Duraisamy, P., 2018a. Green Synthesis of Aluminium Oxide Nanoparticles by using *Aerva lanta* and *Terminalia chebula* Extracts. *International Journal for Research in Applied Science and Engineering Technology* 6, 428-433.

- Duraisamy, P., 2018b. Green synthesis of aluminium oxide nanoparticles by using *Aerva lanta* and *Terminalia chebula* extracts. *IJRASET* 6, 428-433.
- Fernández, V., Eichert, T., 2009. Uptake of Hydrophilic Solutes Through Plant Leaves: Current State of Knowledge and Perspectives of Foliar Fertilization. *Critical Reviews in Plant Sciences* 28, 36-68.
- Galhotra, P., 2010. Carbon dioxide adsorption on nanomaterials.
- Geisler-Lee, J., Wang, Q., Yao, Y., Zhang, W., Geisler, M., Li, K., Huang, Y., Chen, Y., Kolmakov, A., Ma, X., 2012. Phytotoxicity, accumulation and transport of silver nanoparticles by *Arabidopsis thaliana*. *Nanotoxicology* 7, 323-337.
- Gericke, M., Pinches, A., 2006. Biological synthesis of metal nanoparticles. *Hydrometallurgy* 83, 132-140.
- Ghotekar, S., 2019a. Plant extract mediated biosynthesis of Al₂O₃ nanoparticles-a review on plant parts involved, characterization and applications. *Nanochemistry Research* 4, 163-169.
- Ghotekar, S., 2019b. A review on plant extract mediated biogenic synthesis of CdO nanoparticles and their recent applications. *Asian Journal of Green Chemistry* 3, 187-200.
- Gondal, M., Saleh, T.A., Drmash, Q., 2012. Synthesis of nickel oxide nanoparticles using pulsed laser ablation in liquids and their optical characterization. *Applied Surface Science* 258, 6982-6986.
- Goswami, A., Roy, I., Sengupta, S., Debnath, N., 2010. Novel applications of solid and liquid formulations of nanoparticles against insect pests and pathogens. *Thin solid films* 519, 1252-1257.
- Govindaraju, K., Kiruthiga, V., Kumar, V.G., Singaravelu, G., 2009. Extracellular synthesis of silver nanoparticles by a marine alga, *Sargassum wightii* Grevilli and their antibacterial effects. *Journal of Nanoscience and Nanotechnology* 9, 5497-5501.
- Grover, G.M., 1966. Evaporation-condensation heat transfer device. Google Patents.
- Gruère, G., Narrod, C., Abbott, L., 2011. Agricultural, food, and water nanotechnologies for the poor. International Food Policy Research Institute, Washington, DC.
- Guczi, L., Beck, A., Horvath, A., Koppány, Z., Stefler, G., Frey, K., Sajo, I., Geszti, O., Bazin, D., Lynch, J., 2003. AuPd bimetallic nanoparticles on TiO₂: XRD, TEM, in situ EXAFS studies and catalytic activity in CO oxidation. *Journal of Molecular Catalysis A: Chemical* 204, 545-552.

- Hind, A.R., Bhargava, S.K., Grocott, S.C., 1999. The surface chemistry of Bayer process solids: a review. *Colloids and surfaces A: Physicochemical and engineering aspects* 146, 359-374.
- Hulkoti, N.I., Taranath, T., 2014. Biosynthesis of nanoparticles using microbes—a review. *Colloids and Surfaces B: Biointerfaces* 121, 474-483.
- Iatrou, I., Vardas, E., Theologie-Lygidakis, N., Leventis, M., 2010. A retrospective analysis of the characteristics, treatment and follow-up of 26 odontomas in Greek children. *Journal of oral science* 52, 439-447.
- Ismail, R.A., Zaidan, S.A., Kadhim, R.M., 2017. Preparation and characterization of aluminum oxide nanoparticles by laser ablation in liquid as passivating and anti-reflection coating for silicon photodiodes. *Applied Nanoscience* 7, 477-487.
- Issa, B., Obaidat, I.M., Albiss, B.A., Haik, Y., 2013. Magnetic nanoparticles: surface effects and properties related to biomedicine applications. *International journal of molecular sciences* 14, 21266-21305.
- Jalal, M., Ansari, M.A., Shukla, A.K., Ali, S.G., Khan, Haris M., Pal, R., Alam, J., Cameotra, S.S., 2016. Green synthesis and antifungal activity of Al₂O₃NPs against fluconazole-resistant *Candida* spp isolated from a tertiary care hospital. *RSC Advances* 6, 107577-107590.
- Jia, G., Wang, H., Yan, L., Wang, X., Pei, R., Yan, T., Zhao, Y., Guo, X., 2005. Cytotoxicity of Carbon Nanomaterials: Single-Wall Nanotube, Multi-Wall Nanotube, and Fullerene. *Environ. Sci. Technol* 39, 1378-1383.
- Jiang, Q., Lu, H., 2008. Size dependent interface energy and its applications. *Surface Science Reports* 63, 427-464.
- Jiang, W., Mashayekhi, H., Xing, B., 2009. Bacterial toxicity comparison between nano-and micro-scaled oxide particles. *Environmental pollution* 157, 1619-1625.
- Kavitha, R., Jayaram, V., 2006. Deposition and characterization of alumina films produced by combustion flame pyrolysis. *Surface and Coatings Technology* 201, 2491-2499.
- Keyvani, A., Saremi, M., Sohi, M.H., 2010. Microstructural stability of zirconia–alumina composite coatings during hot corrosion test at 1050 C. *Journal of Alloys and Compounds* 506, 103-108.
- Khan, I., Saeed, K., Khan, I., 2019. Nanoparticles: Properties, applications and toxicities. *Arabian journal of chemistry* 12, 908-931.

Khin, M.M., Nair, A.S., Babu, V.J., Murugan, R., Ramakrishna, S., 2012. A review on nanomaterials for environmental remediation. *Energy & Environmental Science* 5, 8075-8109.

Khodakovskaya, M., Dervishi, E., Mahmood, M., Xu, Y., Li, Z., Watanabe, F., Biris, A.S., 2009. Carbon nanotubes are able to penetrate plant seed coat and dramatically affect seed germination and plant growth. *American Chemical Society nano* 3, 3221-3227.

Király, Z., Klement, Z., Solymosy, F., Voros, J., 1970. *Methods in plant pathology*

Kruusing, A., 2010. Handbook of liquids-assisted laser processing. Elsevier.

Krysanov, E.Y., Pavlov, D., Demidova, T., Dgebuadze, Y.Y., 2010. Effect of nanoparticles on aquatic organisms. *Biology Bulletin* 37, 406-412.

Laachachi, A., Ferriol, M., Cochez, M., Cuesta, J.-M.L., Ruch, D., 2009. A comparison of the role of boehmite (AlOOH) and alumina (Al₂O₃) in the thermal stability and flammability of poly (methyl methacrylate). *Polymer Degradation and Stability* 94, 1373-1378.

Leclerc, L., 2011. Internalisation cellulaire et activité biologique de micro et nanoparticules fluorescentes de chimie de surface contrôlée, Génie des procédés. l'École Nationale Supérieure des Mines de Saint-Étienne.

Lee, C., Kim, J.Y., Lee, W.I., Nelson, K.L., Yoon, J., Sedlak, D.L., 2008. Bactericidal effect of zero-valent iron nanoparticles on Escherichia coli. *Environmental science & technology* 42, 4927-4933.

Lee, C.W., Mahendra, S., Zodrow, K., Li, D., Tsai, Y.C., Braam, J., Alvarez, P.J., 2010a. Developmental phytotoxicity of metal oxide nanoparticles to *Arabidopsis thaliana*. *Environmental Toxicology and Chemistry: An International Journal* 29, 669-675.

Lee, S., Cho, I.-S., Lee, J.H., Kim, D.H., Kim, D.W., Kim, J.Y., Shin, H., Lee, J.-K., Jung, H.S., Park, N.-G., 2010b. Two-step sol-gel method-based TiO₂ nanoparticles with uniform morphology and size for efficient photo-energy conversion devices. *Chemistry of Materials* 22, 1958-1965.

Lemine, O., 2009. Microstructural characterisation of α -Fe₂O₃ nanoparticles using, XRD line profiles analysis, FE-SEM and FT-IR. *Superlattices and Microstructures* 45, 576-582.

Lewis, K.E., Golden, D.M., Smith, G.P., 1984. Organometallic bond dissociation energies: laser pyrolysis of iron pentacarbonyl, chromium hexacarbonyl, molybdenum

hexacarbonyl, and tungsten hexacarbonyl. *Journal of the American Chemical Society* 106, 3905-3912.

Li, J., Pan, Y., Xiang, C., Ge, Q., Guo, J., 2006. Low temperature synthesis of ultrafine α -Al₂O₃ powder by a simple aqueous sol-gel process. *Ceramics International* 32, 587-591.

Liang, Z.Y.Y.J.T., Jiu-Lin, N.Y.-N.W., 2007. Study of nano-porous Si/Graphite/C composite anode materials for Li-ion batteries. *Chinese Journal of Inorganic Chemistry* 23, 1882-1886.

Lin, D., Xing, B., 2007. Phytotoxicity of nanoparticles: inhibition of seed germination and root growth. *Environmental pollution* 150, 243-250.

Liu, I., Shen, P., Chen, S., 2010. H⁺-and Al²⁺-codoped Al₂O₃ nanoparticles with spinel-type related structures by pulsed laser ablation in water. *The Journal of Physical Chemistry C* 114, 7751-7757.

Lombardi, R., 2019. Knowledge transfer and organizational performance and business process: past, present and future researches. *Business Process Management Journal*.

Lukić, I., Krstić, J., Jovanović, D., Skala, D., 2009. Alumina/silica supported K₂CO₃ as a catalyst for biodiesel synthesis from sunflower oil. *Bioresource technology* 100, 4690-4696.

Mahajan, P., Dhoke, S., Khanna, A., 2011. Effect of nano-ZnO particle suspension on growth of mung (*Vigna radiata*) and gram (*Cicer arietinum*) seedlings using plant agar method. *Journal of Nanotechnology* 2011.

Mandal, D., Bolander, M.E., Mukhopadhyay, D., Sarkar, G., Mukherjee, P., 2006. The use of microorganisms for the formation of metal nanoparticles and their application. *Applied microbiology and biotechnology* 69, 485-492.

Manias, E., Touny, A., Wu, L., Strawhecker, K., Lu, B., Chung, T., 2001. Polypropylene/montmorillonite nanocomposites. Review of the synthetic routes and materials properties. *Chemistry of Materials* 13, 3516-3523.

Manikandan, V., Jayanthi, P., Priyadharsan, A., Vijayaprabathap, E., Anbarasan, P., Velmurugan, P., 2019. Green synthesis of pH-responsive Al₂O₃ nanoparticles: Application to rapid removal of nitrate ions with enhanced antibacterial activity. *Journal of Photochemistry and Photobiology A: Chemistry* 371, 205-215.

Manivasakan, P., Rajendran, V., Rauta, P.R., Sahu, B.B., Panda, B.K., 2011. Effect of mineral acids on the production of alumina nanopowder from raw bauxite. *Powder technology* 211, 77-84.

- Martin, M., Rabanal, M.E., Gómez, L.S., Torralba, J.M., Milosevic, O., 2008. Microstructural and morphological analysis of nanostructured alumina particles synthesized at low temperature via aerosol route. *Journal of the European Ceramic Society* 28, 2487-2494.
- Mata, Y., Torres, E., Blazquez, M., Ballester, A., González, F., Munoz, J., 2009. Gold (III) biosorption and bio-reduction with the brown alga *Fucus vesiculosus*. *Journal of hazardous materials* 166, 612-618.
- Maximous, N., Nakhla, G., Wan, W., Wong, K., 2009. Preparation, characterization and performance of Al₂O₃/PES membrane for wastewater filtration. *Journal of Membrane Science* 341, 67-75.
- McGraw, R., 1997. Description of aerosol dynamics by the quadrature method of moments. *Aerosol Science and Technology* 27, 255-265.
- Mimani, T., Patil, K., 2001. Solution combustion synthesis of nanoscale oxides and their composites. *Materials Physics and Mechanics* (Russia) 4, 134-137.
- Mirjalili, F., Hasmaliza, M., Abdullah, L.C., 2010. Size-controlled synthesis of nano α -alumina particles through the sol-gel method. *Ceramics International* 36, 1253-1257.
- Mittal, A.K., Chisti, Y., Banerjee, U.C., 2013. Synthesis of metallic nanoparticles using plant extracts. *Biotechnology advances* 31, 346-356.
- Mohamed, Y., Azzam, A., Amin, B., Safwat, N., 2015. Mycosynthesis of iron nanoparticles by *Alternaria alternata* and its antibacterial activity. *African Journal of Biotechnology* 14, 1234-1241.
- Mohanraj, V., Chen, Y., 2006. Nanoparticles-a review. *Tropical journal of pharmaceutical research* 5, 561-573.
- Moradi, M., Abdolhosseini, M., Zarrabi, A., 2019. A review on application of Nano-structures and Nano-objects with high potential for managing different aspects of bone malignancies. *Nano-Structures & Nano-Objects* 19, 100348.
- Mukherjee, A., Mohammed Sadiq, I., Prathna, T., Chandrasekaran, N., 2011. Antimicrobial activity of aluminium oxide nanoparticles for potential clinical applications. Science against microbial pathogens: *communicating current research and technological advances* 1, 245-251.
- Murdock, R.C., Braydich-Stolle, L., Schrand, A.M., Schlager, J.J., Hussain, S.M., 2008. Characterization of nanomaterial dispersion in solution prior to in vitro exposure using dynamic light scattering technique. *Toxicological sciences* 101, 239-253.
- Nair, R., Varghese, S.H., Nair, B.G., Maekawa, T., Yoshida, Y., Kumar, D.S., 2010. Nanoparticulate material delivery to plants. *Plant science* 179, 154-163.

- Narayanan, K.B., Sakthivel, N., 2010. Biological synthesis of metal nanoparticles by microbes. *Advances in colloid and interface science* 156, 1-13.
- Nasibulin, A.G., Moisala, A., Brown, D.P., Jiang, H., Kauppinen, E.I., 2005. A novel aerosol method for single walled carbon nanotube synthesis. *Chemical Physics Letters* 402, 227-232.
- Nehra, P., Chauhan, R., Garg, N., Verma, K., 2018. Antibacterial and antifungal activity of chitosan coated iron oxide nanoparticles. *British journal of biomedical science* 75, 13-18.
- Nyankson, E., Agyei-Tuffour, B., Asare, J., Annan, E., Rwenyagila, E., Konadu, D., Yaya, A., Dodoo-Arhin, D., 2013. Nanostructured TiO₂ and their energy applications-a review.
- Parveen, S., Misra, R., Sahoo, S.K., 2012. Nanoparticles: a boon to drug delivery, therapeutics, diagnostics and imaging. *Nanomedicine: Nanotechnology, Biology and Medicine* 8, 147-166.
- Peelen, J.G.J., 1977. Alumina: sintering and optical properties.
- Perez, C., Pauli, M., Bazerque, P., 1990. An antibiotic assay by the well agar method. *Acta Biol Med Exp* 15, 113-115.
- Pimentel, D., 2005. 'Environmental and Economic Costs of the Application of Pesticides Primarily in the United States'. *Environment, Development and Sustainability* 7, 229-252.
- Piriyawong, V., Thongpool, V., Asanithi, P., Limsuwan, P., 2012. Preparation and characterization of alumina nanoparticles in deionized water using laser ablation technique. *Journal of Nanomaterials*.
- Pirzada, S., Yadav, T., 1998. Method of producing nanoscale powders by quenching of vapors. Google Patents.
- Qu, L., He, C., Yang, Y., He, Y., Liu, Z., 2005. Hydrothermal synthesis of alumina nanotubes templated by anionic surfactant. *Materials Letters* 59, 4034-4037.
- Rajaeiyan, A., Bagheri-Mohagheghi, M., 2013. Comparison of sol-gel and co-precipitation methods on the structural properties and phase transformation of γ and α -Al₂O₃ nanoparticles. *Advances in Manufacturing* 1, 176-182.
- Rajesh, S., Raja, D.P., Rathi, J., Sahayaraj, K., 2012. Biosynthesis of silver nanoparticles using *Ulva fasciata* (Delile) ethyl acetate extract and its activity against *Xanthomonas campestris* pv. *malvacearum*. *Journal of Biopesticides* 5, 119.

- Rajeshkumar, S., Malarkodi, C., Paulkumar, K., Vanaja, M., Gnanajobitha, G., Annadurai, G., 2014. Algae mediated green fabrication of silver nanoparticles and examination of its antifungal activity against clinical pathogens. *International journal of Metals* 2014.
- Reid, C.B., Forrester, J.S., Goodshaw, H.J., Kisi, E.H., Suaning, G.J., 2008. A study in the mechanical milling of alumina powder. *Ceramics International* 34, 1551-1556.
- Riddin, T., Gericke, M., Whiteley, C., 2006. Analysis of the inter-and extracellular formation of platinum nanoparticles by *Fusarium oxysporum* f. sp. lycopersici using response surface methodology. *Nanotechnology* 17, 3482.
- Rogojan, R., Andronescu, E., Ghitulica, C., Vasile, B.S., 2011. Synthesis and characterization of alumina nano-powder obtained by sol-gel method. UPB Buletin Stiintific, Series B: *Chemistry and Materials Science* 73, 67-76.
- Sadiq, I.M., Chowdhury, B., Chandrasekaran, N., Mukherjee, A., 2009. Antimicrobial sensitivity of *Escherichia coli* to alumina nanoparticles. *Nanomedicine: Nanotechnology, Biology and Medicine* 5, 282-286.
- Saha, S., 1994. Preparation of alumina by sol-gel process, its structures and properties. *Journal of Sol-Gel Science and Technology* 3, 117-126.
- Salavati-Niasari, M., Davar, F., Mir, N., 2008. Synthesis and characterization of metallic copper nanoparticles via thermal decomposition. *Polyhedron* 27, 3514-3518.
- Sanghi, R., Verma, P., 2009. Biomimetic synthesis and characterisation of protein capped silver nanoparticles. *Bioresource technology* 100, 501-504.
- Santhosh, P.B., Ulrih, N.P., 2013. Multifunctional superparamagnetic iron oxide nanoparticles: promising tools in cancer theranostics. *Cancer letters* 336, 8-17.
- Santos, M.F.d., 2013. Sistemas baseados em amido termoplástico: pectina contendo hidroxiapatita nanoestruturada visando liberação de fósforo em meio aquoso.
- Schröfel, A., Kratošová, G., Bohunická, M., Dobročka, E., Vávra, I., 2011. Biosynthesis of gold nanoparticles using diatoms—silica-gold and EPS-gold bionanocomposite formation. *Journal of nanoparticle research* 13, 3207-3216.
- Senapati, S., Ahmad, A., Khan, M.I., Sastry, M., Kumar, R., 2005. Extracellular biosynthesis of bimetallic Au–Ag alloy nanoparticles. *Small* 1, 517-520.
- Sheeba, J.M., Thambidurai, S., 2009. Extraction, characterization, and application of seaweed nanoparticles on cotton fabrics. *Journal of applied polymer science* 113, 2287-2292.

Singaravelu, G., Arockiamary, J., Kumar, V.G., Govindaraju, K., 2007. A novel extracellular synthesis of monodisperse gold nanoparticles using marine alga, *Sargassum wightii* Greville. *Colloids and surfaces B: Biointerfaces* 57, 97-101.

Singh, A., Singh, N., Hussain, I., Singh, H., Singh, S., 2015. Plant-nanoparticle interaction: an approach to improve agricultural practices and plant productivity. *Int J Pharm Sci Invent* 4, 25-40.

Sorbiun, M., Shayegan Mehr, E., Ramazani, A., Mashhadi Malekzadeh, A., 2018. Biosynthesis of metallic nanoparticles using plant extracts and evaluation of their antibacterial properties. *Nanochemistry Research* 3, 1-16.

Stadler, T., Buteler, M., Weaver, D.K., 2010. Novel use of nanostructured alumina as an insecticide. *Pest Management Science: formerly Pesticide Science* 66, 577-579.

Stadler, T., Buteler, M., Weaver, D.K., Sofie, S., 2012. Comparative toxicity of nanostructured alumina and a commercial inert dust for *Sitophilus oryzae* (L.) and *Rhyzopertha dominica* (F.) at varying ambient humidity levels. *Journal of Stored Products Research* 48, 81-90.

Stadler, T., garcia, G.P.L., Gitto, J.G., Buteler, M., 2017. Nanostructured alumina: biocidal properties and mechanism of action of a novel insecticide powder. *Bulletin of Insectology* 70, 17-25.

Subramanyam, B., Roesli, R., 2000. Inert dusts, Alternatives to pesticides in stored-product IPM. Springer, pp. 321-380.

Sun, Z.-X., Zheng, T.-T., Bo, Q.-B., Du, M., Forsling, W., 2008. Effects of calcination temperature on the pore size and wall crystalline structure of mesoporous alumina. *Journal of colloid and interface science* 319, 247-251.

Sutradhar, P., Debnath, N., Saha, M., 2013. Microwave-assisted rapid synthesis of alumina nanoparticles using tea, coffee and triphala extracts. *Advances in Manufacturing* 1, 357-361.

Tai, C.Y., Tai, C.-T., Chang, M.-H., Liu, H.-S., 2007. Synthesis of magnesium hydroxide and oxide nanoparticles using a spinning disk reactor. *Industrial & engineering chemistry research* 46, 5536-5541.

Teodoro, S., , L.G.G.P., , G.J.G., , B.M., 2017. Nanostructured alumina: biocidal properties and mechanism of action of a novel insecticide powder. *Bulletin of Insectology* 1, 17-25.

- Thakkar, K.N., Mhatre, S.S., Parikh, R.Y., 2010. Biological synthesis of metallic nanoparticles. *Nanomedicine: nanotechnology, biology and medicine* 6, 257-262.
- Thul, S.T., Sarangi, B.K., 2015. Implications of nanotechnology on plant productivity and its rhizospheric environment, *Nanotechnology and plant Sciences*. Springer, pp. 37-53.
- Tiwari, D.K., Behari, J., Sen, P., 2008. Application of nanoparticles in waste water treatment 1.
- Touzin, M., Goeuriot, D., Guerret-Piécourt, C., Juvé, D., Fitting, H.-J., 2010. Alumina based ceramics for high-voltage insulation. *Journal of the European Ceramic Society* 30, 805-817.
- Tripathi, D.K., Singh, S., Singh, S., Pandey, R., Singh, V.P., Sharma, N.C., Prasad, S.M., Dubey, N.K., Chauhan, D.K., 2017. An overview on manufactured nanoparticles in plants: uptake, translocation, accumulation and phytotoxicity. *Plant Physiology and Biochemistry* 110, 2-12.
- Vigneshwaran, N., Ashtaputre, N., Varadarajan, P., Nachane, R., Paralikar, K., Balasubramanya, R., 2007. Biological synthesis of silver nanoparticles using the fungus *Aspergillus flavus*. *Materials letters* 61, 1413-1418.
- Vivek, M., Kumar, P.S., Steffi, S., Sudha, S., 2011. Biogenic silver nanoparticles by *Gelidiella acerosa* extract and their antifungal effects. *Avicenna Journal of Medical Biotechnology* 3, 143.
- Wang, P., Lombi, E., Zhao, F.-J., Kopittke, P.M., 2016. Nanotechnology: a new opportunity in plant sciences. *Trends in plant science* 21, 699-712.
- Wang, Q., Arash, B., 2014. A review on applications of carbon nanotubes and graphenes as nano-resonator sensors. *Computational Materials Science* 82, 350-360.
- Wani, A., Shah, M., 2012. A unique and profound effect of MgO and ZnO nanoparticles on some plant pathogenic fungi. *Journal of Applied Pharmaceutical Science* 2, 4.
- Wu, S., Zuber, F., Maniura-Weber, K., Brugger, J., Ren, Q., 2018. Nanostructured surface topographies have an effect on bactericidal activity. *Journal of nanobiotechnology* 16, 20.
- Yan, L., Li, Y.S., Xiang, C.B., Xianda, S., 2006. Effect of nano-sized Al₂O₃-particle addition on PVDF ultrafiltration membrane performance. *Journal of Membrane Science* 276, 162-167.

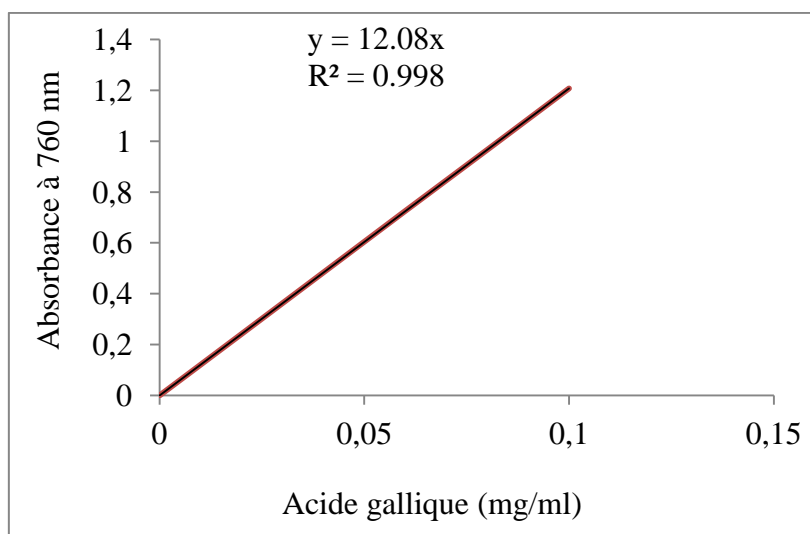
Yan, Z., Bao, R., Huang, Y., Chrisey, D.B., 2010. Hollow particles formed on laser-induced bubbles by excimer laser ablation of Al in liquid. *The Journal of Physical Chemistry C* 114, 11370-11374.

Yasur, J., Rani, P.U., 2013. Environmental effects of nanosilver: impact on castor seed germination, seedling growth, and plant physiology. *Environmental Science and Pollution Research* 20, 8636-8648.

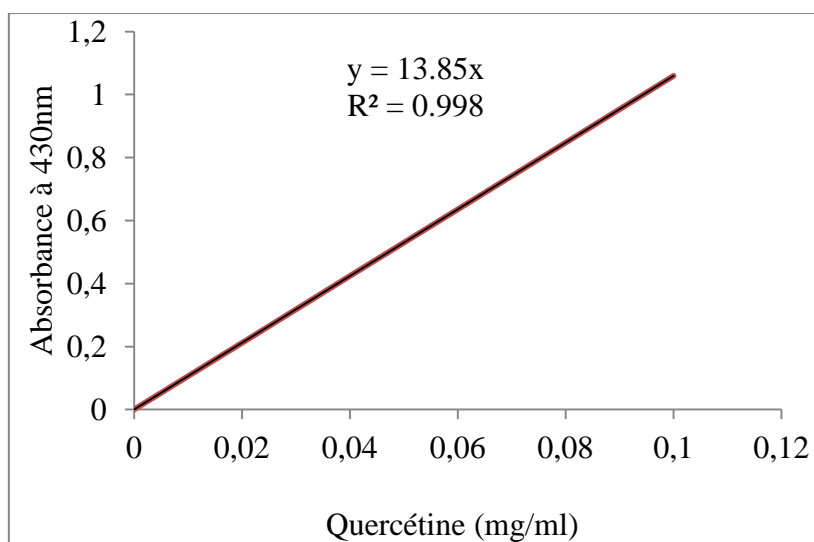
Yong, P., Rowson, N.A., Farr, J.P.G., Harris, I.R., Macaskie, L.E., 2002. Bioreduction and biocrystallization of palladium by *Desulfovibrio desulfuricans* NCIMB 8307. *Biotechnology and bioengineering* 80, 369-379.

Zakharova, O.V., Godymchuk, A.Y., Gusev, A.A., Gulchenko, S.I., Vasyukova, I.A., Kuznetsov, D.V., 2015. Considerable variation of antibacterial activity of Cu nanoparticles suspensions depending on the storage time, dispersive medium, and particle sizes. *BioMed research international*.

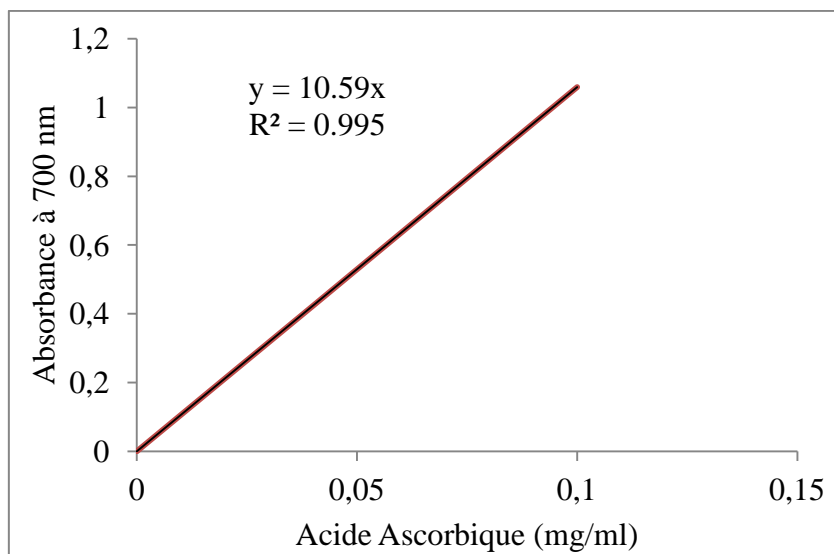
Annexes



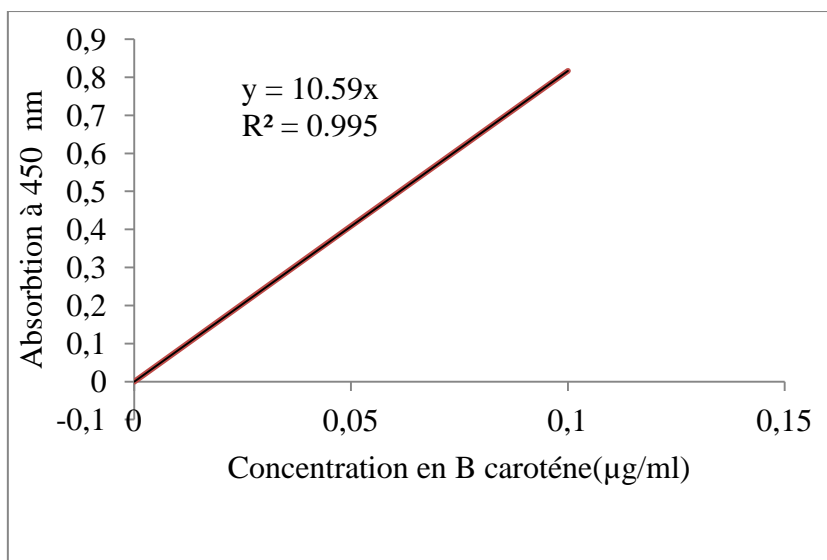
Annexe I: Calibration curve for phenolic compounds.



Annexe II: Flavonoid calibration curve.



Annexe III: Reducing power calibration curve.



Annexe VI: Carotenoid calibration curve.

Résumé : L'extraction solide liquide a été combinée avec la méthodologie de surface de réponse (RSM), pour optimiser l'extraction en composés phénoliques et les activités antioxydantes des feuilles de *Phillyrea angustifolia* et *Rhamnus alaternus*. Un plan d'expérience à trois variables : concentration en éthanol (%EtOH), le temps d'extraction, le ratio et l'étude de deux réponses (teneur en polyphénols totaux et le piégeage du radical DPPH) ont été étudiés. Les conditions optimales obtenues pour les extraits de *P. angustifolia* sont : TPT de 79,40 mg équivalent acide gallique/gMS et un effet de piégeage du radical libre DPPH de 63,75 µg/mL. Tandis que cas de *R. alaternus* donnent une TPT de 70,36 mg équivalent acide gallique/g Ms et un effet de piégeage du radical libre DPPH de 69,49 µm/mL. La plus forte teneur en humidité et en caroténoïdes a été obtenue avec les feuilles de *R. alaternus* avec un taux de 62,14% et une teneur de 93,74 mg β -carotène/100 g, respectivement. L'extrait de *R. alaternus* obtenu dans les conditions optimales possède les plus fortes teneurs en flavonoïdes et en tannins qui sont de 17,17 mg équivalent quercitine/g MS et de 1,86 mg équivalent cyanidine/g MS. Les activités antioxydantes des extraits des deux plantes obtenus dans les conditions optimales ont été déterminée par le test du pouvoir réducteur, ABTS radical, teste d'inhibition de superoxyde et le test de phosphomolybdate d'ammonium. L'extrait de *R. alaternus* possède le plus fort pouvoir réducteur et le plus fort effet réducteur des ions molybdate avec des teneurs de 16,92 mg équivalent acide gallique/g MS et de 112,86 mg équivalent acide gallique/g MS, respectivement. La plus forte activité antibactérienne a été obtenue avec l'extrait de *R. alaternus* sur *Escherichia coli* et *Salmonella enterica* avec des diamètres de zones d'inhibition de 27,37 et de 26,87 mm, respectivement.

Les extraits optimaux obtenus à partir de deux espèces ont été testés ; l'activité anti-inflammatoire a été évaluée *In vitro* à l'aide de deux tests (inhibition de la protéine de dénaturation et antiprotéinase) ; *P. angustifolia* a montré une activité très intéressante. Enfin, deux extraits optimaux Les extraits obtenus par le test de cytotoxicité ne présentent aucune toxicité.

Dans la deuxième partie de la thèse, nous avons évalué l'effet de l'alumina nanostructuré (NSA) en tant que protecteur des semences contre les principaux insectes ravageurs des semences, *Oryzaephilus surinamensis*, *Stegobium paniceum* et *Tribolium confusum*. En outre, nous avons testé les effets de NSA sur la germination des semences et la croissance des plantes et enfin, nous avons évalué la présence de NSA en tant que contaminant dans les feuilles des plants de haricots germés à partir de semences traitées à NSA. Les résultats ont montré une activité insecticide claire de la NSA. Au contraire, un effet positif de la NSA a été observé sur la croissance des pousses avec les plantes traitées qui étaient environ 66% plus élevées que les plantes non traitées. Enfin, aucune contamination par des particules d'alumine n'a été trouvée par le système EDX couplé à la microscopie électronique à balayage (MEB) sur la surface des feuilles de *P. vulgaris* obtenues à partir de haricots traités avec la NSA. L'activité antifongique de NSA a également été enregistrée La zone d'inhibition la plus élevée obtenu par la plus forte concentration NSA.

Mots clés : Activités antioxydantes, Activités antibactériennes, Activités antiinflammatoires, extraction solide/liquide, Méthodologie de réponse de surface, Polyphénols, *Phillyrea angustifolia*, *Rhamnus alaternus*. NSA, activité anifongique et activité insecticide

Abstract: Solid-liquid extraction was combined with the Response Surface Methodology (RSM), to optimise the extraction of phenolic compounds and antioxidant activity from the leaves of *Phillyrea angustifolia* and *Rhamnus alaternus*. An experimental design with three variables: ethanol concentration (%EtOH), extraction time, ratio and the study of two responses (total polyphenol content and DPPH radical scavenging) were studied. The optimal conditions obtained for *P. angustifolia* extracts are : TPT of 79.40 mg gallic acid equivalent/gMS and a DPPH free radical scavenging effect of 63.75 µg/mL. While *R. alaternus* gives a TPT of 70.36 mg gallic acid equivalent/g Ms and a DPPH free radical scavenging effect of 69.49 µm/mL. The highest moisture and carotenoid content was obtained with *R. alaternus* leaves with a 62.14% and 93.74 mg β -carotene/100 g, respectively. The extract of *R. alaternus* obtained under optimal conditions has the highest flavonoid and tannin contents, which are 17.17 mg quercitin equivalent/g DM and 1.86 mg cyanidin equivalent/g DM. The antioxidant activity of the extracts of the two plants obtained under optimal conditions was determined by the reducing power test, ABTS radical scavenging, NO enzymatic superoxide radical scavenging and the ammonium phosphomolybdate test. The extract of *R. alaternus* has the highest reducing power and the strongest reducing effect of molybdate ions with contents of 16.92 mg gallic acid equivalent/g DM and 112.86 mg gallic acid equivalent/g DM, respectively. The strongest antibacterial activity was obtained with *R. alaternus* extract on *Escherichia coli* and *Salmonella enterica* with inhibition zone diameters of 27.37 and 26.87 mm, respectively.

The optimal extracts obtained from two species were tested; the anti-inflammatory activity was evaluated *In vitro* using two tests (denaturation protein inhibition and anti-proteinase); *P. angustifolia* showed very interesting activity. Finally, two optimal extracts The extracts obtained by the cytotoxicity test showed no toxicity. In the second part of the thesis, we evaluated the effect of nanostructured alumina (NSA) as a seed protector against the main seed pests, *Oryzaephilus surinamensis*, *Stegobium paniceum* and *Tribolium confusum*. In addition, we tested the effects of NSA on seed germination and plant growth and finally, we evaluated the presence of NSA as a contaminant in the leaves of bean plants germinated from NSA-treated seeds. The results showed a clear insecticidal activity of NSA. On the contrary, a positive effect of NSA was observed on shoot growth with treated plants which were about 66% higher than untreated plants. Finally, no contamination by alumina particles was found by EDX system coupled with scanning electron microscopy (SEM) on the surface of *P. vulgaris* leaves obtained from beans treated with NSA. The antifungal activity of NSA was also recorded The highest inhibition zone was demonstrated by the highest concentration of NSA

Keywords: Antioxidant activities, Antibacterial activities, NSA, antifungal activities, insecticide activity, solid/liquid extraction, Surface response methodology, Polyphenols, *Phillyrea angustifolia*, and *Rhamnus alaternus*

الخلاصة:

الجمع بين الاستخلاص السائل والصلب مع منهجية سطح الاستجابة (RSM)، لتحسين استخراج المركبات الفينولية والنشاط المضاد للأكسدة من أوراق *Phillyrea angustifolia* و *Rhamnus alaternus*. تمت دراسة تصميم تجريبي مع ثلاثة متغيرات: تركيز الإيثانول (% EtOH)، ووقت الاستخراج، والنسبة ودراسة استجابتين (محتوى البوليفينول الكلي وكسح جذور DPPH). الشروط المثلى التي تم الحصول عليها لمستخلصات *P. angustifolia* هي: TPT من 79.40 ملغ مكافئ حمض الغاليك / جم وتأثير إزالة الجذور الحرة DPPH بنسبة 63.75 ميكروغرام / مل بينما يعطي *R. alaternus* 70.36 ملغ مكافئ حمض الغاليك / جم MS وتأثير مسح الجذور الحرة DPPH من 69.49 ميكرومتر / مل تم الحصول على أعلى محتوى رطوبة وكاروتين مع أوراق *R. alaternus* بنسبة 62.14% و 93.74 مجم كاروتين / 100 جم على التوالي. يحتوي مستخلص *R. alaternus* الذي تم الحصول عليه في ظل الظروف المثلى على أعلى محتوى من الفلافونويد والتانين، وهو 17.17 مجم من مكافئ كيرسيتين / جم DM و 1.86 مجم مكافئ سيانيددين / جم DM. تم تحديد النشاط المضاد للأكسدة لمستخلصات نباتين تم الحصول عليها في ظل الظروف المثلى من خلال اختبار القدرة المختزلة واختبار فوسفوموليبدات الأمونيوم. يمتلك مستخلص *R. alaternus* أعلى قوة اختزال وأقوى تأثير اختزال لأيونات الموليبدات بمحتويات 16.92 مجم مكافئ حمض الغاليك / جم DM و 112.86 مجم مكافئ حمض الغاليك / جم DM، على التوالي. تم الحصول على أقوى نشاط مضاد للجراثيم باستخدام مستخلص *R. alaternus* على الإشريكية القولونية والسالمونيلا المعوية بأقطار منطقة تثبيط 27.37 و 26.87 مم على التوالي.

تم اختبار المستخلصات المثلى التي تم الحصول عليها من نوعين؛ تم تقييم النشاط المضاد للالتهابات في المختبر باستخدام اختبارين (تسخن البروتين تثبيط البروتين ومضاد البروتين)؛ أظهر *P. angustifolia* نشاطاً مثيراً للاهتمام للغاية. أخيراً، لم يُظهر المستخلصان المثاليان اللذان تم الحصول عليهما عن طريق اختبار السمية الخلوية أي سمية.

في الجزء الثاني من الأطروحة، قمنا بتقييم تأثير الألومينا ذات البنية النانوية (NSA) كحماية للبذور ضد آفات البذور الرئيسية، *Oryzaephilus surinamensis* و *Stegobium paniceum* و *Tribolium confusum*. بالإضافة إلى ذلك، قمنا باختبار تأثيرات NSA على إنبات البذور ونمو النبات، وأخيراً، قمنا بتقييم وجود NSA كمثبط في أوراق نباتات الفاصوليا المنبتة من البذور المعالجة بـ NSA. أظهرت النتائج نشاط مبيد حشري واضح لـ NSA. على العكس من ذلك، لوحظ وجود تأثير إيجابي لـ NSA على نمو الفروع بالنباتات المعالجة والتي كانت أعلى بنسبة 66% من النباتات غير المعالجة. أخيراً، لم يتم العثور على أي تلوث بجزيئات الألومينا بواسطة نظام EDX المقترن بالمجهر الإلكتروني (SEM) على سطح أوراق *P. vulgaris* التي تم الحصول عليها من الفاصوليا المعالجة بـ NSA. كما تم تسجيل النشاط المضاد للفطريات لـ NSA. تم إظهار أعلى منطقة تثبيط من خلال أعلى تركيز لـ NSA

الكلمات المفتاحية: نشاط مضاد للأكسدة، نشاط مضاد للجراثيم، نشاط مضاد للالتهابات، الطريقة التقليدية، منهجية الاستجابة السطحية، البوليفينول، *Phillyrea angustifolia*، *Rhamnus alaternus*. NSA، نشاط فطري ونشاط مبيد للحشرات